

**NEURAL RESPONSES TO INJURY:
PREVENTION, PROTECTION, AND REPAIR
Annual Technical Report
1994**

Submitted by

Nicolas G. Bazan, M.D., Ph.D.
Program Director

Period Covered: 20 September, 1993, through 19 September, 1994

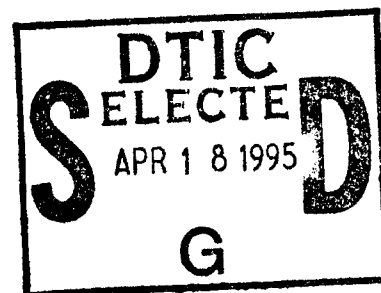
Cooperative Agreement DAMD17-93-V-3013

between

United States Army Research and
Development Command
(Walter Reed Army Institute of Research)

and

Louisiana State University Medical Center
Neuroscience Center of Excellence



**Role of Growth
Factors and Cell
Signaling in the
Response of Brain
and Retina to Injury**

Project Directors:
Prescott Deininger, Ph.D.
Nicolas G. Bazan, M.D., Ph.D.

19950417 158

DISTRIBUTION STATEMENT A

Approved for public release;
Distribution Unlimited

DTIC QUALITY INSPECTED 1

REPORT DOCUMENTATION PAGE			Form Approved OMB No 0704-0188	
1. AGENCY USE ONLY (Leave blank)		2. REPORT DATE 19 October, 1994	3. REPORT TYPE AND DATES COVERED Annual Report: 9/20/93 - 9/19/94	
4. TITLE AND SUBTITLE Neural Responses to Injury: Prevention, Protection, and Repair (Cooperative Agreement # DAMD17-93-V-3013)			5. FUNDING NUMBERS 97304000003758119 61110200000415000 AXZAC1KUF00000000 0AXZA00S18064 -AND- 21220400000275811 9611102H41ZZ41500 0ZYIZC1KUF0000000 00ZYIZ00S18064	
6. AUTHOR(S) Nicolas G. Bazan, M.D., Ph.D., Program Director Director, LSU Neuroscience Center Professor of Ophthalmology, Biochemistry and Molecular Biology and Neurology				
7. PERFORMING ORGANIZATION NAME(S) AND ADDRESS(ES) Louisiana State University Medical Center LSU Neuroscience Center 2020 Gravier Street, Suite B New Orleans, LA 70112			8. PERFORMING ORGANIZATION REPORT NUMBER	
9. SPONSORING/MONITORING AGENCY NAME(S) AND ADDRESS(ES) U. S. Army Research Office P. O. Box 12211 Research Triangle Park, NC 27709-2211			10. SPONSORING/ MONITORING AGENCY REPORT NUMBER	
11. SUPPLEMENTARY NOTES The views, opinions and/or findings contained in this report are those of the author(s) and should not be construed as an official Department of the Army position, policy, or decision, unless so designated by other documentation.				
12a. DISTRIBUTION/AVAILABILITY STATEMENT Approved for public release; distribution unlimited			12b. DISTRIBUTION CODE	
13. ABSTRACT (Maximum 200 words) The LSU Neuroscience Center is a comprehensive, multidisciplinary, and transdepartmental entity that unites fundamental neurobiology and the clinical neurosciences in the common goal of elucidating the workings of the brain and contributing to the treatment of currently incurable diseases of the nervous system. The objective of the present program is to find solutions to neuroscience-related problems of interest to the U.S. Army Medical Research and Development Command. The program is focused on exploiting novel neuroprotective strategies that lead to prevention of and repair after neural injury. Converging approaches using state-of-the-art tools of cell biology, neurochemistry, neuroimmunology, neurophysiology, neuropharmacology, molecular biology and virology are proposed. Over the next four years, this program aims to: 1) carry out seven research projects in the basic and clinical neurosciences; 2) expand central, shared facilities with the addition of highly specialized instrumentation not currently available to our scientists; 3) develop laboratory space to permit the physical consolidation and coordination of this research effort; and 4) institute a coordination unit to monitor, facilitate, and administrate the cooperative research programs, as well as to meet the associated budgetary, human resources, facilities, and communications needs for the attainment of the proposed program goals.				
14. SUBJECT TERMS			15. NUMBER OF PAGES	
			16. PRICE CODE	
17. SECURITY CLASSIFICATION OF REPORT UNCLASSIFIED			18. SECURITY CLASSIFICATION OF THIS PAGE UNCLASSIFIED	19. SECURITY CLASSIFICATION OF ABSTRACT UNCLASSIFIED
			20. LIMITATION OF ABSTRACT UL	

This Technical Report covers the progress made in the first year of this Cooperative Agreement in one project of the original proposal. We hope that this format of the report will facilitate its handling. The table of contents of all the projects has been included in each volume as well letters by members of External Advisory Committee of the LSU Neuroscience Center who have conducted an initial review of the work done supported by this Cooperative Agreement.

Nicolas G. Bazan, M.D., Ph.D.
 Director, LSU Neuroscience Center
 Program Director, USAMRDC Cooperative Agreement For

NTIS	CRA&I	<input checked="" type="checkbox"/>
DTIC	TAB	<input type="checkbox"/>
Unannounced		<input type="checkbox"/>
Justification		
By		
Distribution /		
Availability Codes		
Dist	Avail and/or Special	
A-1		

Table of Contents

Introduction	2
Table of Contents	3
Submission Letter from Dr. Nicolas G. Bazan	10
Letters of Critical Review: External Advisory Committee	16
Dr. Dennis W. Choi	17
Dr. Fred Plum	18

Technical Reports:

Neuroscience Core Research Facilities	
---	--

"Repair and Regeneration of Peripheral Nerve Damage"

Project Directors Roger Beuerman, Ph.D.
 David Kline, M.D.
 Austin Sumner, M.D.

Participating Scientists: John England, M.D.
 Leo Happel, Ph.D.
 Daniel Kim, M.D.,
 Cheryl Weill, Ph.D.

Introduction	
Experimental Procedures	
Conclusions	
Appendices	

Abstracts:

1. Society for Neuroscience: Epidermal growth factor and fibroblast growth factor in human neuroma tissue

"The Neuroimmunology of Stress, Injury, and Infection"

Project Directors: Bryan Gebhardt, Ph.D.
 Daniel Carr, Ph.D.

Table of Contents	
Abstract	
Introduction	

Body

Appendices

Abstracts: Psychoneuroimmunology Research Society

1. HSV-1 latently-infected mice display an altered response to stress: Implications for antiviral immunity.
2. Mouse lymphocytes express an orphan opioid receptor
3. Morphine suppresses peritoneal and splenic CTL activity in a dose-dependent fashion in alloimmunized mice
4. The frequency of exposure to morphine differentially affects CTL activity in alloimmunized mice.

Manuscripts:

1. Carr DJJ, Carpenter GW, Garza HH, Baker ML, Gebhart BM (in press) Cellular mechanisms involved in morphine-mediated suppression of CTL activity. In: *The Brain Immune Axis in Substance Abuse* (Sharp, Friedman, Maddin and Eisenstein, eds), Plenum Press.
2. Carpenter GW and Carr DJJ (submitted) Pretreatment with β -funaltrexamine blocks morphine-mediated suppression of CTL activity in alloimmunized mice.
3. Carr DJJ and Carpenter GW (submitted) Morphine-induced suppression of splenic CTL activity in alloimmunized mice is not mediated through a δ -opioid receptor.
4. Carpenter GW, Garza HH, Gebhardt BM, Carr DJJ (in press) Chronic morphine treatment suppresses CTL-mediated cytotoxicity, granulation and cAMP responses to alloantigen

"Neurochemical Protection of the Brain, Neural Plasticity and Repair"

Project Director: Nicolas G. Bazan, M.D., Ph.D.

Participating Scientists: Geoffrey Allen, Ph.D.
 Gary D. Clark, M.D.
 Victor Marcheselli, M.S.
 John Hurst, Ph.D.
 Leo Happel, M.D.
 Walter Lukiw, Ph.D.

PAF is a Presynaptic Mediator of Excitatory Neurotransmitter Release

Table of Contents

Introduction

Experimental Methods

Results

Conclusions

References

Neuroanatomical Correlation of PAF Antagonist-Affected Gene Expression

Quantitative Reverse Transcription Polymerase Chain Reaction (RT-PCR)

ELISA

Traumatic Brain Injury
 Introduction
 Methods and Experimental Animal Models
 Results
 Summary
 Bibliography

"Neuropharmacology of Delta Receptor Agonists and Antagonists "

Project Director: Joseph Moerschbaecher, Ph.D.

Participating Scientists: Charles France, Ph.D.
 Dennis J. Paul, Ph.D.
 Jayaraman Rao, M.D.

 Table of Contents
 Abstract
 Introduction
 Methods and Results
 Conclusions
 References
 Appendices
A: Figures 1 and 2
B: Figures 1 through 5

Stress, Dopamine, and Opiate Receptors
 Abstract
 Introduction
 Narrative
 Conclusions
 References
 Appendices

Abstract:
1. International Symposium on Nicotine: The Effects of Nicotine on Biological Systems II:
 Bienvenu B, Kiba H, Rao J, and Jayaraman A. Nicotine induced fos intensely in the
 parvocellular paraventricular nucleus and the lateral hypothalamus in rats.
Figures 1 and 2

"Vision, Laser Eye Injury, and Infectious Diseases"

Project Director: Herbert E. Kaufman, M.D.
 Roger Beuerman, Ph.D.

Participating Scientists: Claude A. Burgoyne, M.D.
 Emily Varnell

Mandi Conway, M.D.

Table of Contents
Abstract
A. Confocal Microscopy
B. Glaucoma, Traumatic and Non-traumatic
C. Herpes
Appendies

Manuscripts

2. Chew SJ, Beuerman RW, Kaufman HE (in press) Real-time confocal microscopy of keratocyte activity in wound-healing after cryoablation in rabbit corneas. *Scanning* 16.

TABLE OF CONTENTS FOR THIS VOLUME

"Role of Growth Factors and Cell Signaling in the Response of Brain and Retina to Injury"	21
Project Directors: Prescott Deininger, Ph.D. Nicolas G. Bazan, M.D., Ph.D.	
Participating Scientists: Julia Cook, Ph.D. Haydee E. P. Bazan, Ph.D. William C. Gordon, Ph.D. Elena Rodriguez De Turco, Ph.D. Victor Marcheselli, M.S.	
"Neuropathological responses in transgenic mice having growth factor receptors either depleted or overexpressed."	21
Table of Contents	24
Abstract	25
Introduction	26
Narrative	28
Conclusions	30
References	31

(continued on next page)

Role of Growth Factors and Cell Signaling in the Response of Brain and Retina to Injury (continued)	
Appendices	
Figure 1. A neuron-specific expression vector for the PDGF dominant negative mutant.	
Letter to Rick Huntress, Transgenic Services Coordinator, DNX Corporation	
Manuscript	
1.	Thompson HW, Cook JL, Nguyen D, Rosenbohm T, Beuerman RW, Kaufman HE (submitted) In vivo gene transfer to corneal epithelium by retroviral vector administration in eyedrops.
"The Trigeminal Ganglion as a Model to Study the Effects of Growth Factors in Nerve Repair and Regeneration" 64	
	Summary 65
	Introduction 66
	Methods 68
	Discussion 76
	References 80
"Pathophysiological Events Triggered During Light-induced Damage to the Retina" 89	
	Introduction 90
	References 115

"Protecting the Auditory System and Prevention of Hearing Problems"

Project Directors: Richard Bobbin, Ph.D.
Charles Berlin, Ph.D.

Participating Scientists: Sharon Kujawa, Ph.D.
Carlos ErosteGUI, M.D.
Douglas Webster, Ph.D.

Abstract	
Introduction	
Body	
Conclusions	
References	
Appendices	

Poster presented at the Acoustic Society of America: Kujawa SG, Fallon M, Bobbin RP (1994)
A suppressive "off-effect" in the f_2 - f_1 DPOAE response to continuous moderate level
primary stimulation.

Additional figures for the animals studies

Figures for the human studies

Manuscript: Berlin CI, Hood LJ, Hurley AH, Wen H, and Kemp DT (submitted) Binaural noise

Additional figures for the animals studies

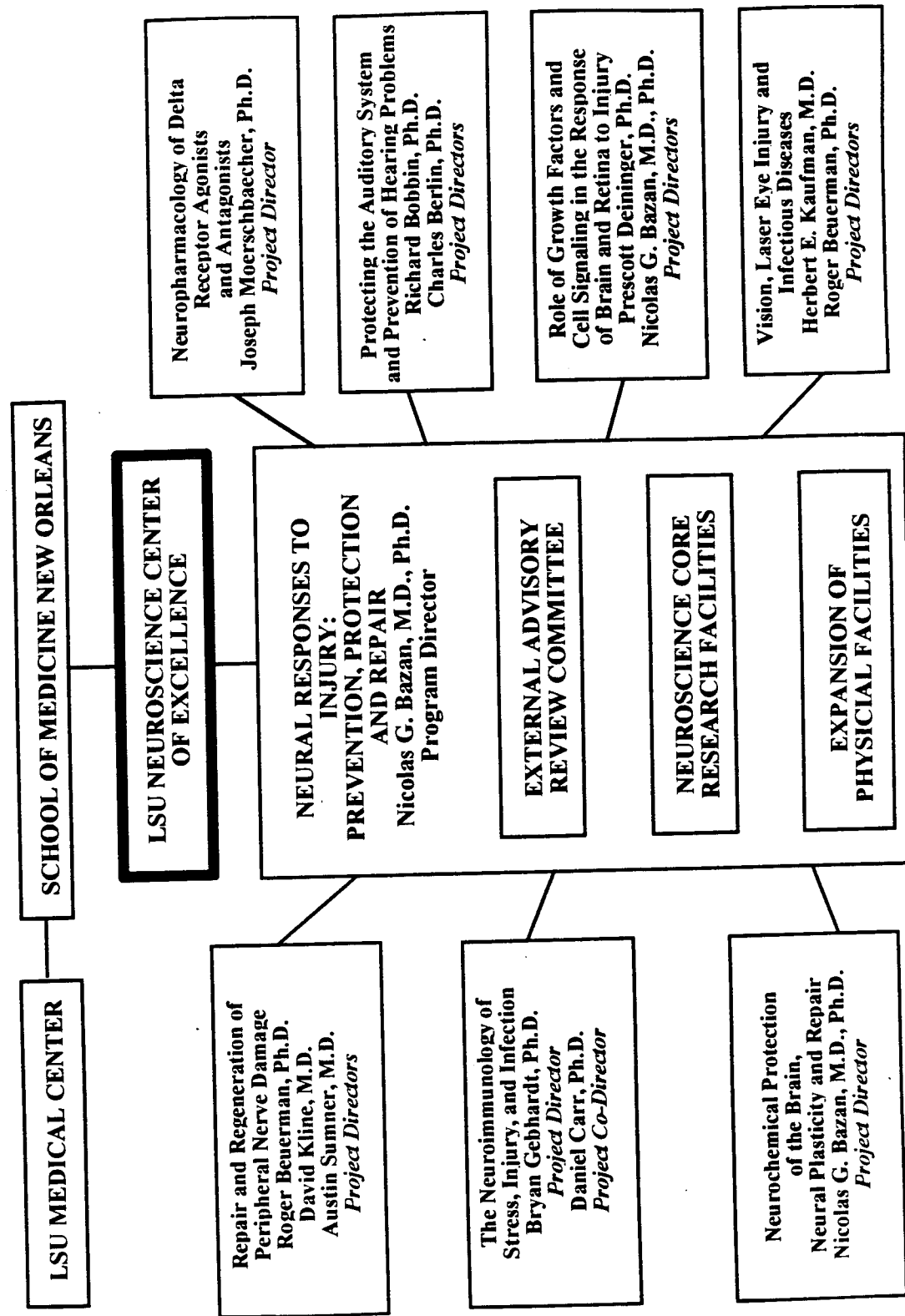
Figures for the human studies

Manuscript: Berlin CI, Hood LJ, Hurley AH, Wen H, and Kemp DT (submitted) Binaural noise suppression linear click-evoked otoacoustic emissions more than ipsilateral or contralateral noise.

Cooperative Agreement Between the US Army Medical Research and Development Command and

The LSU Neuroscience Center of Excellence

DAMD17-93-V-3013 20 September, 1993 - 19 October, 1997 \$13,860,000



SCHOOL OF MEDICINE IN NEW ORLEANS

Louisiana State University
Medical Center
2020 Gravier Street, Suite "B"
New Orleans, LA 70112-2234
Telephone: (504) 568-6700
Telefax: (504) 568-5801

Neuroscience Center
Office of the Director

19 October, 1994

Commander
U.S. Army Medical Research and Development Command (USAMRDC)
ATTN: SGRD-RMI-S
Fort Detrick
Frederick, MD 21702-5012

Re: Annual report, Cooperative Agreement No. DAMD17-93-V-3013
Neural Responses to Injury: Prevention, Protection, and Repair

Dear Sir,

Please find enclosed the original and five copies of the first annual report for the Cooperative Agreement, referenced above, between the USAMRDC and the Louisiana State University Medical Center School of Medicine, Neuroscience Center of Excellence. This report represents the research carried out during the first year of this agreement (20 September, 1993, to date). It is organized per project, each corresponding to a chapter of the original application.

In addition to the research conducted in the first year of this agreement, the planning for the two additional floors of research space which are to be added to the Lions/LSU Clinics Building, 2020 Gravier Street, New Orleans, LA, has been completed, including all specifications necessary for the start of bidding. Enclosed is one copy each of the program manual (1 vol.) and the project manual (3 vols.) which has been generated by Cimini, Meric and Duplantier, Architects and Planners, for bidding purposes. It should be noted that there will actually be three floors constructed in this one project, two as funded by this Cooperative Agreement and one which is funded by LSU to be used by the School of Medicine for other purposes.

As planned, I arranged to have three meetings between the LSU investigators and their counterparts in the Army to provide program briefings for the work that they were planning to conduct under this agreement as well as to exchange ideas and information of mutual interest. The agendas for each of these meetings are enclosed. These provided both the LSU scientists and those of the Army the opportunity to discuss the work being done, the direction, and the significance to problems of interest to the Department of Defense.

On 2 December, 1993, several of our investigators, excluding the Auditory and Laser/Vision groups, met at the Walter Reed Army Institute of Research, Washington, D.C., with Drs. Frank Tortella, Joseph Long, Mark DeCoster and Jit Dave. These discussions revolved around the neurochemical and neuropharmacological aspects of the program project and provided a forum for the Army scientists to begin interactions and exchange of information with our investigators.

On 31 January, 1994, the LSU auditory physiology group, represented by Drs. Charles Berlin and Richard Bobbin, and I met at Fort Rucker, AL, with Dr. Kent Kimball and Dr. Ben T. Mozo. These meetings involved presentations and discussions about the protection of the auditory system and prevention of hearing problems in humans.

The LSU investigators involved with the vision research, composed of Dr. Herbert Kaufman, Dr. Roger Beuerman and myself, met on 7 February, 1994, at Brooks Air Force Base, San Antonio, TX. These scientists and those of the Ocular Hazards Research Unit of the US Army Medical Research Detachment made presentations and conducted discussions focused on protection from, repair of, and prevention of laser injuries, specifically to the eye. Each of these information exchanges provided very useful direction and advice for the LSU investigators. These workshops will be conducted annually for the term of this agreement.

At the end of the first year of this program, as planned, I requested that two of the members of the External Advisory Committee of the LSU Neuroscience Center, Dr. Dennis W. Choi, Jones Professor and Head of the Department of Neurology, Washington University School of Medicine, and Dr. Fred Plum, Anne Parrish Titzell Professor and Chairman of the Department of Neurology, Cornell University Medical College, provide a critical review and a written report of the progress of the research accomplished under this Cooperative Agreement. Dr. Choi was given a copy of this annual report and subsequently made a site visit on 15 September, 1994, to the LSU Neuroscience Center. (The agenda for his meeting is attached.) At that time he met with a number of the investigators and administrators involved with whom he discussed many facets of the research being performed under this Agreement. His opinion of the work being done is attached.

Dr. Fred Plum made a site visit on 26 September, 1994, having also been provided previously with a copy of this annual report. He was also given the opportunity to examine the research and other progress made under this agreement and his written critique is also attached. Please note that, near the end of his letter (bottom of page two, first four paragraphs of page 5), Dr. Plum also included a description of projects not directly supported by the Cooperative Agreement but which are very positively impacted by any support of Neuroscience projects. The

Annual Report
DAMD17-93-V-3013
19 October, 1994
Page 3

reviewers were very complimentary of the positive consequences resulting from this support.

We are very pleased with the progress that has been made. We would like to thank you for the assistance you have given us. Please let me know if there is any further information that I can provide you.

Sincerely,



Nicolas G. Bazan, M.D., Ph.D.
Villere Professor of Ophthalmology,
Biochemistry and Molecular Biology,
and Neurology
Director, LSU Neuroscience Center

NGB/eh
enclosures

13

**JOINT WORKSHOP ON "NEURAL RESPONSES TO INJURY: PREVENTION,
PROTECTION AND REPAIR"**

*Sponsored by the LSU Neuroscience Center and Walter Reed Army
Institute of Research, Department of Medical Neurosciences*

December 2, 1993
Building 40, Room 2133

"Overview of LSU Program"	9:00
N. Bazan	
"Repair and Regeneration of Peripheral Nerve Damage"	9:20
R. Beuerman, D. Kline, J. England	
"The Neuroimmunology of Stress, Injury and Infection"	10:10
D. Carr	
Break	10:20
"Neurochemical Protection of the Brain, Neural Plasticity and Repair"	10:40
N. Bazan	
"Neuropharmacology of Delta Receptor Agonists and Antagonists"	11:15
J. Moerschbaeher	
"Stress and the Dopamine System"	11:45
J. Rao	
Box Lunch Served (\$2.00 each)	12:00
"Role of Growth Factors and Cell Signaling in the Response of Brain and Retina to Injury"	12:10
N. Bazan and J. Cook	
"An Overview of Neuropharmacology Research at WRAIR on Nervous System Injury and Protection"	13:00
Frank Tortella	
"Animal Models of Spinal Cord Injury and Mechanisms of Blood Flow Changes"	13:30
Joseph Long	
"Evaluation of Excitatory Amino Acids in Neuronal Cell Culture"	13:50
CPT DeCoster	
"Molecular Biology of Nervous System"	14:10
Jit Dave	
Overall Discussion	14:30
Adjourn	15:00

Joint Workshop on Neural Responses to Injury:
Prevention, Protection and Repair
Walter Reed Army Institute of Research, Dept. of Medical Neuroscience
U.S. Army Aeromedical Research Laboratory, Fort Rucker, AL
SCHEDULE FOR JANUARY 31, 1994

January 30

12:00 PM - depart New Orleans by car

Hotel: **Comfort Inn, 615 Boll Weevil Circle, Enterprise, AL 36330**
Tel. 205-393-2304, Fax. 205-347-5954

January 31

Visiting - **Dr. Kent Kimball, Director, Plans and Programs, USAARL**
Dr. Ben T. Mozo, Research Physicist, USAARL
Fort Rucker, AL 36362-5292
Tel. (205) 255-6917, Fax. (205) 255-6937

9:00 AM - Welcome
9:20 AM - Overview of LSU Program - **Nicolas G. Bazan**
9:45 AM - Protection the Auditory System and Prevention of Hearing Problem via Efferent
Activation in Humans - **Charles Berlin**
10:30 AM - Break
11:00 AM - Prevention of Hearing Problems in Animals - **Richard Bobbin**
12:00 PM - General Discussion and Lunch
13:00 PM - Adjourn

15

OCULAR HAZARDS RESEARCH
U.S. ARMY MEDICAL RESEARCH DETACHMENT
7914 A DRIVE (Bldg 176)
BROOKS AIR FORCE BASE, TEXAS 78235-5138

February 7, 1994

Leave New Orleans on Continental flight #1445 at 6:00 PM, arrive San Antonio on Continental flight #1120 at 8:53 PM.

Hyatt Regency San Antonio
123 Losoya St., San Antonio, TX 78205
Confirmation #HY0000605552

February 8, 1994

8:30 *Overview of USAMRD program*

Bruce Stuck, Director, USAMRD

8:45 *Review of Accidental Laser Exposures and Human Tissue Response*

Donald Gagliano, Commander, USAMRD

9:00 *Overview of LSU Program*

Nicolas G. Bazan, Director, LSU Neuroscience Center

9:10 *The Program: Vision, Laser Eye Injury, and Infectious Diseases*

Herbert Kaufman, Chairman, Ophthalmology Dept. LSU

10:00 *Confocal Approach to Cellular Reactions in Wound Healing and of the Lamina Cribrosa.*

Roger Beuerman of the LSU Neuroscience Center

10:30 **BREAK AND LAB TOUR**

10:50 *Neurochemical Protection of the Brain, Neural Plasticity, and Repair*

Nicolas Bazan, Director, LSU Neuroscience Center

11:40 *Basic Fibroblast Growth Factor (bFGF) Treatment of Laser-Injured Retina*

Steven T. Schuschereba, Chief, Biology Section, USAMRD

12:10 *Role of Growth Factors and Cell Signaling in the Response of Brain and Retina to Injury: Focus on the Retina*

Nicolas Bazan, Director, LSU Neuroscience Center

12:50 **LUNCH**

2:50 Depart San Antonio on Southwest flight #803

5:55 Arrive New Orleans on Southwest flight #1055

**LETTERS FROM MEMBERS OF THE
EXTERNAL ADVISORY COMMITTEE**

17

**WASHINGTON
UNIVERSITY
SCHOOL OF
MEDICINE**
AT WASHINGTON UNIVERSITY MEDICAL CENTER

NEUROLOGY

Dennis W. Choi, M.D., Ph.D.

Andrew B. and Gretchen P. Jones Professor and Head
Neurologist-in-Chief, Barnes Hospital

October 17, 1994

Nicholas G. Bazan, MD, PhD
Director, LSU Neuroscience Center
School of Medicine in New Orleans
Louisiana State University Medical Center
2020 Gravier Street, Suite "B"
New Orleans, LA 70112-2234

Dear Nick:

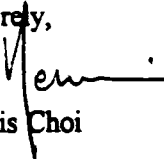
Thank you for the invitation to visit LSU on September 15 and review early progress made under the LSU Neuroscience Center of Excellence Cooperative Agreement with the U.S. Army Medical Research and Development Command.

You have assembled an impressive array of faculty researchers to study diverse aspects of nervous system injury. Overall, I find the individual projects to be thoughtful and well chosen. With you as director, I am sure that they will be most ably integrated. Your project 3 "Neurochemical Protection of the Brain, Neuroplasticity and Repair" is in my view the clear focal point of the overall program. The identification of new PAF antagonist drugs capable of regulating excitatory synaptic transmission and excitotoxic central nervous system injury, is an attractive and attainable goal. The novel pharmacology theme is also well developed in Dr. Moerschbaecher's Section 4 "Neuropharmacology of Delta Receptor Agonist and Antagonist". Involvement of clinician-investigators in clinical departments, such as Dr. Sumner in Project 1 or Dr. Kaufman in Project 5 are strengths of the program that will enhance its ability to identify human therapeutic interventions.

Progress in the first months of operation appears to be on target. Substantial synergy can be expected between the research programs specifically outlined in this collaborative agreement, and the larger intellectual framework formed the LSU Neuroscience Center of Excellence. Your role as director of both efforts is a vital feature that will ensure maximization of this synergy. In summary, I am most enthusiastic about this LSU-U.S. Army Cooperative Agreement, both for its specific merit and as a prototype mechanism for facilitating effective collaboration between academic and military institutions.

Best regards.

Sincerely,


Dennis Choi

Box 8111

660 South Euclid Avenue

St. Louis, Missouri 63110

(314) 362-7175 • FAX (314) 362-2826

THE NEW YORK HOSPITAL-CORNELL MEDICAL CENTER

FRED PLUM, M.D., CHAIRMAN
 ANNE PARRISH TITZELL, PROFESSOR OF NEUROLOGY
 CORNELL UNIVERSITY MEDICAL COLLEGE
 NEUROLOGIST-IN-CHIEF
 THE NEW YORK HOSPITAL-CORNELL MEDICAL CENTER
 (212) 746-6141
 FAX (212) 746-8532

September 28, 1994

Nicholas G. Bazan, M.D., Ph.D.
 LSU Neuroscience Center
 2020 Gravier Street
 Suite B
 New Orleans, LA 70112-2234

Dear Dr. Bazan:

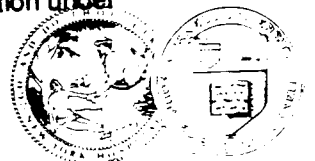
I am pleased to submit this reviewer's report of a Cooperative Agreement between the LSU Neuroscience Center and the US Department of the Army entitled, "Neural Response to Injury: Prevention, Protection and Repair" (henceforth designated as "Injury Study"). The agreement will span four years of effort by the LSU Center; this report describes progress obtained during its first year, extending from September 1, 1993 to August 31, 1994.

Nicholas G. Bazan, M.D., Ph.D. both directs the LSU Neuroscience Center of Excellence and serves as the Program Director of the Injury Study. In addition to Dr. Bazan's personal investigative efforts, seven additional study groups are engaged in research directly related to the Injury Study, as indicated in the administrative diagram attached to this report.

Dr. Bazan's outstanding personal and scientific qualities are the two most important factors in assuring the future success of the LSU-U.S. Army Cooperative Agreement. His leadership and intellectual "taste", as well as his joy in and dedication to brain science penetrate every aspect of the LSU Neuroscience Institute. His enthusiasm has spread to infect his colleagues and many other departments of the Medical School with his high scientific standards and integrity. His knowledge suffuses every dimension of basic neuroscience. His diplomacy and gentle handling of his staff creates their huge loyalty. His energy is contagious. Furthermore, he has the wonderful quality of scientific generosity: always ready to help and encourage others, he is entirely responsible for the continuously improving quality of young persons who are coming to LSU to learn and do important neuroscience.

In addition to the above, Dr. Bazan's specific research is internationally recognized as being of the highest caliber. His personal research contributions to the Injury Study during the past year reflects these high qualities in several ways. They have been published in the most competitively prestigious biomedical research journals. They also add new understandings to both the normal and potentially abnormal effects of the platelet-activating factor (PAF). PAF already is known to be a potent mediator of inflammatory and immune responses. What Bazan and his team now have found is that in low concentrations, PAF transmission may enhance memory and repair mechanisms in brain. Alternately, if released in excessively large concentrations or in combination with certain other molecules, PAF appears capable of causing immune-related tissue damage such as occurs with intense inflammation and/or the induction of genetic prostaglandin synthesis, a step that also may injure brain tissue. This fundamental research emphasizes the complexity and often bidirectional responses that may occur when injury strikes the brain. The results are important and illustrate the difficulties which must be overcome in establishing prevention, protection and repair of brain injuries.

Drs. Bazan and Prescott Delninger have succeeded in developing a series of transgenic mice expressing a dominant mutant of platelet derived growth factor (PDGF). Remarkably enough, the animals thus far have shown no major behavioral alteration under



19

normal developmental conditions. Their reaction to ischemia, seizures and other circumstances has not yet been tested.

Let me turn now to some of the other, supporting projects: **Drs. R. Benerman, D. Kline and A. Sumner** have made good progress in their studies of neurotrophic factors and other mechanisms in human and experimental neuromas resulting from blunt and crush nerve injuries. Basic fibroblast growth factor (bFGF) was the most prominent factor found in human post-nerve injury neuromas with other specific factors either absent or reaching only very low levels of concentration. More precisely analytic experiments await the analyses of fresh neuronal material from the experimental preparations.

Drs. Herbert Kaufman and Roger Benerman have made brilliant advances using confocal microscopy to examine the cellular details of the human retina. To a degree never before possible they have safely demonstrated in awake human subjects the acute pathophysiology of laser injuries to cornea and their early transformation into fibroblasts. Detailed identification of anterior chamber cells has been possible and current efforts are underway to examine at great magnification the optic disc itself. Ocular fungus and herpes infections can be identified immediately and without introducing foreign substances against the cornea or into the eye. Application of the tool should have an important place in clinically applied military medicine.

During the past year, the investigators also have pursued their earlier discovery that ambient chilling of monkeys latently infected with H. Simplex induces an acute recurrence of cutaneous herpes. Furthermore, chronic ingestion of the beta blocker, propranolol, has been found to ameliorate or prevent the active recurrence. Clinical trials of this important discovery must be pursued as it has important practical aspects.

During the year, the necessary work to establish and equip the glaucoma research laboratory was undertaken. Next year's report can be expected to provide research results from that laboratory.

Dr. Joseph Moerschbaeher and his colleagues in pharmacology have initiated preliminary studies on the influence of delta opoid agonists-antagonists on learning and antinociception. Somewhat surprisingly, the agent damps the CO₂ response of breathing but has no antinociceptive effect. The same investigator is analyzing how anxiogenic drugs affect dopamine neurons in the ventral tegmental area of the rodent brain.

In another preliminary approach, **Drs. H.W. Thompson et al** have initiated experiments passing retroviral gene carriers into the eye with externally applied eye drops, thereby developing a new approach to deliver protection against certain ophthalmologic infections or enhancing the potential success of corneal transplant.

Drs. Richard Bobbin and Charles Berlin, thanks to the DOD grant, have added an excellent postdoctoral student as well as important new equipment to their laboratory. The laboratory's principal subject of interest is to find mechanisms for preventing the audiologic damage produced by intense sound. In guinea pigs, this has been achieved by stimulating calcium-dependent mechanisms in cochlear neurons. In another study, the laboratory has found in human studies that during the delivery of loud, binaural sounds, men and women suppress the noise in opposite sided ears from each other.

The above individual achievements provide only a part of the considerable effort, enthusiasm and success that the U.S. Army grant has brought to the LSU Neuroscience Center of Excellence (NCE). The following steps forward can also be emphasized:

- 1) Morale in the LSU-NCE rides at high pitch, encouraging scientific collaboration and the generation of new ideas.

- 2) Funds have been granted to subsidize the necessary equipment and technical personnel to establish a brain bank. Presently, approximately 50 specimens are available in storage with the Center holding good clinical records of the preterminal illness.
- 3) A program of "starter" grants designed to assist young investigators in conducting merit-deserving, self designed research projects has been initiated.
- 4) A highly popular state-wide Graduate School outreach summer program has been successfully concluded, attracting a strong interest in neuroscience among gifted college students.
- 5) An interdisciplinary graduate program in neuroscience was initiated and strongly encouraged by the faculty during 1993-94. As a result, nearly all of the graduate students (including the new entering class) are of very good quality. Indeed, other participating departments say that the Neuroscience graduate students are the best among the LSU biological sciences programs.

Summary. Under the generous auspices of a U.S. Army Cooperative Agreement, the LSU Neuroscience Center of Excellence is not only thriving but headed for far greater future productivity than at any time in the past. The admirable success of the program depends heavily on the foresight, intelligence, creativity and energy of two outstanding scientists, Herbert Kaufman and, especially, Nicholas G. Bazan. Their achievements and those of their colleagues totally warrant continuation of support. Indeed, every indication is that their extramural, non-Army support will continue to grow, making the program stronger and stronger as the years elapse.

One serious problem remains - that of sufficient space in which to do the studies that Dr. Bazan and his colleagues already have conceived so well. Prompt attention to and effective application of must be given to the DOD funds already awarded to construct new research space which will greatly increase the LSU Neuroscience team's opportunities for creative discovery.

I and my colleagues on the External Advisory Board of the LSU Neuroscience Center of Excellence strongly endorse the quality and number of achievements that have come from the U.S. Army-LSU-NCE collaboration. Thanks to strong leadership for the Center and a high degree of internally high morale and interdependence within the Center, it can be anticipated that the Cooperative Agreement will have a major impact on national neuroscience research as well as the specific medical needs of the U.S. Army.

Sincerely,



Fred Plum, M.D.

FP/moc

NEUROCHEMICAL PROTECTION OF THE BRAIN, NEURAL PLASTICITY AND REPAIR

Transgenic mice having growth factors either depleted or overexpressed.

The trigeminal ganglion as a model to study the effects of growth factors in nerve repair and regeneration.

Pathological events triggered during light-induced damage to the retina.

Project Directors:

Prescott Deininger, PhD

Nicolas G. Bazan, M.D., Ph.D.

Participating Scientists:

William C Gordon, PhD

Elena B Rodriguez de Turco, PhD

Haydee EP Bazan, PhD

Julia Cook, PhD

Victor Marcheselli, MS

FOREWARD

Opinions, interpretations, conclusions and recommendations are those of the author and are not necessarily endorsed by the U.S. Army.

(✓) Where copyrighted material is quoted, permission has been obtained to use such material.


(✓) Where material from documents designated for limited distribution is quoted, permission has been obtained to use the material.

(PB) Citations of commercial organizations and trade names in this report do not constitute an official Department of the Army endorsement or approval of the products or services of these organizations.

(PB) In conducting research using animals, the investigator(s) adhered to the "Guide for the Care and Use of Laboratory Animals," prepared by the Committee on Care and Use of Laboratory Animals of the Institute of Laboratory Resources Commission on Life Science, National Research Council (NIH Publication no. 86-23, Revised 1985).

(✓) For the protection of human subjects, the investigator(s) have adhered to policies of applicable Federal Law 45 CFR 46.

(PB) In conducting research utilizing recombinant DNA technology, the investigator(s) adhered to current guidelines promulgated by the National Institutes of Health.

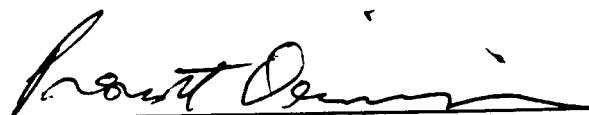

Investigator Signature

ANIMAL USE
20 SEPTEMBER, 1993, THROUGH JULY, 1994

DAMD17-93-V-3013

The experimental animals used during this period for the project, Neural Responses to Injury: Prevention, Protection, and Repair, **Subproject: Role of Growth Factors and Cell Signaling in the Response of Brain and Retina to Injury**, are as follows:

Species	Number Allowed	Number Used	LSU IACUC #
mice	1260	70	1034


 Investigator Signature

4. Table of Contents:

Front Cover	1
Forward	2
Animal Usage	3
Table of Contents	4
Abstract	5
Introduction	6
Body	8
Conclusion	10
References	11
Appendix Materials	
• Map of recombinant construct	12
• Submission to DNX	13
• Manuscript	17

5. Abstract:

Our goal is an understanding of the role of specific growth factors and cytokines on development and wound healing in the central nervous system (CNS). We have initially focussed on platelet derived growth factor (PDGF) by developing a series of transgenic mice expressing a dominant negative mutant of PDGF which should produce greatly lowered levels of this growth factor in neurons. A great deal of effort has been put into making the recombinant DNA construct in a manner that will allow us to readily assay its expression and effectiveness in the transgenic mice. We are now prepared to measure the effectiveness of the dominant negative mutant in the ten transgenic mice we have generated and to assess the affect of this lowered PDGF levels on CNS development and response of the CNS to injury models. These mice will be studied, along with normal mice, for general characteristics in their ability to respond to injury, as well as an assessment of the expression of other growth factors that might influence wounding or be altered by changes in PDGF expression.

6. Introduction:

This project addresses the identification of growth factors, differentiation factors, neurotrophic factors and corresponding receptors that are involved in wound healing events in the CNS and eye. We propose to use two different methods to study the roles of these different factors in wounding healing.

First, using the injury models described in our original application, we will screen for changes in mRNA levels of nerve growth factor, platelet-derived growth factor (PDGF) A and B forms, ciliary neurotrophic factor, basic and acidic fibroblast growth factors, insulin, insulin-like growth factors, glial fibrillary acidic protein, brain-derived neurotrophic factor, and corresponding receptors. We have revised our original methodology to employ a procedure which will permit us to simultaneously screen many mRNAs (1). In this method, expression patterns of a hundred or more different genes can be examined from a single 10 μ g RNA sample. Specifically, RNA will be isolated from control tissue and from tissue immediately after injury or at various time points following injury. The RNA samples will be reverse transcribed into DNA using oligo (dT) primers and then complementary strands of DNA will be synthesized using 32 P-dCTP, random hexamers and klenow. The 32 P-ds cDNA will then be hybridized to filter bound probes for the various genes of interest. Control clones such as GAPDH, G6PD, and actin (RNA levels of which are not expected to change during wounding and wound healing) will be included to standardize for "between sample" differences in reverse transcription and cDNA synthesis. Autoradiography and densitometry will be performed to quantify changes. We had initially proposed to use quantitative reverse transcription/polymerase chain reaction to examine mRNA levels for each gene individually (a truly arduous task). We think that our current strategy represents a monumental improvement.

Second, we propose to study the roles of growth factors *in vivo* using transgenic mouse models. We have made considerable progress in this particular specific aim during

the past year. We have focused our first efforts on platelet-derived growth factor which is proposed to have important roles in the brain in normal development and in wound healing. Based on *in vitro* data, PDGF is believed to be the major mitogen responsible for clonal expansion of precursor cells which differentiate into oligodendrocytes. A deficiency of CNS PDGF *in vivo*, therefore, might lead to neurological abnormalities characteristic of hypomyelination. Secondly, PDGF has a putative role in wound healing. Therefore, PDGF deficiencies might affect the ability of these transgenic mice to heal following CNS injury. This has implications for the use of growth factors or growth factor-encoding genes in the treatment of CNS injury.

While it was not a subject of the specific goals proposed in our portion of the DOD proposal, we have included in the appendix, a related manuscript (to be submitted to Gene Therapy). In this paper, we examine the expression of genes delivered (in retroviral vectors) to rabbit corneal epithelium and stroma by eyedrop application and to endothelium by anterior chamber injection. We also examine the efficacy of gene introduction to human corneas in eyebank transplantation medium. We include this paper so that the reviewer will understand that we are developing techniques related to gene therapy of the eye and CNS. Identification of the growth and neurotrophic factors which augment wound healing will precede the development of genetic therapies.

7. Body:

a) Preparation of a Dominant Negative Mutant Expression Construct:

The first step in the generation of mice deficient in neuron-derived PDGF involved the construction of an expression construct encoding a dominant negative mutant (DNM) of PDGF. Specifically, we prepared a construct in which expression of the 1308 DNM is regulated by the neuron-specific enolase (NSE) promoter. For preparation of the promoter, the NSElacZ plasmid (2) was digested with Eco RI and Hind III, end-filled, and electrophoresed on an agarose gel. The 1800 bp fragment was eluted. For vector preparation, the adenovirus late promoter/enhancer of pMT2 was removed by digestion with Dra II to generate pMT2/ Δ Dra. Dra II-digested pMT2 was phosphatased, endfilled and electrophoresed on a 1% gel. The vector was isolated free of the 1168 bp Dra II fragment. This vector (pMT2/ Δ Dra) was then ligated to insert (promoter). The promoter orientation was determined using XhoI/Hind III. This expression construct is called NSE/pMT2 Δ Dra and should direct expression specifically to CNS neurons (as does NSElacZ).

Next, the 1308 PDGF DNM was ligated into the NSE/pMT2 Δ Dra. Specifically, the 1308/Bluescript clone (3) was digested with Eco RI, electrophoresed on a 1% gel, and the 1 kb PDGF DNM was electroeluted. NSE/pMT2 Δ Dra was digested with Eco RI and phosphatased. The insert was ligated to vector and orientation determined using Hind III. This plasmid is called NSE/pMT2 Δ Dra/PDGF₁₃₀₈.

Finally, a small fragment of the luciferase gene was inserted into the DHFR portion of pMT2 to permit easy identification of expressed transgene-derived mRNA. This fragment was removed from pXP2 (4) using Xba I/Eco RI, end-filled, and ligated into Afl II site of NSE/pMT2 Δ Dra/PDGF₁₃₀₈ to generate NSE/pMT2 Δ Dra/PDGF₁₃₀₈/luc (7301 bp in length, see appendix Figure 1).

Procaryotic or plasmid sequences have been found in some instances to negatively impact expression of transgenes. Therefore, generally every attempt is made to reduce or eliminate these sequences prior to microinjection of the transgenes into animals. NSE/pMT2 Δ Dra/PDGF1308/luc was digested with Bam HI/Ssp I to generate fragments of 4817, 2021 and 463 bp. The 4817 bp fragment was isolated by gel electrophoresis, purified on Elutip-D spin columns and quantified by ETBr staining of DNA electrophoresed in parallel with known standards. This DNA was supplied to DNX (Princeton NJ) on 5/24/94 for microinjection into recipient mice.

Also supplied to DNX were PCR amplification primers designed to differentiate transgenic from non-transgenic mice. Primers Amp 5 and Amp 6 are of sequence 5'-CAGAGAACTTGAAAGCATCTTCCTG-3' and 5'-GACTTATTGAACAACCGGAATTGGC-3' and hybridize to the DHFR cDNA in the transgene construct to generate a 300 bp amplification product. In contrast, PCR of endogenous genomic DNA with these primers generates a product in excess of 6 kb (due to intervening introns). These primers will permit technical personnel at DNX to identify founder transgenic mice and ship these to us.

Upon receipt of the animals, which we expect within 2 weeks, we will confirm their transgenic status using PCR. They will then be monitored for any phenotypic deviations from wild-type and assayed for expression of the transgene in brain and control tissues (lung, liver, gonads, muscle, kidney, spleen, and eye). Amp 5 and Amp 6 PCR primers will not be useful in detecting expression. They are unable to differentiate RNA from the transgene cDNA. Therefore, we will use PCR primers designed to hybridize to and amplify the luciferase fragment within the transgene. In this expression vector the PDGF 1308 is expressed as a chimeric mRNA with DHFR (and consequently luciferase). In the appendix we have included copies of materials sent to DNX early this year. These include 1) a letter describing the plasmid, 2) DNA fragment information, 3) PCR analysis information and 4) a map of the construct.

8. Conclusion:

According to Rick Huntress at DNX, they have had 52 young mice born following egg injection with our mutant PDGF construct. This resulted in ten founder mice carrying the dominant negative PDGF transgene. This is very close to the expected percentage of transgenics in such an experiment and indicates that the transgene has not produced any strong lethal effects on the animals. We should be receiving transgenic mice within one-two weeks. If any of these mice or their homozygous offspring have a visible phenotype, we will proceed with examination of tissue-specificity of expression, cell-type specificity of expression, gross brain morphology, visual evoked potentials and auditory evoked potentials. They will also be assessed with respect to their response to CNS injury. Even if the mice display no obvious phenotype, they will be examined with regard to gene expression in the CNS (to ensure that the transgene is being expressed) and response to injury. We will assess the results of this first transgene before making modifications to generate further transgenic models.

The preparation of the transgene construct has been very tedious and has limited the time devoted to the growth factor panel screening model but we plan to devote a major effort to this second project within the next year. This process will also be most efficient if carried out simultaneously with normal and transgenic mice.

9. References

1. Chalifour, L. E., R. Fahmy, E.L. Holder, E.W. Hutchinson, C.K. Osterland, H.M. Schipper and E. Wang. 1994. A method for analysis of gene expression patterns. *Anal. Biochem.* 216:299-304.
2. Sonja F.-P., P.E. Danielson, S. Catsicas, E. Battenberg, J. Price, M. Nerenberg and J.G. Sutcliffe. 1990. Transgenic mice expressing β -galactosidase in mature neurons under neuron-specific enolase promoter control. *Neuron* 5:187-197.
3. Mercola, M., P.L. Deininger, S.M. Shamah, J. Porter, C. Wang and C.D. Stiles. 1990. Dominant-negative mutants of a platelet-derived growth factor gene. *Genes & Dev.* 4:2333-2341.
4. Nordeen, S.K. 1988. Luciferase reporter gene vectors for analysis of promoters and enhancers. *BioTechniques* 6:454-457.

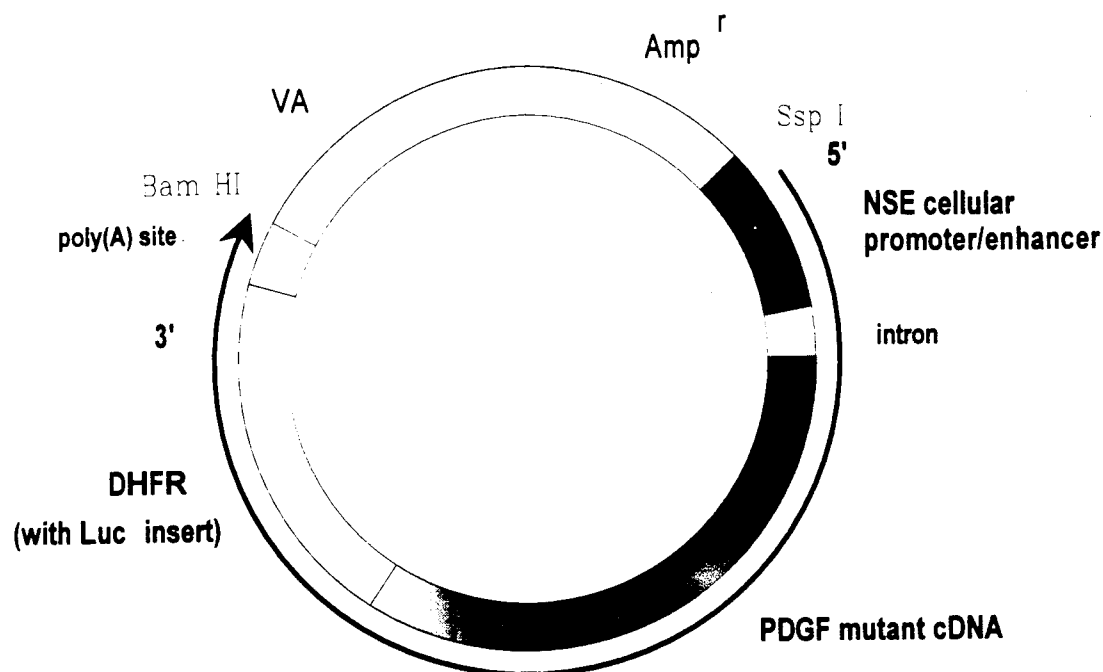


Figure 1. A neuron-specific expression vector for the PDGF dominant negative mutant. This vector was modified from the pMT2 expression vector. The neuron-specific enolase promoter/enhancer region is ligated upstream of a chimeric set of SV40 donor/acceptor splice junctions that allow splicing of the expressed RNA. The full length PDGF cDNA is inserted so that the initiator ATG represents the first ATG of the RNA produced. DHFR cDNA sequences have been left in the vector from the original pMT2 vector and generally provide some stabilization of otherwise short-lived mRNAs. The translation product will initiate at the first ATG in the PDGF A chain cDNA and terminate at the normal A chain termination signal and therefore will form normal PDGF (not a chimera with the DHFR). The poly(A) addition site is provided by the double SV40 poly (A) site. The VA RNA genes are irrelevant to this particular construct. Cleavage with *Bam* HI and *Ssp* I permits removal of the relevant portions of the expression cassette from the plasmid sequences.

ALTON OCHSNER
MEDICAL FOUNDATION
1516 Jefferson Highway
New Orleans, Louisiana 70121
Phone: 504 838-3000
Fax: 504 837-0977
Cable Address: OCHSCLINIC

Ochsner

Rick Huntress, Transgenic Services Coordinator
DNX Corporate Headquarters
303B College Road East
Princeton, New Jersey 08540

February 22, 1994

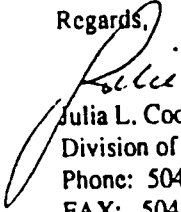
Dear Rick:

We have assembled a plasmid within which an expression construct for a PDGF dominant negative mutant (1) exists. The promoter is from the neuron-specific enolase gene and should direct expression to neuronal tissue (2). In previous transgenic mice, this promoter lead to specific expression of a regulated β -galactosidase gene in CNS neurons (2). Since the expression construct is assembled in the plasmid, pMT2, the mRNA is expressed as a fusion construct of PDGF-DHFR (mouse dihydrofolate reductase cDNA) (3). We have constructed our primers to the DHFR portion of the transgene. The primers can amplify the transgene to produce a 300 bp product. The primers can also amplify endogenous genomic DNA but will produce a >6 kb fragment. We have had no problems with amplification of the endogenous genomic DNA (no visible high MW band and no obvious competition with the transgene for primer binding). The transgene fragment has been prepared according to your specifications and has been purified free of most plasmid sequences by digestion with Bam III and Ssp I. The fragment is 4817 bp in length and a circular map is provided. The gene will produce no infectious condition which could be harmful to other animals, humans or the environment and experimentation involving the gene does not require containment conditions greater than those required under NIH RAC BL-2 standards.

We are providing you with purified transgene (200 ng/ul) and PCR primers (20uM). In addition, we are providing photographs and related information regarding quantification and PCR amplification of the fragment. Please contact me if I can provide additional information or if I can answer any questions. Thanks very much, Rick.

- 1) Mercola, M., Deininger, P. L., Shamah, S. M., Porter, J., Wang, C. and Stiles, C. D. 1990. Dominant-negative mutants of a platelet-derived growth factor gene. *Genes and Devel.* 4:2333-2341.
- 2) Forss-Petter, S., Danielson, P. E., Catsicas, S., Battenberg, E., Price, J., Nerenberg, M., and Sutcliffe, J. G. 1990. Transgenic mice expressing β -galactosidase in mature neurons under neuron-specific enolase promoter control. *Neuron* 5:187-197.
- 3) In Molecular Cloning: A Laboratory Manual, eds, Sambrook, Fritsch, Maniatis, Cold Spring Harbor Laboratory Press, 1989.

Regards,


Julia L. Cook
Division of Research
Phone: 504-842-3316
FAX: 504-842-3381

DNX**DNA FRAGMENT INFORMATION**Investigator Name: Julia L. CookInstitution: Ochsner Medical FoundationAddress: Molecular Genetics, Research Division1516 Jefferson Hwy. LA 70121Phone#: (504) 842-3316 Fax #: (504) 8 - 3381DNA Fragment Name: NSE/PDGFR308 (NSE/pMT2ΔDra/PDGFR308/Luc)Total DNA Fragment Length: 4817bp

DNA Fragment Purified By (check one):

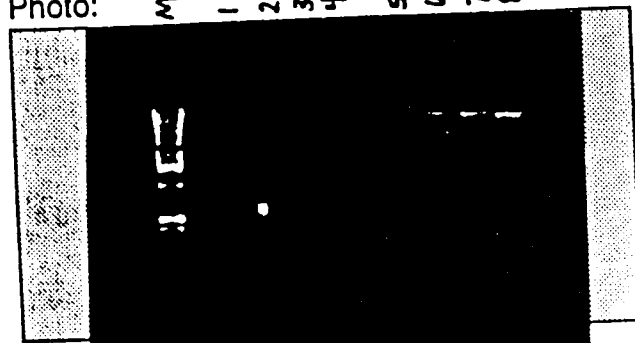
ELUTIP-D (Schleicher & Schuell) XXQiagen Column (Qiagen, Inc.) Other (Prior consultation with DNX required) Please describe:

DNA Fragment Stock Concentration:

200 ng/μl

DNA fragment should be dissolved in 10mM Tris/0.25mM EDTA, pH 7.5. A photo of the fragment on an agarose gel with the appropriate size and quantitative markers is required.

Photo:



Comments:

Marker - 1 kb ladder
1-4 = Control, 10-50ng respectively.
5-8 = 1, 2, 4 and 5, 1μl of dilute transgene.
1 μl dilute transgene (1/5) = 40ng
40ng · 5 (diln factor) = 200ng/μl
(conc. of transgene)

NTDF

PCR ANALYSIS

If PCR analysis is to be used to identify transgenic mice, NTDF requires appropriate oligonucleotides and a specification of proven conditions for the reaction. If necessary, NTDF will provide endogenous mouse DNA for evaluating oligonucleotide performance. Completion of the following information is required. Include photographs of the primer and photographs of the requested controls (originals or quality copies).

If these criteria are not met, all remaining DNA materials will be returned to the investigator with explanation and documentation and NTDF shall not be obligated to proceed further.

5' Primer name: Amp 6 3' Primer name: Amp 5
 Length: 25 nt Length: 25 nt
 Molar Concentration of Stock: 20 μ M Molar Concentration of Stock: 20 μ M

Reaction Conditions

All primers must be tested prior to submission. Controls should include:

1. Normal mouse DNA (NM)
2. NM + 1 gene copy/cell equivalent of the DNA fragment
3. NM + 5 gene copy/cell equivalent of the DNA fragment
4. NM + 10 gene copy/cell equivalent of the DNA fragment
5. 1 gene copy/cell equivalent of the DNA fragment alone
6. 5 gene copy/cell equivalent of the DNA fragment alone
7. DNA from a donor of same species as the DNA fragment (if applicable)

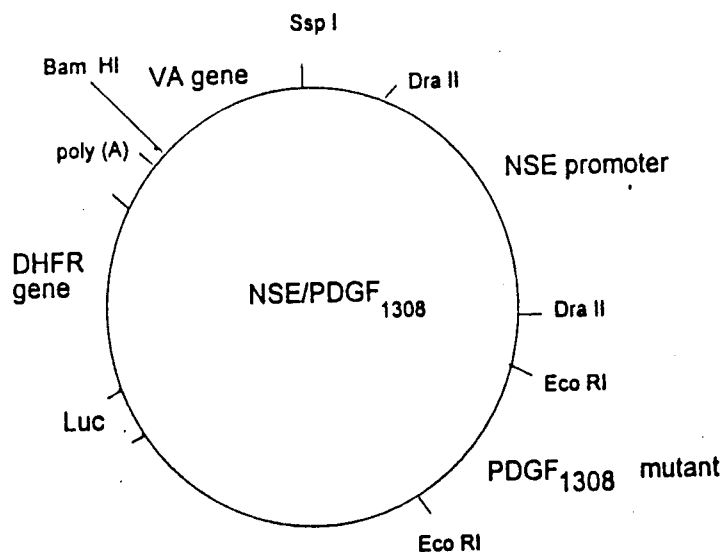
Primer Concentration in Reaction: 0.5 μ M
 Template concentration in the Reaction: 1-10 μ g/ml

Denaturing Temp: 94°C Denaturing Time: 1'5"
 Annealing Temp: 55°C Annealing Time: 1'5"
 Extension Temp: 72°C Extension Time: 2'5"

of Cycles: 35

Please include a copy of the results (original or quality copy).





Luc is 540 bp Xba I/ Eco RI frgmt from pKP2 (end-filled)
ligated into AflII site of pMT2.

$NSE/PDGF_{1308} = (NSE/pMT2 \Delta Dra / PDGF_{1308} / luc)$
is a total of 7301 bp.

The transgenic frgmt:

Cut $NSE/PDGF_{1308}$ with Bam HI/ Ssp I
to generate a 4817 bp transg. frgmt.

In Vivo Gene Transfer to Corneal Epithelium by Retroviral Vector
Administration in Eyedrops.

Hilary W. Thompson, Ph.D., Julia L. Cook, Ph.D.*, Doan
Nguyen, Trisha Rosenbohm *, Roger W. Beuerman, Ph.D., Herbert E.
Kaufman. M.D..

L.S.U. Eye Center Lions Eye Research Laboratories and
Laboratory of the Molecular Biology of the Ocular Surface,
Division of Research, Alton Ochsner Medical Institutions*, New
Orleans, LA.

Corresponding Author: RWB.

Submitted to: *Gene Therapy*.

SUMMARY.

The cornea of the eye can undergo wounding, infectious ulceration, scarring and loss of transparency as a result of its exposed position. The cornea is the site of refractive surgery that is reduced in effectiveness when over-exuberant healing causes regression. Failure of healing or over-exuberant healing lead to common pathologies of the cornea including reluctant healing of ulceration, loss of transparency, graft failure and regression after refractive surgery. All of these processes are potential targets for genetic manipulation if a means of delivery of genes to corneal tissues, especially the mitotically active fraction of the tissues, can be developed. Gene delivery from solution could also have a positive impact on the success of corneal transplantation if gene expression in donor corneas could be manipulated to enhance the success of transplantation by vector addition to eyebank media. The results presented here indicate that retroviral vector delivery and gene expression are feasible with vector administration in eyedrops or in eyebank media. Wounding of epithelium causes vector uptake and expression in vivo, as well as uptake and expression in endothelium of human donor corneas.

INTRODUCTION.

The epithelium and endothelial tissues of the cornea, bathed by tears and isolated from direct blood perfusion, are an ideal candidate tissue for *in vivo* genetic manipulation. Several recent publications have presented data that show the feasibility of gene delivery to tissues of the anterior segment [1-3].

As pointed out in a recent comment [4] different viral-derived vectors have proclivities for infecting interphase cells or mitotic cells; the use of retroviral vectors should allow specific administration of genetic material to dividing cells. The herpes virus or adenovirus-derived vectors applied to deliver genes to the anterior segment target non-dividing cells as well. However, since cell division is correlated with important ocular events such as reepithelialization of the corneal surface following wound healing [5] or proliferation of stromal keratocytes after refractive surgery [6], retroviral vectors could be used to target mitotically active cells in gene therapy of eye tissue.

Historically, the most serious concern encountered when using RVVs was that the helper genome (encoding the components of the virion particle and the reverse transcriptase) and the vector genome (encoding the protein of interest) could recombine through homologous sequences to generate replication competent virus. However, site-directed mutagenesis has been used to generate RVV genomes which, upon homologous recombination, inactivate the helper virus [7]. These vectors have been approved for use in human clinical protocols and thus far have shown no recombination

THOMPSON et al. In vivo gene transfer eyedrops 4
to generate replication-competent virus.

Genetic diseases such as forms of retinitis pigmentosa, in which a specific genetic defect is known, are most often discussed as targets for ophthalmic gene therapy [8]. Alternatively, our demonstration that genes can be delivered to mitotically active cells by topical administration to ocular tissues, suggests the use of exogenous genes in a pharmacologic manner rather than in targeting genetic defects.

Direct transfection of mitotic cells in vivo provides a simple direct means of producing a subgroup of recombinant cells in ocular tissue, and since the mitotic cells have an active role in wound healing and scar formation [9], this technique provides the means to explore pathologic mechanisms and intervene therapeutically at the genetic level in the eye.

Development of genetic manipulation in corneal tissues will have monumental impact since corneal transplantation is the most commonly performed organ transplant and much research is devoted to improving the preservation techniques of the human donor material. Among the possible target tissues for ocular gene therapy: corneal epithelium, stromal keratocytes, and corneal endothelium, we demonstrate that either topical administration in eyedrops, anterior chamber injection, or addition to eyebank media are effective routes for selectively targeting mitotically active cells for vector uptake and transgene expression, or in the case of adult endothelium, cells stimulated by wounding epithelial cells in the tissue. The future development of these

THOMPSON et al. In vivo gene transfer eyedrops 5 techniques will require the delivery of genes for expression such as growth factors or their receptors, ion channels or neurotransmitter receptors, enzymes of extracellular matrix formation or other genes which are involved at key points in the processes we wish to control.

In order to evaluate the relative effectiveness of retroviral gene delivery we also tested a plasmid DNA/lipofectin mix, a plasmid DNA/collasome mix, naked plasmid DNA and an adenoviral vector for gene delivery under circumstances similar to those used for retroviral gene delivery to corneal epithelium.

RESULTS.

The quantities of luciferase assayed in the tissue samples from wounded and control rabbit eyes are shown in figure 1. The background of the assay is the light from all reaction reagents minus tissue. There is no endogenous luciferase activity in mammalian tissues to give a tissue background [10]. The duration of expression in epithelium and endothelium is illustrated graphically for levels of luciferase assayed at various times following retroviral vector transduction (figure 2).

Plasmid DNA was delivered to corneal epithelium by several different methods (each performed in duplicate). The relative efficacy of gene transfection to different ocular tissues by drops, liposomes and collagen bits is shown in figure 3. Note that the maximum value of RLU in figure 3 is ten times less than that of figure 1, indicating the lower level of expression when

THOMPSON et al. In vivo gene transfer eyedrops 6
DNA plasmid rather than RVV transduced the target tissues.

The luciferase assay results on tissues from human donor corneas in which we used plasmid DNA to deliver the gene, show that none of these samples had activity distinguishable from background (data not shown).

Luciferase assay results for four human corneas are shown as means and standard deviations for each tissue assayed (Figure 4).

The appearance of positive X-gal staining in rabbit corneal epithelium when the tissue was developed following wounding and retroviral vector administration. In a low magnification view (10 X, figure 5 a) shows the staining when the tissue was collected at 36 hours after viral administration. The Blue staining was visible macroscopically as well. Figure 5 b shows no staining in a wounded, uninfected cornea. The β -galactosidase expressing cells have a distribution after wounding that reflects of the pattern of migration of epithelial cells that have undergone mitosis on the corneal surface. This suggests that gene transfection may be a tool in corneal physiology where the fate of mitotically active cells can be traced after an event such as corneal wounding.

The histological appearance of the X-gal positive cells in shown in figure 6 a and 6 b. In Figure 6 a the labelling of basal epithelial cells is evident as well as labelling of some superficial stromal keratocytes. In figure 6 b, taken from a more central and deeper area of the same corneal stroma, the labeling of keratocytes in deeper layers is shown.

THOMPSON et al. In vivo gene transfer eyedrops 7

Figure 7 a shows the labelled endothelial cells on the human donor material. Two lines of evidence suggest that this activity is not due to endogenous β -galactosidase activity, first similar positive results are observed using luciferase gene transduction (figure 4), and secondly a control in which RVV is applied to unwounded corneas demonstrates no β -Gal activity (figure 7 b).

MATERIALS AND METHODS.

Viral and Plasmid Vectors.

An amphotropic retroviral vector (RVV) was generated from the ecotropic Ψ 2 BAG α cell line [11] (ref1 ATCC CRL 9560). Ψ 2 BAG α cells, which produce a packaged β -galactosidase, neomycin phosphotransferase expressing RVV, were plated at 70% confluence on a T75 flask and the medium was changed to a volume of 10 ml the following day. The medium was harvested 24 h later, filtered through a 0.2 μ M Nalgene filter (Nalge CO., Rochester, NY) and supplemented with polybrene (to a 8 μ g/ml final concentration). This medium was immediately used to infect the PA 317 amphotrophic helper cell line [12] (ref 2, ATCC CRL 9078) and infected colonies were selected using the neomycin analogue Geneticin (Gibco/BRL, Grand Island, NY). Bag α /PA 317 (a clonal cell line generated in this manner) was grown to confluence. These producer cells generate virus at a titer of 2×10^6 /ml.

THOMPSON et al. In vivo gene transfer eyedrops 8
Medium was harvested 24 hours after application to confluent cells and immediately applied to eye tissues.

The luciferase-encoding RVV (LNC-luc) was constructed in LNCX (LNCX is a gift from Dr. Dusty Miller, [13] ref 3). Expression of the luciferase gene in this construct is regulated by the human Cytomegalovirus promoter/enhancer. The RVV was transfected into ecotropic Ψ 2 cells [14] (ref 4) and then media collected from these cells was used to transduce PA 317 cells (this being the procedure used by Miller and Rosman to optimize expression, [7] ref 3). These producer cells generate virus at a titer of $5 \times 10^5 - 1 \times 10^6$ cfu/ml.

A β -galactosidase-encoding adenoviral vector was obtained from Dr. J. Kolls [14] (ref 5). This virus was generated by an *in vivo* recombination event between a modified pACCMVpLpA shuttle vector and the pJM17 modified adenoviral genome [15,16] (ref 6 and 7). This virus was propagated in 293 human embryonic kidney cells (ATCC CRL 1573) and isolated on cesium chloride gradients. The virus stock concentration used in these experiments was 5×10^9 /ml.

Plasmid expression vectors encoding luciferase include RSV/pXP1 and SV2/pXP1 [17] (ref 8).
Luciferase Assays.

Tissues were harvested and immediately placed at 4° C in serum-free culture medium. The tissue was minced and manually homogenized in a Tekmar polytron (Tekmar Co., Cincinnati, OH) in an extraction buffer containing 1% Triton-X. Assays were

THOMPSON et al. In vivo gene transfer eyedrops 9
performed according to Braiser et al. [18] (ref 9). Luciferin and purified luciferase were obtained from Analytical Luminescence Laboratory (San Diego, CA). Luciferase activity in relative light units (RLUs) was measured on an Analytical Luminescence Laboratory Monolight 2010 luminometer for a ten second integrated interval. Background was measured by mixing all components except tissue. In several initial background measurements, control was included and no difference in background was obtained.

RABBIT IN VIVO EXPERIMENTS.

An initial experiment involving In vivo transfection of the anterior segment was carried out in 6 New Zealand albino rabbits of 1 to 1.5 kg. All animal handling techniques were in conformance with the ARVO resolution on the use of animals in research. The experiment compared retroviral gene introduction in wounded and unwounded corneal epithelium and endothelium. Six animals were used, three received bilateral 6 mm anterior corneal keratectomies by previously described methods [19]. Three additional rabbits anesthetized as described for the corneal wounds, were bilaterally wounded by 25 gauge needle puncture of the anterior chamber at the level of the iris and endothelial cell disruption in a 10 mm band under the central cornea. Intact corneal endothelial and epithelium in wounded rabbits served as controls.

At 36 hours after wounding the animals received 200ul of retrovirus (@ 10^6 pfu/ ml) dropped into the eyes once an hour for four hours. Animals in which the endothelium had been disrupted

THOMPSON et al. In vivo gene transfer eyedrops 10
had an injection of the same quantity of retrovirus into the
anterior chamber after an equal volume of aqueous had been
removed.

At 36 hours after treatment of the animals with retrovirus
(72 hours after wounding) all rabbits were sacrificed. Corneal
epithelium and scleral epithelium was scraped from the eye
surface of three animals, (six eyes) of each treatment group. The
eyes were enucleated and further dissected to allow collection of
iris, retina, stroma, endothelium and scleral epithelium.

A second experiment was designed to determine the duration
of expression in the wounded corneal epithelium. This was
conducted using a wound of the cornea surface which we devised to
give maximal exposure of the deeper layers of basal cells in the
cornea epithelium to retroviral transfection. Seven rabbits were
anesthetized and the cornea was wounded with the 6 mm diameter
trephine as described above. 36 hours after scraping all eyes
were dropped with retrovirus (conc = 1×10^6 cfu/ml, total amount
delivered = 200 μ l) once an hour for four hours. After 72 hours
for retroviral RNA to be expressed, animals were sacrificed and
tissues harvested for luciferase determination at 48, 72, 96, 1
week, 2 weeks, 3 weeks, and 1 month. Four more rabbits were
treated in the above described manner except that an E.coli β -
galactoside gene was the RVV-reporter gene rather than
luciferase. The animals were one control which was sacrificed at
72 hours post-wound time (36 hours after sham vector
administration), and two animals sacrificed at 36 hours after RVV

THOMPSON et al. In vivo gene transfer eyedrops 11
administration. Xgal color development techniques [20] were
applied and these corneas photographed as whole mounts or
sectioned for higher magnification views.

Another series of experiments was undertaken using DNA
constructs as the gene delivery vectors. These were carried out
on animals wounded on the epithelial surface with limbus to
limbus gentle debridement with a number 11 scalpel blade. Slit
lamp examination revealed this procedure left a thin epithelial
layer after the superficial layers were scraped away. Three
different methods of DNA delivery, drops, liposomes and collagen
bits were evaluated in these experiments. 36 hours after
epithelial debridement 4 animals were given 100 ug of DNA plasmid
in 100 ul of eye drops. The drops were instilled into the cul-de-
sac and the eye gently massaged for one minute. In two other
animals 12 mg of collagen bits were hydrated in 100 ul of sterile
water containing 100 ug of DNA. This quantity of rehydrated bits
was mixed into 200 mg of Murocel (corp) and introduced into the
cul-de-sac. The same amount of DNA was introduced into liposomes
(Lipofectin, BRL corp ref) and instilled in the cul-de-sac. At 72
hours after DNA administration these animals were sacrificed and
tissue collected for luciferase expression analysis as described
above.

HUMAN DONOR CORNEA IN VITRO EXPERIMENTS.

Human corneas not used for transplantation because of donor
age were obtained within 36 hours post-mortem. An area of the
central epithelium was demarcated with a 6 mm diameter trephine,

and the epithelium scraped away within that area, the other member of a pair was left unwounded as a control. Retrovirus was added to fresh Optisol corneal storage media in 12 well tissue culture dishes with retrovirus at a concentration of 1×10^6 cfu/ml. Corneas were incubated at 37° C for 24 hours before tissue collection for luciferase assay or fixation and sectioning for detection of β -galactosidase.

DISCUSSION.

The prospectus for gene therapy of genetic deficiencies of the retina has been examined [21] and the feasibility of such therapy experimentally evaluated [22,23]. In contrast to these studies which address the possibility of the rescue of genetic defects due to gene mutation in heritable retinal disorders, another avenue for gene therapy in the eye is the direct administration of novel genetic material to the surface of the eye. Such a route of administration could considerably enhance the therapeutic possibilities of gene therapy in ophthalmology.

Our results suggest that retroviral vectors are better suited to this application than DNA plasmids. The efficiency of DNA plasmid delivered gene expression was much lower than that due to retroviral vector infection, and it was not enhanced by DNA delivery in collagen bits or in liposomes. The infection of mitotic cells in wound healing on the corneal epithelium, or in stromal keratocytes is an aspect of this method that offers potential advantage for manipulation of this tissue since it targets the active cells during events such as reepithelization

THOMPSON et al. In vivo gene transfer eyedrops 13
during wound healing, or stromal repair.

The strategy of gene administration, its goals and purposes in the anterior segment will be different from those envisioned for the retina. In retinal conditions proposed as candidates for gene therapy, [8,22,23] specific genes are known to mutated. In cornea anomalies classed as congenital, the specific genes are not know as yet.

Corneal disease and surgical treatment of the cornea suggest that a different spectrum of problems may be amenable to genetic manipulation. The possibility of ease of topical delivery of genes to the anterior segment suggested by our study allows gene expression that could act to produce substances such as growth factors, growth factor receptors, antisense gene products to inhibit specific biosynthetic products such as collagens, metallo-proteinase or other lytic enzymes. This role of gene delivery would provide gene products that would have roles similar to pharmacologic agents, acting on specific mechanisms to influence cell behavior. Instances where such an approach might be useful would include limiting of extracellular matrix production by stromal keratocytes in refractive surgery, and thus limiting haze, aiding healing or reducing regression to the pre-surgical curvature. Corneal transplantation growth into recipient tissues and re-endothelialization might be enhanced, and reluctant healing speeded.

These applications of gene delivery could use the fraction of mitotically active cells available for transfection by

retrovirus as producers of protein transgene products which could act on the entire tissue they are part of. In reepithelialization of the corneal surface, dividing cells appear distributed across the surface at early times after wound closure and center in the reepithelialized area at later times, as our results show.

ACKNOWLEDGEMENTS

This work was supported by a Neuroscience Center Incentive Grant Award to HWT and JLC, an Eye Bank Association of America grant to HWT and also supported by the Department of the Army, Cooperative Agreement DAMD17-93-V-3013. This does not necessarily reflect the position or the policy of the government and no official endorsement should be inferred.

REFERENCES.

1. Mashhour, B., Couton, D., Perricaudet, M., & Briand, P. In vivo adenovirus-mediated gene transfer into ocular tissues. *Gene Therapy* 1,122-126(1994).
2. Thompson, H.W., Cook, J.L., Nguyen, D., Beuerman, R.W., Kaufman, H.E. High levels of in vivo gene transfer to corneal epithelium and endothelium. *Invest. Ophthalm. Vis. Sci.* 35,1383 (abstract#604) (1994)
3. Feldman, S.T., Tozer, J.R., Whang, S., Johnson, P., Feramisco, J.R. & Friedman, T. Gene transfer to the anterior segment of the eye by infection with recombinant viral vector. *Invest. Ophthalm. Vis. Sci.* 35,1383 (abstract#605) (1994)
4. Pepose, J.S., Leib, D.A. Herpes simplex viral vectors for therapeutic gene delivery to ocular tissues. *Invest. Ophthalm. Vis. Sci.* 35,2662-2666 (1994).
5. Thompson, H.W., Malter, J.S. & Beuerman, R.W. Flow cytometry measurements of DNA content of corneal epithelial cells during wound healing. *Invest. Ophthalm. Vis. Sci.* 32:433-436 (1991).
6. Roger corneal keratocyte paper new ref.

THOMPSON et al. In vivo gene transfer eyedrops 16

7. Miller, A.D. & Rosman, G.J. Improved retroviral vectors for gene transfer and expression. *Biotechniques* 7,980-990 (1989).
8. Piatigorsky, J. Gene Therapy: Is it feasible? In: The Cornea: Transactions of the World Congress on the Cornea III. Chapter 80 pp 439-444 (1988).
9. Beuerman, R.W., and Schimmelpfennig, B. Sensory denervation of the rabbit cornea affects epithelial properties. *Exp. Neurol.* 69:196-201(1988).
10. Alam, J., Cook, J.L. 1990. Reporter genes: application to the study of mammalian gene transcription. *Anal. Biochem.* 188,254-254(1990).
11. Price, J., Turner, D., & Cepko, C. Lineage analysis in the vertebrate nervous system by retrovirus-mediated gene transfer. *Proc. Natl. Acad. Sci.* 84,156-160 (1987).
12. Miller, A.D., & Buttimore, C. Redesign of retrovirus packaging cell lines to avoid recombination leading to helper virus production. *Mol. Cell. Biol.* 6,2895-2902 (1986).
13. Mann, R., Mulligan, R.C. & Baltimore, D. Construction of a retrovirus packaging vector mutant and its use to produce helper-free defective retrovirus. *Cell* 33,153-159(1983).

- THOMPSON et al. In vivo gene transfer eyedrops 17
14. Kolls, J., Peppel, K., Silva, M., & Beutler, B. Prolonged and effective blockade of tumor necrosis activity through adenovirus-mediated gene transfer. *Proc. Natl. Acad. Sci.* **91**,215-219(1994).
15. Gomez-Foix, A.M., Coats, W.S., Baque, S., Alam, T., Gerard, R.D., & Newgard, C.B. Adenovirus-mediated transfer of the muscle glycogen phosphorylase gene into hepatocytes confers altered regulation of glycogen metabolism. *J. Biol. Chem.* **267**,25129-25134(1992).
16. McGrory, W.J., Bautista, D.S. & Graham, F.L. A simple technique for the rescue of early region I mutations into infectious human adenovirus type 5. *Virology* **163**,614-617(1988).
17. Barbee, R.W., Stapleton, D.D., Perry, B.D., Re, R.N., Murgu, J.P., Valentino, V.A. & Cook, J.L. Prior arterial injury enhances luciferase expression following in vivo gene transfer. *Biochem. Biophys. Res. Comm.* **190**,70-78(1993).
18. Brasier, A.R., Tate, J.E. & Habener, J.F. Optimized use of the firefly luciferase assay as a reporter gene in mammalian cell lines. *Biotechniques* **7**,1116-1122(1989).
19. Frantz, J.M., Dupuy, B.M., Kaufman, H.E. & Beuerman, R.W. 1989. The effect of collagen shields on epithelial wound healing in rabbits. *Am. J. Ophthal.* **108**,524-528(1989).

20. Bondi, A., Chieriegatti, G., Eusebi, V., Fulcheri, E. & Bussolati, G. The use of β -galactosidase as a tracer in immunohistochemistry. *Histochem.* **76**,153-158 (1982).
21. Bok, D. Retinal transplantation and gene therapy. *Invest. Ophthalm. Vis. Sci.* **34**(3),473-476(1993).
22. Bennett, J., Wilson, J., Sun, D., Forbes, B., Maguire, A. Adenovirus vector-mediated in vivo gene transfer into adult murine retina. *Invest. Ophthalm. Vis. Sci.* **35**,2535-2542(1994).
23. Li, T., Adamian, M., Roof, D.J., Berson, E.L., Dryja, T.P., Roessler, B.J. & Davidson, B.L. In vivo transfer of a reporter gene to the retina mediated by an adenoviral vector. *Invest. Ophthalm. Vis. Sci.* **35**,2543-2549(1994).

FIGURE LEGENDS.

FIGURE 1. Graph of relative light units produced by luciferase gene expression in rabbit ocular tissues after administration of retroviral vectors as eyedrops, (in epithelium wounded and unwounded controls) or injections to the aqueous humor (endothelium wounded and unwounded controls). Also shown are luminometer assay results from other tissues in these same eyes. Each bar represents the means and standard error from assays on six eyes from three rabbits. LEGEND: epi_UW= unwounded epithelium, epi_W= wounded epithelium, endo_UW= unwounded endothelium, endo_W= wounded endothelium, iris_UW = iris in proximity to unwounded endothelium, no retroviral vector in anterior chamber, iris_W= iris in proximity to wounded endothelium, retroviral vector in anterior chamber, ret_UW= retina from eye with no endothelial wound, no vector in anterior chamber, ret_W= retina from eye with wounded endothelium and vector in anterior chamber, conj_UW= conjunctival epithelium from eye with no epithelial wound, no vector administered as eyedrops, conj_W= conjunctival epithelium from eye with epithelial wound and vector administered in eyedrops, BKG= assay background, all reagents without tissue sample.

FIGURE 2. Duration of luciferase expression in wounded endothelium and epithelium. Each point represents expression from pooled tissue from the two eyes of one rabbit at each time point. Endothelial expression was not followed beyond 72 hours.

FIGURE 3. Relative efficiency of different delivery methods of DNA vectors to rabbit eyes with epithelial wounds. No method gives significant increase over DNA vectors delivered in eyedrops. LEGEND: bkg= background light production, no tissue in reaction, epith_DNA= corneal epithelial expression following vector DNA in eyedrops, epith_BITS= DNA administered in collagen bits (collasomes), epith_LIPO= DNA administered in liposomes, conj_DNA= conjunctival epithelium assayed after DNA administered in eyedrops, conj_BITS= conjunctival epithelial expression after DNA administration in collasomes, conj_LIPO= DNA administration in liposomes.

FIGURE 4. Luciferase expression results from human donor corneas in culture. LEGEND: BKG= background light production, UW Epi= expression in unwounded corneal epithelium, all samples represented in this graph were exposed to retroviral vector, with retroviral vector in medium, W Epi= wound on corneal epithelium, W Endo= expression in endothelium where the corneal epithelium was wounded, (No endothelial wounds were made in these experiments), UW stroma= expression from stroma where the cornea epithelium was intact, W Stroma= stromal expression with corneal epithelium wounded, UW Conj= expression on epithelium on scleral rim left on cornea with no wound, W Conj=conjunctival expression where the cornea was wounded.

FIGURE 5. A. Low power (10X) micrograph of whole mount of rabbit cornea 36 hours after retroviral vector administration at 36 hours after corneal wound (72 hours total post wound time).

B. Control Xgal development of wounded rabbit cornea without administration of retroviral vector (5 X).

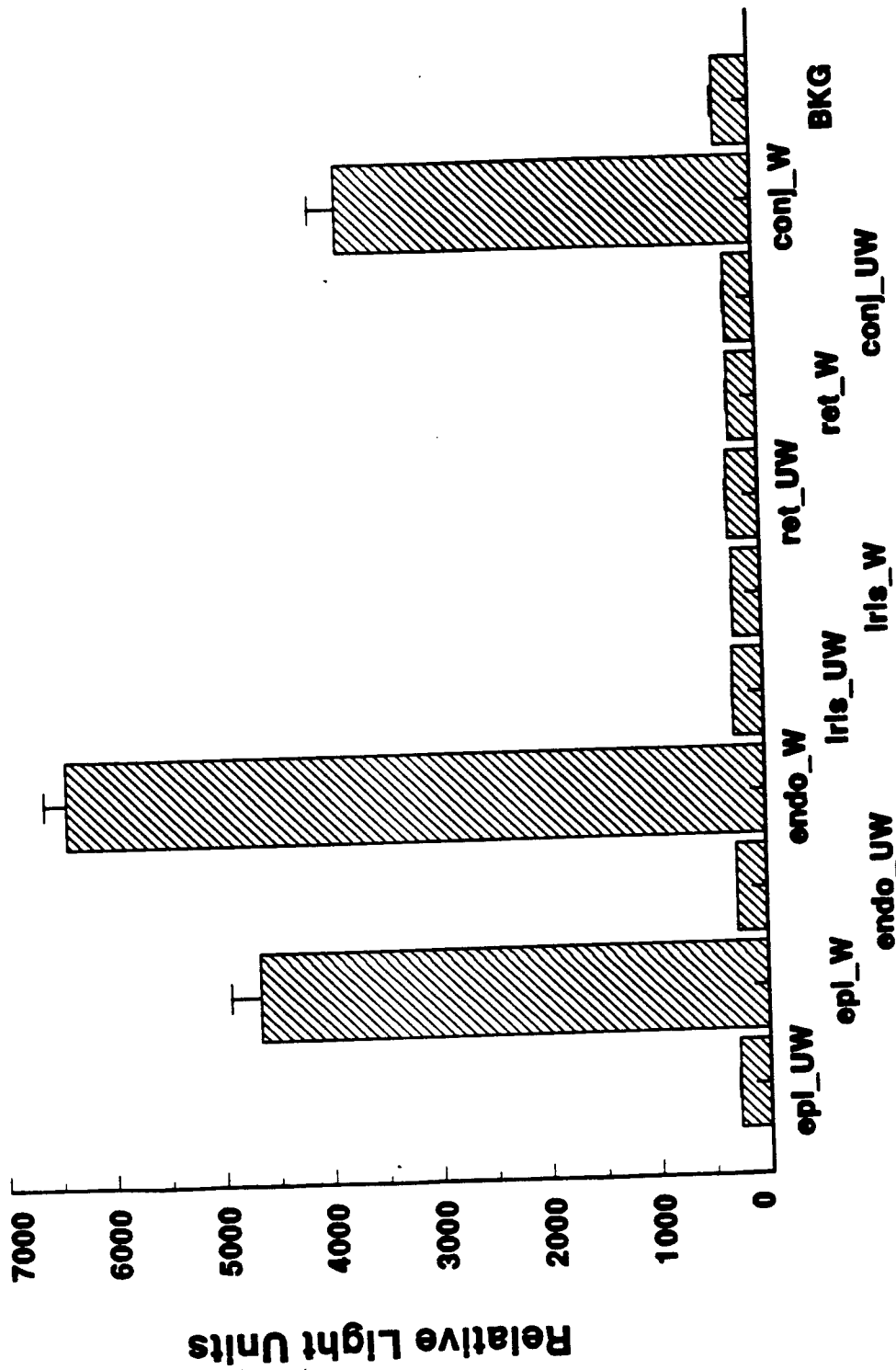
FIGURE 6 A. Rabbit cornea epithelial section from margin of keratectomy wound at 36 hours after retroviral vector administration. Note Xgal development identifying enzyme expression in basal and more superficial epithelial cells, and in superficial stromal keratocytes (100 X).

B. Deeper stromal layers of section from same rabbit cornea. β -gal expression is evident in deeper stromal keratocytes in this section (150 X).

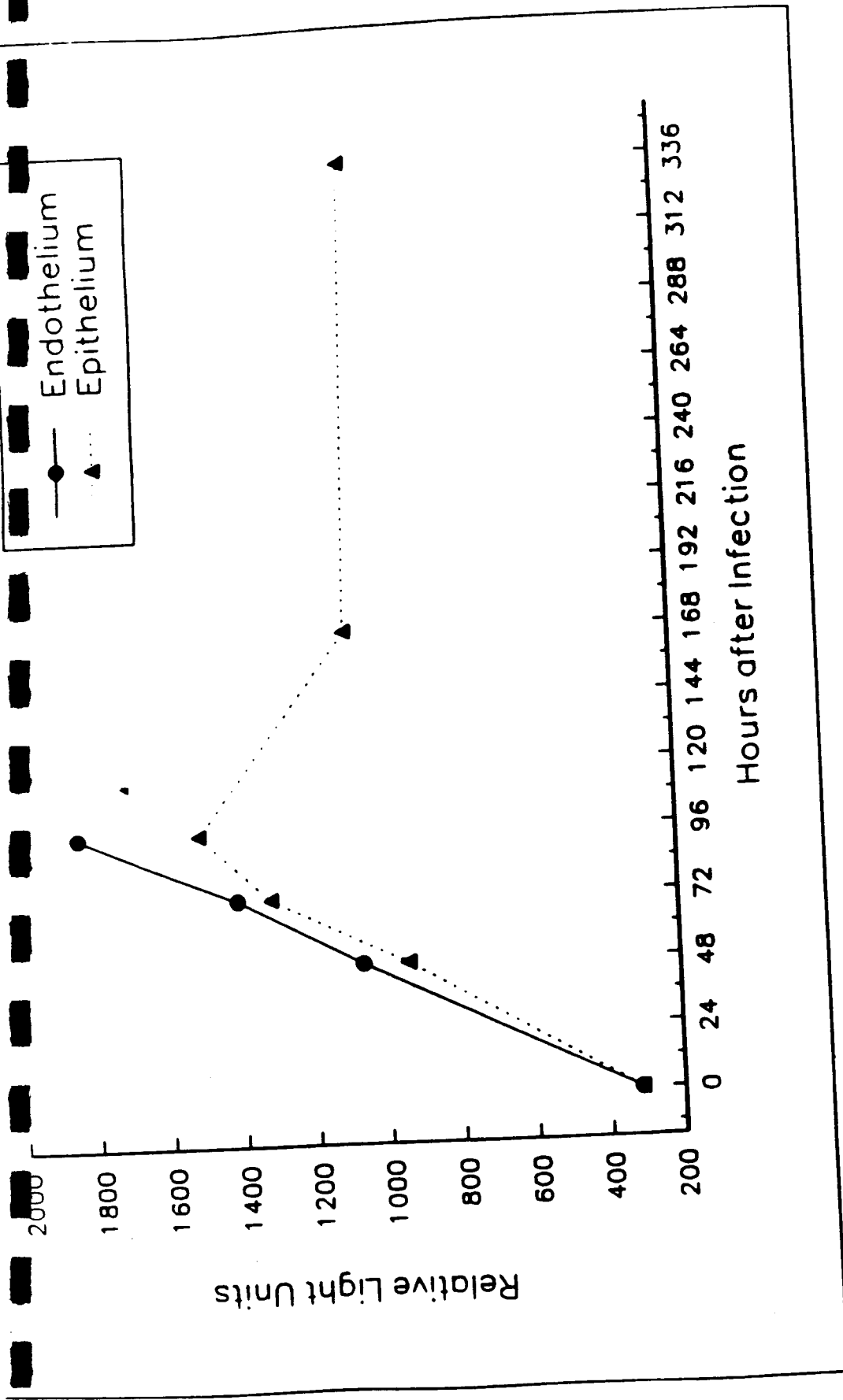
THOMPSON et al. In vivo gene transfer eyedrops 22

FIGURE 7 A. Endothelial cell staining in human cornea with wound on epithelium (20 X).

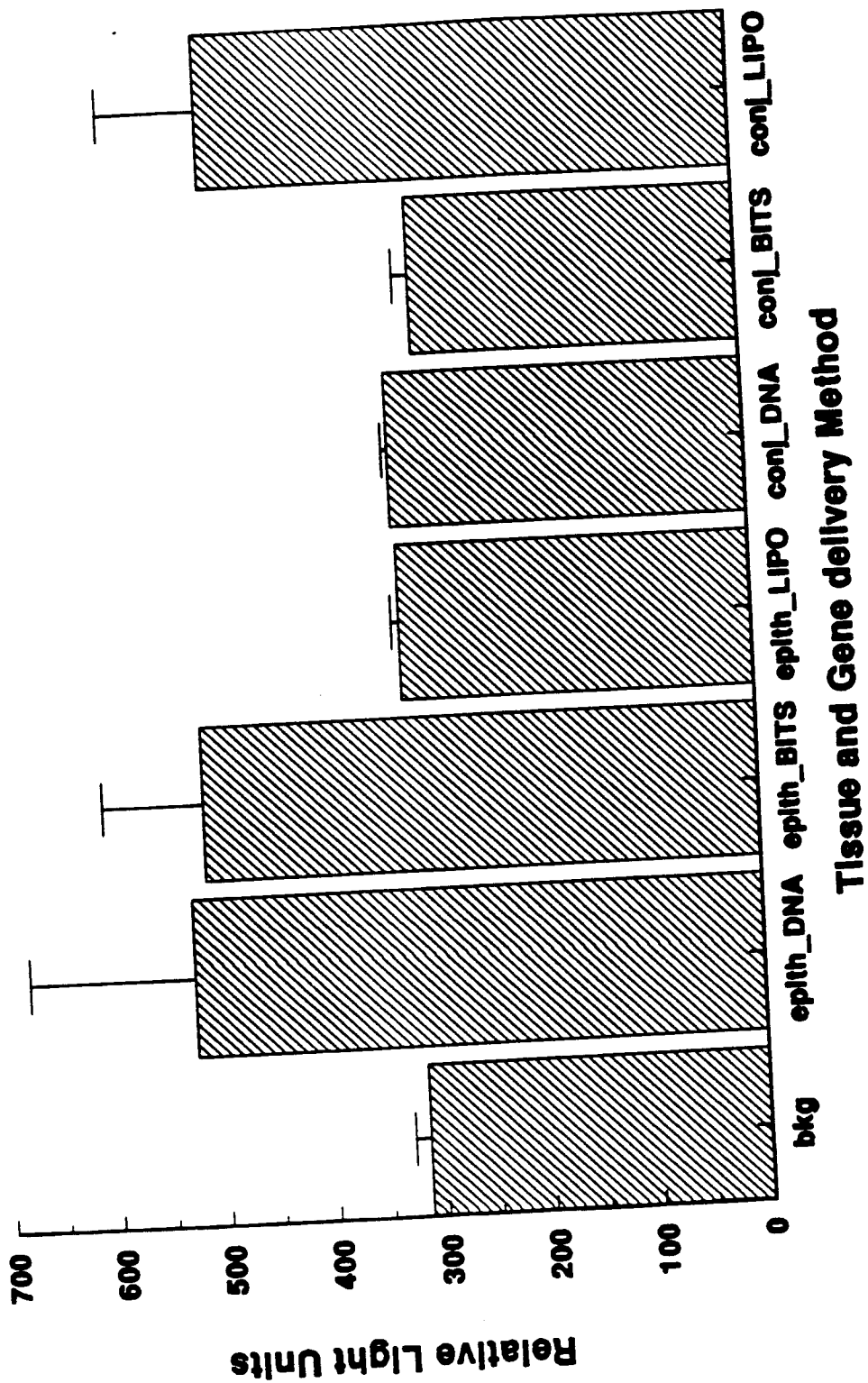
B. There was no staining in unwounded control corneas exposed to RVV.



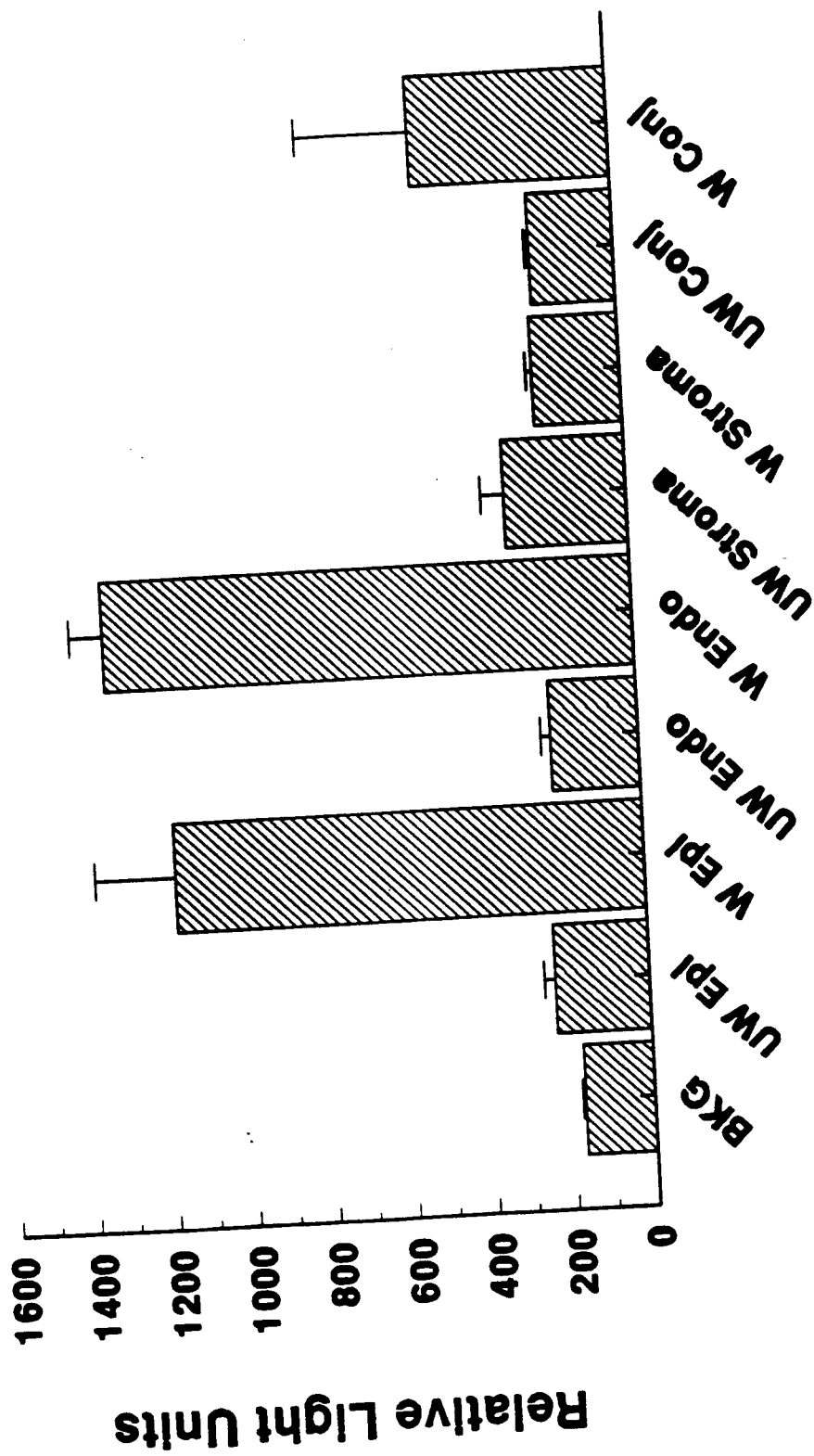
Thompson et al. FIG 1



Thompson et al. FIG 2.



Thompson et al Fig 3



Tissue and Treatment

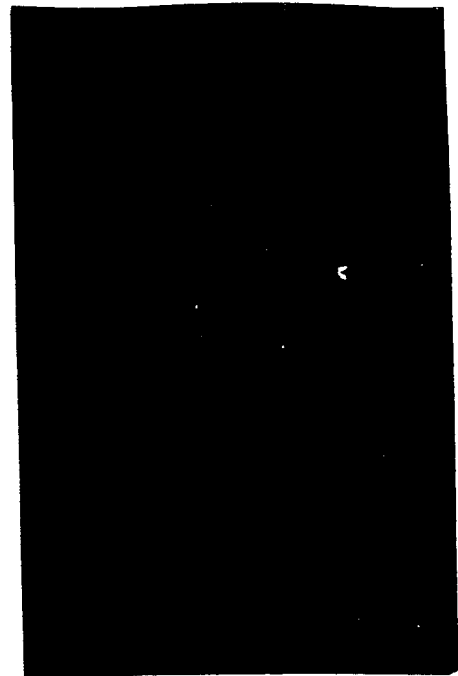
Thompson et al. FIG 4

Thompson
etal

FIG 5



A



63

B

FIG 6



A



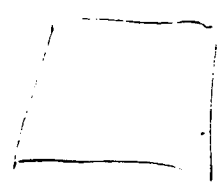
B

FIG 7

A



B



NEUROCHEMICAL PROTECTION OF THE BRAIN, NEURAL PLASTICITY AND REPAIR

The trigeminal ganglion as a model to study the effects of growth factors in nerve repair and regeneration.

The Trigeminal Ganglion as a Model to Study the Effect of Growth Factor in Nerve Repair and Regeneration

Summary

Reinnervation after corneal injury or surgery is critical for the tissue to restore its function. Growth-associated protein 43 (GAP-43) is a phosphoprotein, abundant in growth cones and involved in nerve regeneration. In this study, the expression of GAP-43 mRNA in the trigeminal neurons that innervate the cornea and the expression of the protein in the corneal epithelial layer were studied after injury of corneal nerve endings.

The fluorescent dye fast blue, applied to the surface of the cornea, was used as a retrograde tracer to identify the specific trigeminal neurons that innervate the tissue. The expression of GAP-43 mRNA was quantitated by *in situ* hybridization in the cell bodies of trigeminal neurons after the nerve terminals had been destroyed by a cryogenic corneal injury. GAP-43 protein was analyzed in the corneal epithelium by Western blot analysis.

A four-fold increase in GAP-43 mRNA was found in the neurons 3 days after corneal wounding and this level remained constant for 7 days. At 14 days, the level decreased to three-fold over non-wounded neurons. Increased expression of GAP-43 coincided with the post-injury period during which there is regeneration of corneal nerves. Three days after injury, a weak GAP-43 immunoreactivity was detected in the

the corneal epithelium layer associated to a membrane fraction. The signal was much stronger 7 days after injury.

Our results demonstrate that injury of the nerve terminals in the cornea increased GAP-43 mRNA expression in the trigeminal neurons, followed by translation and axonal transport of the protein to the nerve terminals. This study also shows that GAP-43 was expressed even when the injury was inflicted at a long distance from the neuronal cell body of the peripheral nervous system. The results suggest that GAP-43 can be an important protein in the structural and functional restoration of the corneal nerve terminals after injury.

Introduction

The cornea, the most densely innervated tissue of the body, receives sensory nerve fibers from pseudo-unipolar neurons located in the ipsilateral trigeminal ganglion. These neuronal cell bodies are found in the ophthalmic (medial) region, interspersed among neurons innervating other tissues (Marfurt, et al., 1989). Corneal afferent nerves, mostly of A-delta and C types, form branches around the limbal region and expand as a plexus beneath the corneal epithelium (Rozsa and Beuerman, 1982). In the epithelium, nerves run parallel to the basal layer and appear as free nerve endings without myelination (Rozsa and Beuerman, 1982; de Leeuw and Chan, 1989).

In addition to transmitting sensory input, the nerves contribute to the functional integrity of the cornea. For example, the nerve fibers exert important trophic

influences on the corneal epithelium and stimulate wound-healing following epithelial lesions (Beuerman and Schimmelpfennig, 1990). Diseases, injuries, and ocular surgeries that damage corneal nerves can cause severe impairments in the cornea. In fact, corneal denervation results in neurogenic corneal ulcers (Cavanagh and Colley, 1989). Therefore, a complete regeneration of the nerves after damage of the cornea is an important factor for avoiding chronic pathologies.

GAP-43 (also known as B-50, F1, pp46, p57, or neuromodulin) is a neural tissue-specific phosphoprotein expressed during neuronal growth, regeneration, and synaptic plasticity (for review see Skene, 1989; Gispen et al., 1992). It is also implicated in neuronal signal transduction since it is a protein kinase C (PKC) substrate and its phosphorylation is involved in neurotransmitter release (Dekker et al., 1989) and long-term potentiation (Benowitz and Routtenberg, 1988). GAP-43 also stimulates the GTPase activity of the G_0 -protein, suggesting a role in regulating G-protein coupled receptors (Strittmatter et al., 1990). The protein is a major component of the membranes of growth cones, which are the leading edges of extending neurites. A relationship between the expression of GAP-43 and axon growth had been suggested. There is more GAP-43 in certain neurons during development, and synthesis of GAP-43 increases when adult neurons regenerate injured axons (Skene, 1989).

To better understand the factors that are involved in corneal nerve regeneration after corneal injury, we studied the expression of GAP-43 in trigeminal neurons that innervate the cornea. Using *in situ* hybridization, we found that GAP-43

mRNA expression increased in cornea-innervating trigeminal neurons in response to corneal injury and the pattern of induction correlates with reported morphological changes of the corneal nerves (Chan et al., 1990). We also show that, after injury, the protein GAP-43 was expressed in detectable amounts in the membrane fraction of the corneal epithelium layer that contained regenerating nerve terminals.

Methods

Fifty New Zealand albino rabbits of either sex weighing between 2-3 kg were used in this study. The animals were kept under a 12 hr light-dark cycle and were given food and water ad libitum. All procedures were performed under general anesthesia produced by an intramuscular injection of a mixture of 10% ketamine and 10% xylazine.

Retrograde tracing

To differentiate neurons that innervate the cornea from those that do not, the fluorescent dye fast blue (Sigma, St. Louis, MO) was used. Briefly, corneas of anesthetized rabbits were gently scratched with a 27 gauge needle in a grid fashion (3 lines horizontally and 3 lines vertically). This was done under a microscope to ensure that only the superficial epithelium was disrupted to allow fast blue to diffuse into the corneal stroma and be taken up by the nerves. Nerve injury resulting from this procedure was minimal compared to that by the experimental procedure cryoinjury. A piece of filter paper (6 mm in diameter) soaked in 5% fast blue was

applied to the center of the cornea for 1 hour, covered with parafilm to prevent evaporation and tissue damage. Then the eyes were thoroughly rinsed with normal saline and the rabbits allowed to recover. The corneal scratches generally healed overnight.

Cryoinjury

Six days after fast blue administration, a 5 mm diameter copper probe chilled in liquid nitrogen was applied for 20 sec to the center of one cornea of anesthetized rabbits. This created a transcorneal frozen zone of about 7 mm in diameter, damaging corneal nerve terminals in the epithelium as well as axonal trunks in the stroma. The damaged epithelium regenerated between one and two days. Three, 7, and 14 days following the injury, the rabbits were anesthetized and killed by transcardial perfusion of 0.5 liter phosphate-buffered saline, 1 liter 4% paraformaldehyde, and 1 liter of ice-cold 10% sucrose. Trigeminal ganglia (both control and wounded) were harvested, soaked in 25% sucrose for 4 hours, and frozen at -20°C before being sectioned with a cryostat. Sections 20µm thick were cut and collected on Superfrost/plus microscope slides (Fisher, Pittsburgh, PA). Control and wounded ganglia were frozen on the same tissue block, so that they could be cut and mounted on the slides side by side for comparison.

In situ hybridization

In situ hybridization was performed as described (Bloch et al., 1986). Briefly, the sections were prehybridized for 5 h at 42°C in a buffer containing 50% formamide, 2X Denhardt solution, 4X SSC, 10% dextran sulfate, 0.1% salmon sperm DNA, and 0.1% SDS. The buffer was replaced with fresh buffer containing the radioactive probe, a GAP-43 cDNA fragment of 1.4 Kb encompassing the entire coding region (a gift from Dr. P. Skene), labeled with ³³P-dCTP (Zagursky, Conway and Kashdan, 1991) by a random-priming method (Amersham labeling kit; Feinberg and Vogelstein, 1983; 1984). Final probe concentration was 4x10⁶ cpm/ml. The vector plasmid (pGEM3) was labeled in the same way and incorporated into the hybridization buffer for a few slides as a control for hybridization specificity. Following 16 to 18 hours of hybridization, the slides were washed in 2X SSC (room temperature, 10 min), 1X SSC (50°C, 20 min), and 0.5X SSC (50°C, 10 min). After drying, the slides were dipped in Kodak NTB-2 emulsion diluted 1:1 with 600 mM ammonium acetate and subsequently exposed for 2 weeks. After being developed, fixed, and cover-slipped, the slides were viewed simultaneously, using a Nikon microscope, under UV light (wavelength=360 nm) to visualize blue fluorescence and visible light to see the silver grains in a dark field. With this combination of lights, the silver grains looked yellowish and the fast blue-labeled neurons appeared blue. Fluorescent microscopy was also combined with phase microscopy to visualize both fast blue-labeled and unlabeled neurons using a Zeiss microscope. As the size of corneal innervating neurons is predominantly small to medium relative to other

trigeminal neurons (Marfurt et al., 1989), silver grains were counted with a Coulter counter in 75 neurons labeled with fast blue in randomly selected fields from each experimental and control ganglion. Student's t-test was applied to the mean counts per cell and p values of less than 0.05 were considered significant. Photographs were taken with Kodak Ektachrome 200 color-slide film.

Northern blot analysis

The anterior medial part (the ophthalmic region (Marfurt et al., 1989)) of rabbit trigeminal ganglia was dissected and homogenized in 0.25 ml of ice-cold 4M guanidine isothiocyanate and then diluted to 1.4 ml with the same solution. The homogenate was then layered on top of 400 μ l of 6.5M CsCl and centrifuged at 50,000 rpm in a Beckman TL 100 rotor for 5 hours. The pelleted RNA was extracted with 20mM EDTA in chloroform/butanol (4:1, v:v) (Sambrook, Fritsch and Maniatis, 1989). Ten μ g of total RNA from each sample per lane was loaded on a 1.2% agarose/formaldehyde gel and electrophoretically separated. The RNA was transferred by blotting onto a Hybond nylon membrane and cross-linked by exposure to UV light for 5 min. Membranes were prehybridized at 42°C for 6 hrs in a solution containing 50% formamide, 5X SSPE (1X SSPE=0.18M NaCl, 10mM sodium phosphate, and 1mM EDTA, pH 7.4), 5X Denhardt's solution and 150 μ g/ml salmon sperm DNA. Hybridization was performed under the same conditions using a 32 P-labeled GAP-43 cDNA probe ($2-4 \times 10^6$ cpm/ml) for 18 hrs at 42°C. The membranes were washed in 2X SSPE for 15 min at room temperature, 2X SSPE for 30 min at

55°C, and 0.1X SSPE for 10 min at 55°C. Autoradiographs were obtained by exposing the membranes for 24 hrs to Kodak X-Omat film with an intensifying screen at -70°C.

Western blot analysis of GAP-43 in the corneal epithelial layer

Anesthetized rabbits were wounded by removing the corneal epithelium with a scalpel as previously described (Lin and Bazan, 1992). The denuded cornea was covered with new epithelium within 2 days. Thus, the time required for reepithelialization is similar to that necessary after cryoinjury. This kind of injury was chosen because it does not leave any intact epithelium, as does cryoinjury, thus giving a more homogenous sample. Epithelium from eight corneas was collected at day 0 (control) and at 3 and 7 days after injury and homogenized in a glass grinder with six volumes of homogenization buffer (20 mM Tris-HCl, 10 mM EGTA, 2 mM EDTA, 1 mM phenyl methylsulfonyl fluoride, 10 mM β -mercaptoethanol, 50 mg/ml leupeptin and 0.25M sucrose, pH 7.5). The homogenate was centrifuged in a Beckman TL-100 ultracentrifuge at 100,000 x g for 35 min and the supernatant (cytosolic fraction) was collected. The pellet (membrane fraction) was resuspended in the homogenization buffer. All the procedures were done at 4°C. Protein was determined in both fractions (Bradford, 1976).

Samples were subjected to 10% sodium dodecyl sulfate polyacrylamide gel electrophoresis (SDS-PAGE). To enhance the immunochemical recognition of GAP-43, the procedure of Dunn was followed (Dunn, 1986). Briefly, the gels were

incubated in 50 mM Tris-HCl (pH 7.4) containing 20% glycerol for 1 h at room temperature. The gels were transferred using a carbonate blot buffer (10 mM NaHCO_3 , 3 mM Na_2CO_3 , 20% methanol, pH 9.9) for 2 h at a constant 250 mA to a nitrocellulose membrane (Amersham, Arlington Heights, IL). The membrane was blocked with 3% non-fat milk in PBS (blocking solution) and then incubated with mouse anti-GAP-43 monoclonal antibody (Boehringer, Germany) (0.5 $\mu\text{g/ml}$ in blocking solution) at 4°C overnight. After three washes in PBS containing 0.05% Tween (PBS-T), and an incubation of 1 h at room temperature with sheep anti-mouse [^{125}I]IgG in blocking solution (0.5 $\mu\text{Ci/ml}$), the membrane was washed three times for 10 min in PBS-T, dried, and subjected to phosphorimaging analysis.

Results

Our preliminary *in situ* hybridization studies showed that GAP-43 was constitutively expressed in some of the trigeminal ganglion neurons. Northern blot analysis showed that the probe recognized a single mRNA species of 1.4 kb, coinciding with the size of GAP-43 mRNA (Karns et al., 1987). A discrete increase in GAP-43 mRNA was also seen 3 days after corneal wounding (Fig. 1).

Cornea-innervating trigeminal neurons constitute only a small fraction of those of the trigeminal ganglia. In the cat, for example, approximately 300 out of 14,000 trigeminal ganglion neurons innervate the cornea (Holland and Robinson, 1990). In the rabbit, this ratio is slightly higher, and a positive correlation between corneal size and the number of corneal primary afferent neurons in the trigeminal ganglion has

been demonstrated among different species (Marfurt et al., 1989). In order to differentiate them from the other trigeminal ganglion neurons, we labeled the cornea-specific trigeminal neurons with fluorescent fast blue by retrograde tracing. Fast blue has been used to trace ocular innervation (Bortolami et al., 1991) and has been shown to be compatible with *in situ* hybridization procedures (Tetzlaff et al., 1991). This technique consistently labeled about 350 to 450 neurons per ganglion (data not shown), which is within the range reported for rabbit trigeminal neurons innervating the cornea as determined by horseradish peroxidase retrograde tracing (Marfurt et al., 1989). These results indicate that fast blue was effectively transported by the corneal nerves to the soma when applied to the periphery, and that this is a reliable method for labeling neurons that innervate the cornea.

In situ hybridization showed that 3, 7, and 14 days after corneal wounding, the level of GAP-43 mRNA was increased in the cornea-innervating neurons, while the GAP-43 mRNA level in controls was consistently low (Fig. 2). In the control side, more than half (55%) of the cornea-innervating neurons did not express GAP-43 mRNA, while the rest of them expressed low levels (less than 10 silver grains per neuron) of this message. After wounding, these neurons shifted from having low or no GAP-43 mRNA to high expression of the message. By counting the same number of randomly selected, fast blue-stained neurons from both the control side and the injured side of each sample slide, a four-fold increase of GAP-43 mRNA abundance was noted at 3 and 7 days after lesioning. This was due to both the increase in the number of GAP-43 positive neurons and the higher amounts of the message

expressed in each neuron. 40% of the cells counted contained more than 36 grains per cell. Fourteen days after the injury, the increase was three-fold over controls. The changes are best seen by plotting the ratio of signal intensities of wounded side over control side as a function of time (Fig. 3).

There were a number of clusters of hybridization signals (silver dots) outside the fast blue-labeled neurons in both the wounded and non-wounded ganglia (Fig. 2). Those clusters represent neurons that hybridized to the GAP-43 probe but did not innervate the cornea. This was demonstrated by combining phase microscopy with fluorescent microscopy, as shown in Fig. 4. The results confirmed our previous findings that trigeminal ganglion neurons innervating other target tissues express various amounts of GAP-43 and that Northern blot analysis is not a sufficiently sensitive technique for studying the differences in GAP-43 expression in the trigeminal neurons after corneal nerve injuries.

The increase in GAP-43 mRNA in the trigeminal neurons innervating the cornea was accompanied by an augmentation of GAP-43 protein which was detected by Western blot in the membrane fraction of the corneal epithelium (Fig. 5). Three days after wounding by total corneal deepithelialization, a discrete GAP-43 immunoreactive band was seen, and the intensity increased at 7 days. The blot shows the band migrated with an R_f similar to the 60 kDa molecular weight standard. The size of GAP-43, a hydrophobic protein, has been reported to be between 40 and 60 kDa, depending on the conditions of electrophoresis (Skene, 1989)

Discussion

The transcorneal freezing technique accomplishes the equivalent of nerve transection without cutting through the cornea. In this model, most of the nerve regeneration occurred between 3 and 10 days after the injury (Chan et al., 1990). After wounding, two types of nerve growth have been identified: sprouting of new, long neurites that appeared as soon as 2 days after the injury and could still be seen 21 days later, and a genuine regrowth of stromal and subepithelial nerves in a centripetal direction that occurred between 3 and 7 days after injury.

Our results show that GAP-43 mRNA expression in the trigeminal neurons that innervate the cornea was induced from days 3 through 7 after the corneal cryoinjury and declined by 14 days (but was still 3 times higher than control), coinciding with the period when injured neurons regenerate and extend their neurites. Western blot analysis showed that GAP-43 protein was indeed detected in the corneal epithelial layer at 3 days and was more abundant at 7 days after corneal injury. The increase in the amount of GAP-43 protein in the corneal epithelial layer at 7 days may reflect the enhanced regeneration and remodeling processes of the epithelial nerves at that time (Rosza, Guss and Beuerman, 1983), with enrichment of growth cones and concurrent newly synthesized GAP-43 (Skene, 1989). Mechanical deepithelialization and cryogenic injury similarly destroyed epithelial nerves. In each of these wounds, regeneration of the epithelium was accomplished in 1 to 2 days and repair of the epithelial nerves was initiated soon after the epithelium regenerated, at 3 day after injury (Chan et al., 1990). The time required for total repair of corneal epithelial

nerves is similar to keratectomy wounding (4 weeks) (Rosza, Guss and Beuerman, 1983) and cryodamage wounding (3 weeks) (Chan et al., 1990), and the mechanism of their reinnervation may be the same (Chan et al., 1990). Our results, therefore, although from different types of injury, may also represent a general temporal relationship in terms of the increase in GAP-43 mRNA in the neural cell body and the increase of GAP-43 protein in the corneal epithelial layers after corneal wounding (regardless of the type of corneal insult).

We found a weak expression of GAP-43 mRNA in soma of the cornea-innervating trigeminal neurons on the control side. The presence of GAP-43 in normal adult central nervous system (CNS) neurons has been noticed in areas presumably having a relatively high degree of plasticity, such as the hippocampus. As for the peripheral nervous system (PNS), Verge et al. (1990) reported that certain rat dorsal root ganglion neurons that contain substance P (SP)- or calcitonin gene-related peptide (CGRP) also express GAP-43 constitutively. These authors suggest that constitutive expression of GAP-43 in such neurons may be involved in lateral sprouting of the nerves. Previous studies from our lab have shown the presence of GAP-43 immunoreactivity in some of the corneal sensory nerves (Martin and Bazan, 1992). It is conceivable that the constitutive expression of GAP-43 is due to the continuous remodeling of the corneal nerve endings during the normal life cycle of corneal epithelium (Harris and Purves, 1989). The remodeling process in the cornea is similar to the changes that occur during development and in synaptic plasticity

(Benowitz and Routtenberg, 1988; Tetzlaff et al., 1991), and may require the participation of GAP-43.

The mechanisms by which GAP-43 expression is activated are not clear. It has been suggested that the cell body increases GAP-43 synthesis in response to retrograde signals related to the interruption of the contact between the peripheral axon and its target, since blockers of retrograde axonal transport can induce the expression of GAP-43 (Woolf et al., 1990). A neurotrophic factor that is secreted by the corneal epithelial cells after wounding (epithelial neurotrophic factor or ENF), has been reported (Chan and Haschke, 1981). ENF induces neurite outgrowth of sensory neurons in culture, stimulates protein synthesis in trigeminal neurons, and has been suggested to mediate corneal nerve regeneration (Chan et al., 1987). Although the present results do not clarify what mechanisms activate GAP-43 expression in the ganglion, such signals, whether from the target tissue or from the axon itself, could be derived from the periphery, since the injury was performed near (and included) the terminus of the nerve.

Following corneal injury there is an increase in PKC activity in the corneal epithelial layer (Lin and Bazan, 1992). This may suggest a change in the phosphorylation of GAP-43, a specific PKC substrate, and a role of the protein in signal transduction mechanisms activated after injury to lead to corneal nerve regeneration (Bazan and Bazan, 1990). Experiments are in progress in our lab to determine the role of PKC on GAP-43 in the cornea.

It is well known that neurons of the mammalian PNS can regenerate their axons after injury, while those of the CNS typically do not regenerate. Interestingly, the distance from injury appears to be a factor modulating the capacity of CNS neurons to increase GAP-43 expression. Axotomy of corticospinal and retinal ganglion cells at long distances from their cell bodies does not increase the amount of axonally transported GAP-43 (Richardson, Issa, and Shemie, 1982) and these neurons do not regenerate into peripheral nerve transplants, which would provide a favorable milieu for growth. However, when axotomy is performed close to the eye, there is an increase in GAP-43 immunoreactivity in retinal ganglion cells (Doster et al., 1991), and a significant number of these cells regenerate their axons into peripheral transplants (Vidal-Sanz et al., 1987). Our results show that a distant injury like the one reported here can induce GAP-43 mRNA expression in the PNS neuron. Therefore, while distance from injury can be a factor affecting the expression of GAP-43 and the regenerative capacity of CNS neurons, it is not a factor to the PNS neurons even when the injury affects only the nerve terminals.

In conclusion, the results of this study demonstrate that, after corneal injury, there is an increase in GAP-43 mRNA in the trigeminal neurons that innervate the cornea followed by an increase in GAP-43 in the corneal epithelial layer. The pattern of increased expression of GAP-43 correlates with the time when corneal nerve regeneration takes place. Thus, GAP-43 induction may be an important component involved in the regeneration of the trigeminal neurons after nerve injury that will determine a proper wound-healing and the repair of the corneal nerves.

References

- Bazan, N.G., and Bazan, H.E.P. (1990). Ocular responses to inflammation and the triggering of wound healing: Lipid mediators, proto-oncogenes, gene expression and neuromodulation. In *Lipid Mediators in Eye Inflammation. New Trends in Lipid Mediators Research* (Ed N.G. Bazan) Basel, S. Karger, **5**, 168-180.
- Benowitz, L.I., and Routtenberg, A. (1988). A membrane phosphoprotein associated with neural development, axonal regeneration, phospholipid metabolism and synaptic plasticity. *Trends Neurosci.* **10**, 527-532.
- Beuerman, R.W., and Schimmelpfennig, B. (1990). Sensory denervation of the rabbit cornea affects epithelial properties. *Exp Neurol.* **69**, 196-201.
- Bloch, B., Popovici, T., LeGuellec, D., Normand, E., Chouham, S., Guitteny, A.F., and Bohlen, P. (1986). *In situ* hybridization histochemistry for the analysis of gene expression in the endocrine and central nervous system tissues: A 3-year experience. *J Neurosci Res.* **16**, 183-200.
- Bortolami, R., Calza, L., Lucchi, M.L., Giardino, L., Callegari, E., Manni, E., Pettotossi, V.E., Barazzoni, A.M., and Costerbosa, G.L. (1991). Peripheral territory and neuropeptides of the trigeminal ganglion neurons centrally projecting through the oculomotor nerve demonstrated by fluorescent retrograde double-labeling combined with immunocytochemistry. *Brain Res.* **547**, 82-88.
- Bradford, M.M. (1976). A rapid and sensitive method for the quantitation of microgram quantities of protein utilizing the principle of protein-dye binding. *Anal. Biochem.* **72**, 248-254.
- Cavanagh, H.D., and Colley, A.M. (1989). The molecular basis of neurotrophic keratitis. *Acta Ophthalmol Suppl.* **192**, 115-134.
- Chan, K.Y., and Haschke, R.H. (1981). Action of trophic factor(s) from rabbit corneal epithelial culture on dissociated trigeminal neurons. *J. Neurosci.* **1**, 1155-1162.
- Chan, K.Y., Jones, R.R., Bark, D.H., Swift, J., Parker, J.A., and Haschke, R.H. (1987). Release of neurotrophic factor from rabbit corneal epithelium during wound healing and nerve regeneration. *Exp Eye Res.* **45**, 633-646.
- Chan, K.Y., Jarvelainen, M., Chang, J.H., and Edenfield, M.J. (1990). A cryodamage model for studying corneal nerve regeneration. *Invest Ophthalmol Vis Sci.* **31**, 2008-2021.
- de Leeuw, A.M., and Chan, K.Y. (1989). Corneal nerve regeneration. Correlation between morphology and restoration of sensitivity. *Invest Ophthalmol Vis Sci.* **30**, 1980-1990.
- Dekker, L.V., DeGraan, P.N.E., Versteeg, D.H.G., Oestreicher, A.B., and Gispen, W.H. (1989). Phosphorylation of B-50 (GAP-43) is correlated with neurotransmitter release in rat hippocampal slices. *J Neurochem.* **52**, 24-30.

- Doster, S.K., Lozano, A.M., Aguayo, A.J., and Willard, M.B. (1991). Expression of the growth-associated protein GAP-43 in adult rat retinal ganglion cells following axon injury. *Neuron*. **6**, 635-647.
- Dunn, S.T. (1986). Effects of the modification of transfer buffer composition and the renaturation of proteins in gels on the recognition of proteins on western blots by monoclonal antibodies. *Anal Biochem*. **157**, 144-153.
- Feinberg, A.P., and Vogelstein, B. (1983). A technique for radiolabelling DNA restriction endonuclease fragments to high specific activity. *Anal Biochem*. **132**, 6-13.
- Feinberg, A.P., and Vogelstein, B. (1984). A technique for radiolabelling DNA restriction endonuclease fragments to high specific activity. *Addendum. Anal Biochem*. **137**, 266-267.
- Gispen, W.H., Nielander, H.B., DeGraan, P.N.E., Oestreicher, A.B., Schrama, L.H., and Schotman, P. (1992). Role of the growth-associated protein B50/GAP-43 in neuronal plasticity. *Mol Neurobiol*. **5**, 61-85.
- Harris, L.W., and Purves, D. (1989). Rapid remodeling of sensory endings in the corneas of living mice. *J. Neurosci*. **9**, 2210-2214.
- Holland, G.R., and Robinson, P.P. (1990). Cell counts in the trigeminal ganglion of the cat after inferior alveolar nerve injuries. *J Anat*. **171**, 179-186.
- Karns, L.R., Ng, S.G., Freeman, J.A., and Fishman, M.C. (1987). Cloning of complementary DNA for GAP-43, a neuronal growth-related protein. *Science*. **236**, 597-600.
- Lin, N., and Bazan, H.E.P. (1992). Protein kinase C subspecies in rabbit corneal epithelium: Increased activity of α subspecies during wound healing. *Curr Eye Res*. **11**, 889-907.
- Marfurt, C.F., Kingsley, R.E., and Echtenkamp, S.E. (1989). Sensory and sympathetic innervation of the mammalian cornea. A retrograde tracing study. *Invest Ophthalmol Vis Sci*. **30**, 461-472.
- Martin, R.E., and Bazan, N.G. (1992). Growth-associated protein GAP-43 and nerve cell adhesion molecule in sensory nerves of cornea. *Exp Eye Res* **55**, 307-314.
- Richardson, P.M., Issa, V.M.K., and Shemie, S. (1982). Regeneration and retrograde degeneration of axons in the rat optic nerve. *J. Neurocytol*. **11**, 949-966.
- Rozsa, A.J., and Beuerman, R.W. (1982). Density and organization of free nerve endings in the corneal epithelium of the rabbit. *Pain*. **14**, 105-120.
- Rozsa, A.J., Guss, R.B., and Beuerman, R.W. (1983). Neural remodeling following experimental surgery of the rabbit cornea. *Invest. Ophthalmol. Vis. Sci*. **24**, 1033-1051.
- Sambrook, J., Fritsch, E.F., and Maniatis, T. (1989). *Extraction of RNA with Guanidinium thiocyanate Followed by Centrifugation in Cesium Chloride Solutions. Molecular Cloning*. 2nd ed. Cold Spring Harbor Laboratory Press. Vol. 1, 7.19-7.22.

- Skene, J.H.P. (1989). Axonal growth-associated proteins. *Ann Rev Neurosci.* **12**, 127-156.
- Strittmatter, S.M., Valenzuela, D., Kennedy, T.E., Neer, E.J., and Fishman, M.C. (1990). G_o is a major growth cone protein subject to regulation by GAP-43. *Nature.* **344**, 836-841.
- Tetzlaff, W., Alexander, S.W., Miller, F.D., and Bisby, M.A. (1991). Response of facial and rubrospinal neurons to axotomy: changes in mRNA expression for cytoskeletal proteins and GAP-43. *J. Neurosci.* **11**, 2528-2544.
- Verge, V.M.K., Tetzlaff, W., Richardson, P.M.L., and Bisby, M.A. (1990). Correlation between GAP-43 and nerve growth factor receptors in rat sensory neurons. *J. Neurosci.* **10**, 926-934.
- Vidal-Sanz, M., Bray, G.M., Villegas-Perez, M.P., Thanos, S., and Aguayo, A.J. (1987). Axonal regeneration and synapse formation in the superior colliculus by retinal ganglion cells in the adult rat. *J. Neurosci.* **7**, 2894-2909.
- Woolf, C.J., Reynolds, M.L., Molander, C., O'Brien, C., Lindsay, R.M., and Benowitz, L.I. (1990). The growth-associated protein GAP-43 appears in dorsal root ganglion cells and in the dorsal horn of the rat spinal cord following peripheral nerve injury. *Neurosci.* **34**, 465-478.
- Zagursky, R.J., Conway, P.S., and Kashdan, M.A.. (1991). Use of ³³P for Sanger DNA sequencing. *Biotechniques.* **11**, 36-38.

FIGURE LEGENDS

FIG. 1 Northern blot analysis of GAP-43 from the ophthalmic region of rabbit trigeminal ganglia after corneal injury. Each lane was loaded with 10 μ g of total RNA. The probe recognizes a single band at 1.4kb. The intensity of the GAP-43 mRNA signal increased at 72 hours with respect to controls.

FIG. 2 Light microscopic autoradiographs of cornea-innervating neurons after GAP-43 *in situ* hybridization. The trigeminal neurons innervating the cornea appear as light blue spots due to the fluorescent dye fast blue. Wounded neurons are displayed on the left and the contralateral controls are on the right. A and D are 3 days, B and E are 7 days, and C and F are 14 days after injury. Control neurons showed little expression of GAP-43 mRNA (contained few silver grains on the blue spots), while the signals were enhanced on wounded neurons. Also, some clusters of silver grains can be seen that are not on the blue spots. Those are localized on neurons that do not innervate the cornea but do hybridize to GAP-43 (x950). These neurons were not used for quantitation.

FIG. 3 Time course of GAP-43 expression in trigeminal neurons innervating the cornea after wounding. For both wounded and control conditions at each time point, the number of silver grains in 75 randomly selected, fast blue-labeled neurons were determined with a Coulter counter. The mean values of grains of wounded neurons divided by that of controls results in the percent increase. Three and 7 days after the injury, GAP-43 mRNA expression increased more than four-fold over control and started to decrease 14 days after the wounding.

FIG. 4 Light microscopic autoradiographs (A and C) after GAP-43 *in situ* hybridization showing that certain trigeminal neurons of unknown destination also express GAP-43. A was taken combining UV and fluorescent lights. C was taken combining UV and phase to visualize the boundaries of the neurons. B is a schematic illustration delineating the neuronal boundaries with the black dots representing the silver grains. Large arrow in A and C indicate a GAP-43 labeled, cornea-innervating (containing fast blue) neuron. Clusters of silver dots not appearing on the blue spots (small arrows in A) are GAP-43-expressing neurons that do not innervate the cornea (small arrow in C). The section was from a trigeminal ganglion 3 days after corneal cryoinjury.

FIG. 5 Western blot using monoclonal mouse anti-GAP-43 antibody and [125 I]-IgG. Each lane contained 19 μ g of protein from the cytosol (C) or membrane (M) fraction. GAP-43 immunoreactivity was detected in the membrane fraction of the corneal epithelial layer 3 days after injury and increased significantly 7 days after injury. The band on the top of the gel corresponds to nonspecific binding according to controls incubated without the primary antibody. The experiment was repeated twice with similar results.

GAP-43 >

0 24 48 72
Hours after injury

Figure 1

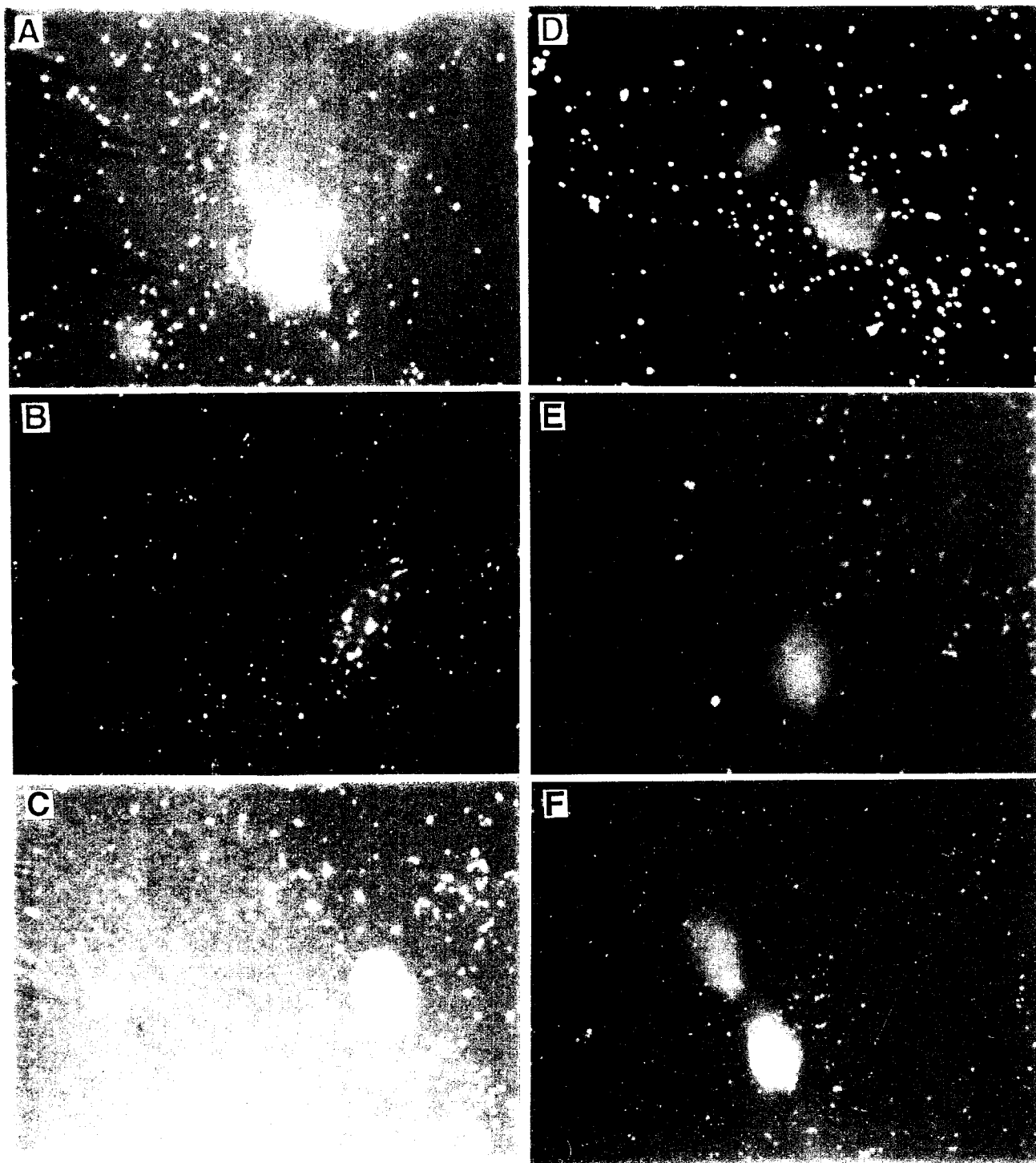


Figure 2

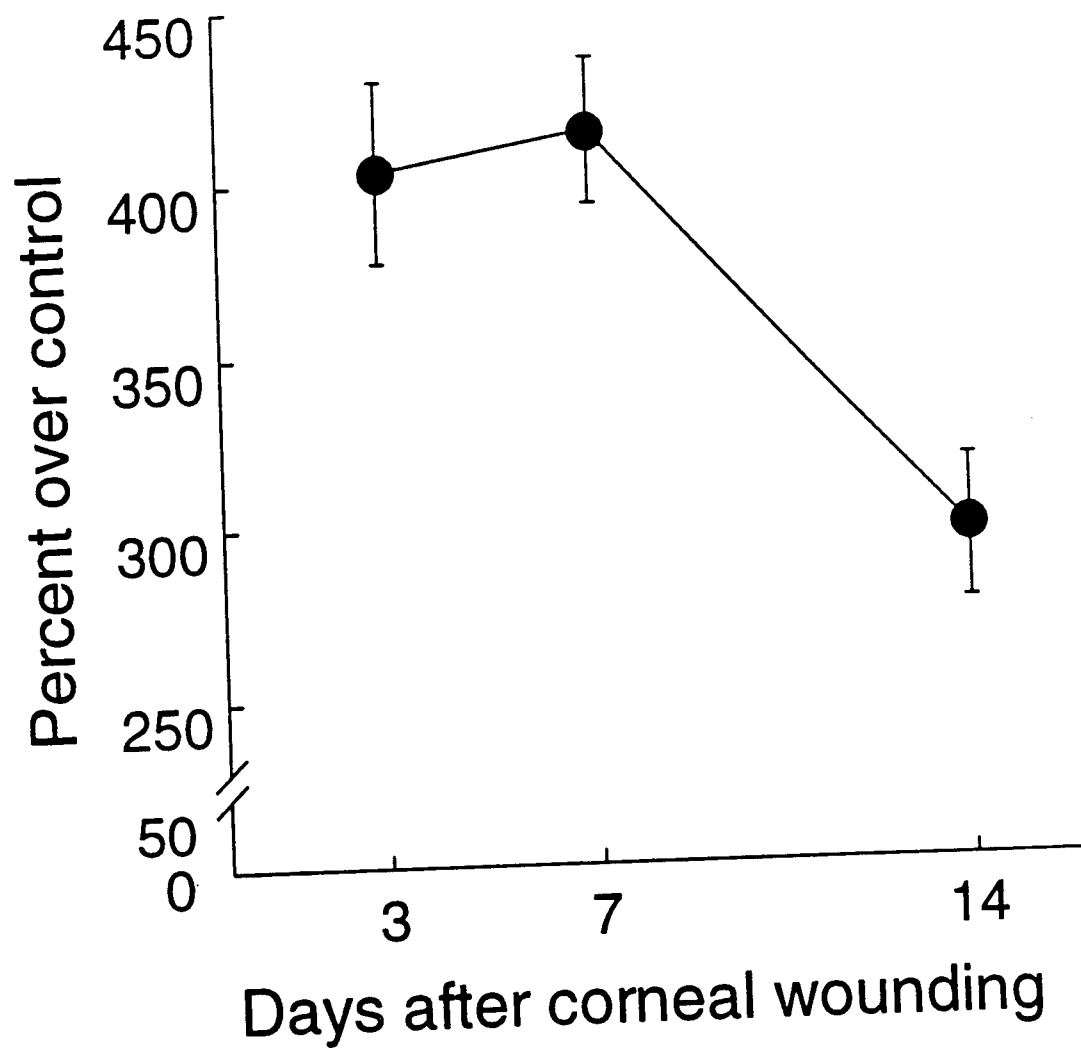


Figure 3

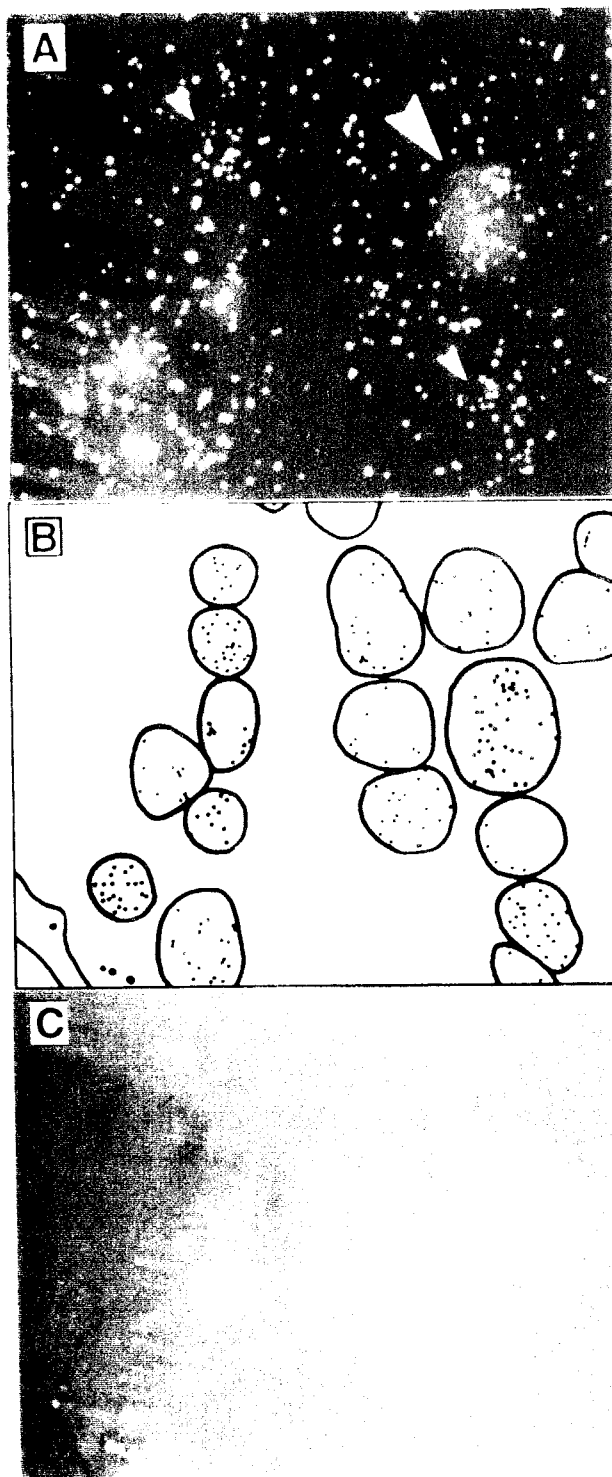


Figure 4

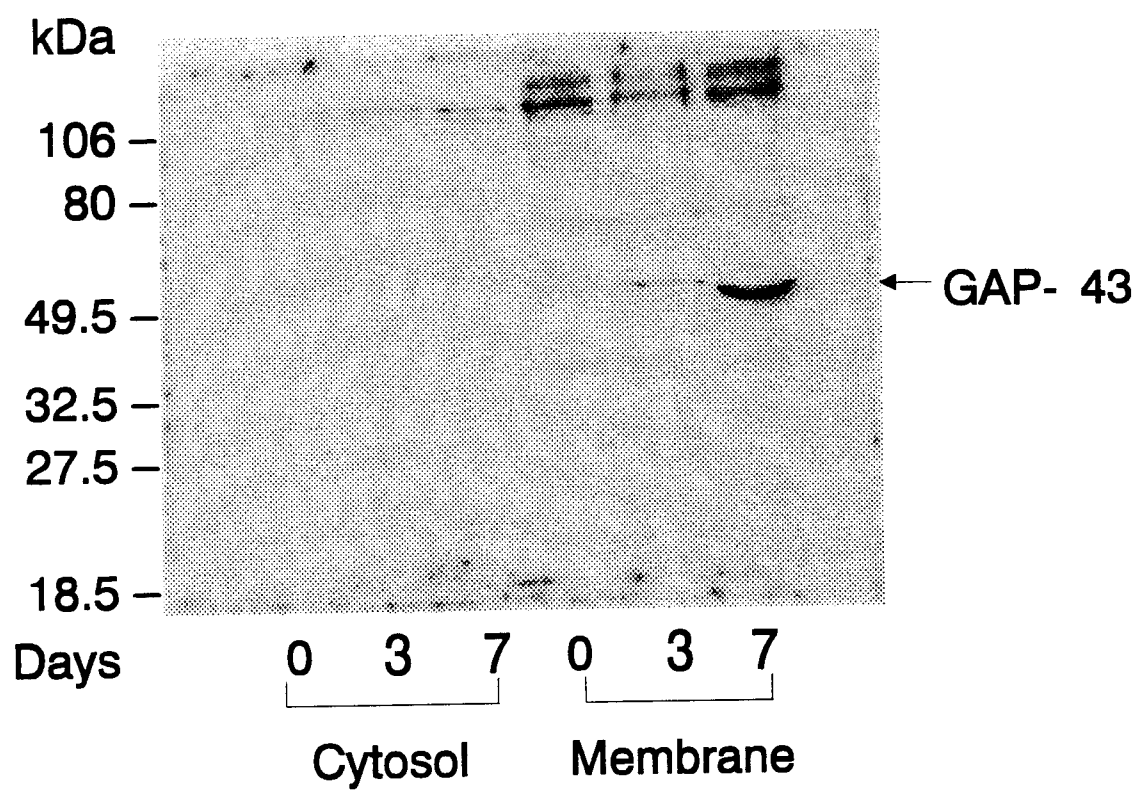


Figure 5

Light Damage Progress Report

1 Outline

- Background
- Long-term light damage
- Short-term light damage
 - Histology
 - TUNEL
 - Ladder
- The effects of PAF on glutamic acid release
- Summary
- General methods and procedures
- References

2 Introduction/background

We have set out to describe the pathophysiological events that are triggered during light damage to the retina and to develop neuroprotective strategies that can prevent or counter these light-induced changes that will lead to delayed cell death. Foremost was the development of a reliable model upon which to conduct these studies. Male albino Wistar rats were used and two models are described. The first model utilizes normal light intensities to slightly prolong the sequence of events, facilitating a physical description of the changes induced within the photoreceptors; the second makes use of higher intensity light to study the nature of the delayed photoreceptor cell death. We have structurally described the temporal sequence of events occurring within the photoreceptors and shown that cell death results from light triggering the process of apoptosis. Finally, we have localized platelet activating factor (PAF) to the photoreceptor terminals and have shown that the presence of PAF will induce the release of glutamate from these cells, while the PAF inhibitor BN52021 blocks the PAF

effect.

3 Demonstrate general, long-term light damage in rat retina

For reference, a section of the rat retina is illustrated in Figure 1, showing the photoreceptors and other relevant retinal layers. In this light micrograph, the four levels along the photoreceptors from which electron microscope sections were taken are localized by squares A, B, C, and D.

Brief Background: White rats are very sensitive to levels of light, and, consequently, light damage easily, making it a possibility that retinal light damage is triggered under normal rat housing conditions. Therefore, it is extremely important to determine precise levels under which retina will be adversely affected.

Question or Statement of Intent: Under what lighting conditions will rat retinas be light damaged when normally housed in our holding incubators, and what form does the light damage take?

Specific Methods: Male, white Wistar rats (see Section 7, General Methods and Procedures, Part A) were placed in either stainless steel cages with metal, slotted tops, or white plastic cages with wire tops. Fluorescent lighting (G.E.® cool white) (see Section 7, General Methods and Procedures, Part B) was adjusted to a 14 h light:10 h dark photocycle, or kept on for the duration of the experiment. Rats were maintained under these conditions for 3 and 6 days. Light intensity was determined by the type of cage in which the rats were housed; within the incubator, light intensity measured on the floor of metal cages with metal, slotted tops was 300 lux, while 1400 lux reached the

floor of white plastic cages with wire tops. An accompanying diagram (Figure 2) outlines these procedures. Following the light damage period, retinas were collected, fixed, and prepared for analysis by light and electron microscopy (see Section 7, General Methods and Procedures, Parts D and F).

Results: Light microscopy of retinal tissue from the light treatment series demonstrates the sequence of events leading to photoreceptor loss. Excessive light first affects the tips of photoreceptor cells (Figure 2, Condition 1), causing apical discs within outer segments to become separated and swollen (Figure 3). However, nuclei appear healthy. Several cone nuclei are visible among the rod nuclei.

Electron microscopy of this tissue reveals that all apical discs are affected, many appearing to be separated from others within the stack (Figure 4). Close examination of the disc rims, however, discloses that disc membranes of sequential discs do not separate. Instead, the upper and lower membranes of the disc disengage, ballooning open to form a large void. Structurally, the basal regions of outer segments and the inner segments (Figure 5) appear to be normal, as well as the outer nuclear layer (Figure 6) and photoreceptor synaptic terminals (Figure 7). An abnormally high number of photoreceptor tips (phagosomes) have been phagocytized by the RPE (Figure 4), but the cytoplasm of these cells remains rich, containing well-structured mitochondria and smooth ER. (See Figure 1 for electron microscope sampling regions.)

With an increase in light intensity (Figure 2, Condition 2), the area of disc swelling slowly extends proximally toward the inner segment, causing the entire outer segment to increase in both length and diameter (Figure 8). Additionally, some vesiculation occurs,

usually near the outer segment - inner segment junction, probably from expansion and separation of these two regions near the connecting cilium. The number of photoreceptor nuclei within the outer nuclear layer has not yet decreased, but some are noticeably dark, suggesting that these pycnotic cells will rapidly disappear.

Electron micrographs reveal numerous old and new phagosomes within the RPE cells (Figure 9), as well as extensive cytoplasmic membrane systems and healthy mitochondria. However, there is extensive microvesiculation within the apical region of the outer segments (Figure 9), and basal discs now show separation and ballooning (Figure 10). Generally, photoreceptor inner segments remain healthy (Figure 11), with rich cytoplasm and intact mitochondria, although occasional degenerating cells are present (Figures 10,11). Photoreceptor terminals maintain dense arrays of synaptic vesicles and well-structured synaptic ribbons (Figure 12), although some evidence of light damage is suggested from the occasional darkened terminal.

By doubling the amount of damaging light over the same period of time (Figure 2, Condition 3), the rate of cell death is increased, reducing the number of nuclei within the outer nuclear layer by half (Figure 13). Interestingly, rod photoreceptors are affected first, since cones represent the majority of the remaining healthy nuclei. Outer segments have remained swollen, but at least half their mass has disintegrated and the fragments phagocytized by RPE cells. Additionally, much more vesiculation is evident, especially near the base of outer segments. Many of the remaining photoreceptor cell nuclei are pycnotic, indicating that additional cell death has already been triggered. Finally, the synaptic region (the outer plexiform layer) appears altered, probably from swelling and

cell dropout.

Electron microscopy of Condition 3 (Figure 2) shows extensive outer segment debris filling the interphotoreceptor matrix, especially in the area adjacent to the RPE cells, and abnormally large phagosomes within the RPE cytoplasm (Figure 14). The more basal portions of the outer segments have some normal portions, but the majority of cells have darkened, swollen, and ballooned discs with associated regions of extensive microvesiculation (Figure 15). Inner segments are disorganized, often with damaged mitochondria, and many cells are darkened, although some remain generally healthy. Occasionally, large, rounded packets of outer segments, located near the inner limiting membrane, are observed in the process of being phagocytized by the Müller cells (Figure 16). Some nuclei appear normal, while others appear darkened and pycnotic, and synaptic terminals can appear healthy, dark, and condensed, or anywhere between (Figure 17). Many dark, residual masses are present within the lighter cytoplasm of the Müller cells, indicating that these cells have been phagocytizing photoreceptor fragments, as well.

Photoreceptors have almost disappeared after 6 days of constant light (Figure 2, Condition 4). Some pycnotic nuclei, presumably from rods, are present, as well as a few healthy cone cells (Figure 18), but these would also rapidly disappear if given more time. There is no evidence of outer segments at the light level, and, interestingly, no sign of phagocytized material within RPE cells. The synaptic layer is greatly reduced since only 12% of the photoreceptors remain. At the electron microscope level, little is left of the photoreceptor fragments, although there is some continual degradation of the remaining

cells. No outer segments are present. Throughout these initial studies there has been no evidence that cells other than photoreceptors have been affected.

Discussions-Conclusions: In this rat model, fluorescent light selectively damages photoreceptors, effecting rods first, then cones. However, the RPE is not damaged but responds by phagocytizing fragments of photoreceptor cells, especially outer segments. Generally, when photoreceptors are light damaged, apical tips of the outer segments are affected first. This response gradually progresses proximally, finally reaching the inner segments. The nucleus then becomes a dark pycnotic mass, followed by inner segment, nuclear, and synaptic degradation. Müller cells appear to be unaffected during these intensities and durations, but do respond by phagocytizing some photoreceptor fragments.

Retinal ultrastructure of these intensity-time sequences suggests an interesting series of events leading up to outer segment disintegration and cell death as light damage proceeds through the stack of discs. It has been suggested that the two membranes of each disc are held in close apposition by the interaction of carbohydrate moieties located near the *N*-terminal on the extracellular side (intradiscal space) of the opsin molecule, and aided by the occurrence of several specific rim proteins (e.g. rom-1 and peripherin/rds) that form the tight, hairpin loops of the disc edges. Ultrastructurally, discs first balloon, probably swelling by the accumulation of fluid within the intradiscal space. For separation to occur, opsin-opsin interactions must be inhibited. This suggests that light first acts on the transmembrane opsin molecule, perhaps through oxidation, altering its structure. By changing the nature of the disc membrane in this

way, permeability could be altered, allowing fluid inside to displace the upper and lower disc surfaces. Despite this, disc rim structures appear normal, suggesting that light damages only components of the disc lamellar regions. Since 85-90% of disc proteins are opsin, it is possible that light has a direct effect on these molecules.

Following initial disc swelling, membrane spheres or tubes appear. These are composed of single membranes (not double membranes as from discs rolling up) that occur in orderly rows or packets across the outer segment, often separated by short regions of intact discs, suggesting formation from single discs. This could occur by local fusions of top and bottom disc lamellae, or rounding up of disc membrane pieces produced from disc distension.

Finally, outer segments appear to fragment, perhaps coming apart in regions where discs have been severely altered. Large masses of packed outer segment portions are then phagocytized, depleting the interphotoreceptor space of outer segments. While it is apparent that damage begins at the distal tips of photoreceptor outer segments and then proceeds proximally toward the inner segment, it is not known why the apical region of photoreceptors is more susceptible to light damage.

4 Demonstrate short-term light damage

Brief Background: Retinal light damage in the rat can occur under normal [human] light levels. To make use of this model, it is important to establish a paradigm for light damage that can be reliably manipulated to produce a constant response. This should result in a regional description of affected areas, a time course for the response,

and evidence for the nature of the mechanism leading to photoreceptor cell loss.

A. Demonstrate light damage histologically

Question or Statement of Intent: When light damage is initiated within the retina, are there regions that are more susceptible than others, and if so, where are they and what is their response time-course?

Specific Methods: Rats were light damaged according to the short-term light damage protocol (7000 lux, 125 $\mu\text{E}/\text{m}^2$ sec, 7.5×10^{19} photons/ m^2 sec) for 2 hours (see Section 7, General Methods and Procedures, Part C), plus time, and retinas prepared for histology (see Section 7, General Methods and Procedures, Part D) immediately before (control) and after (0 days) the 2 h light period, as well as at 1, 2, 4, and 8 days. Retinal layers were measured and nuclei counted from high resolution, 1 μm -thick plastic sections.

Results: A region located in the inferior-temporal retina receives maximal light during unrestrained, *in vivo* conditions (Figure 19). Sections through the optic nerve contain this region on one side and an intact region on the other. Comparisons between these two areas reduce animal variation and demonstrate the degree of light damage. Massive loss of photoreceptors, beginning between 24 and 48 h following light treatment, occurred in the area of light damage, with little or no cell loss in the intact region, as demonstrated by reductions in thicknesses of the photoreceptor outer segment and outer nuclear layers (Figure 20) and numbers of photoreceptor nuclei (Figure 21). The number of photoreceptor nuclei remains constant through 24 h post-

treatment, but then begins to rapidly decrease. By 48 h, loss is greater than 50%, and after 4 days, the numbers have been further reduced by about 20%; by day 8 post-damage, only about 12% of the original number remain. Morphology of the surviving nuclei reveals them to be of cone photoreceptors (10-15% of all rat photoreceptors in normal retinas are cones). As rod nuclei disappear, their corresponding outer and inner segments become reduced, shrinking the thicknesses of these retinal layers.

Discussions-Conclusions: This response to excessive light occurs within the portion of the retina normally positioned beneath the light source (the inferior-temporal region). Retinal regions across the optic nerve (e.g., inferior-nasal) appear to be less damaged, presumably because they receive less light, not because they are less sensitive. However, this remains to be tested.

Light damage, while brief (2 h), triggers a sequence of long-term alterations, culminating in photoreceptor cell death as evidenced by nuclear dropout. Disappearance begins after 24 h post-treatment, and has progressed far beyond the midpoint by 48 h. Plots of the percent of nuclei lost per time interval (rate of loss) suggest that the peak of nuclear dropout occurs at or just before 48 h post-light damage (Figure 21). Moreover, the induced, local degeneration is nonreversible, with cell loss occurring up to 2 days later under a dim light cycle, suggesting that the initial damage occurs rapidly, triggering a sequence of events that results in photoreceptor death and disappearance 24 h later.

B Demonstrate the mechanism through which light induces photoreceptor

cell loss

Question or Statement of Intent: Photoreceptor death can result from damage leading to disruption of cell membranes and organelles, a process referred to as necrosis, or through apoptosis by the induction of DNA endonucleases that cut DNA between the nucleosomes into specifically sized, recognizable fragments. Is the loss of photoreceptor cells following light-induced degeneration triggered by an apoptotic mechanism?

Specific Methods: Rats were light damaged according to the short-term light damage protocol described above (see Section 7, General Methods and Procedures, Part C). Retinas were prepared for paraffin histology (see Section 7, General Methods and Procedures, Part D) before (control) and after (0 days) light damage, as well as at 1, 2, 4, and 8 days post-damage. Retinas were sectioned at 5 μ m thickness and the number and location of apoptotic (pink) photoreceptor nuclei observed in the light microscope (see Section 7, General Methods and Procedures, Part F) by the Terminal dUTP Nick End Labeling (TUNEL) technique, as described by Gavrieli et al. (1992) and Portera-Cailliau et al. (1994) (see Section 7, General Methods and Procedures, Part E).

Results: Control retinas (no light damage) showed no TUNEL labeling. When the TdT enzyme was omitted, no labeling occurred, and when sections were treated with DNase (positive control), all nuclei labeled. Within the region of light damage (the inferior-temporal region), most nuclei labeled throughout the time series, beginning somewhere around 24 h post-damage. However, some (10% or less) remained clear. There was always a small population of densely labeled cells, with the remaining labeled

nuclei appearing a lighter pink-purple. The number of nuclei declined as in previous experiments, dropping to about 50% of normal by 48 h post-treatment. By 8 days, 1-2 rows of nuclei were left, but no defined inner or outer segment regions existed. Many of the residual nuclei appeared pink.

Discussions-Conclusions: The appearance of TUNEL-label within the nuclei of photoreceptors in the inferior-temporal region indicates that the process of apoptosis has been triggered. Since these nuclei labeled from day 1 post-damage onward, but not in light damage controls (prior to 2 h treatments), excessive light is initiating apoptosis. Further, because there were some cells that appeared more heavily labeled than others, it can be assumed that some photoreceptors enter the apoptotic pathway earlier, and thus, have more extensive damage to their DNA than cells just entering. A wave of cell death, spread over several days, could imply: 1) photoreceptors have different apoptotic thresholds, some requiring more light damage than others; 2) the rate at which apoptosis proceeds, once triggered, varies within the photoreceptors-- some progress faster, while others proceed more slowly, dying after a longer time interval. Since all photoreceptors were light-exposed for the same brief 2 h period, and then placed under dim cycled light for the duration of the experiment, different apoptotic thresholds can be ruled out. In addition, there is no evidence that multiple rod types, with different sensitivities, exist within the rat retina.

This wave of rod photoreceptor apoptosis is concluded by about 8 days (probably even less), leaving a small number of photoreceptor nuclei presumed to be from cone cells. Interestingly, many of these nuclei also appear to label (by 8 days), suggesting

that the remaining, less sensitive cones, are also damaged and will eventually drop out as well. This could mean that cone cells: 1) are also light-triggered, but have a slower apoptotic rate; or 2) undergo cell death through apoptosis that is triggered much later, perhaps even by a rod-mediated (local environment) mechanism.

It can be concluded that light can trigger, in a nonreversible manner, apoptosis within photoreceptors, beginning at about 24 h post-damage, and that once initiated, the process will run to completion, but at a rate independent of other nearby cells. There appear to be two retinal apoptotic processes, one early wave of cell death involving rod photoreceptors and a later, or longer lasting, wave that results in cone photoreceptor cell death.

C Demonstrate by an alternative method (the Ladder technique) that light damage triggers apoptosis

Question or Statement of Intent: It can be argued that once a cell begins to die, if detected early enough, the endonuclease-damaged DNA (apoptosis) and DNA undergoing random degradation (necrosis) will have enough available 3'-ends that TUNEL could give a false positive result. Therefore, it is important to demonstrate that the cut DNA lengths that are labeling by the TUNEL technique are all 120-140 base pairs long, or are multiples of these lengths. Electrophoretic comparisons with commercially prepared 123 base pair DNA ladders will demonstrate specific apoptosis-triggered endonuclease DNA cutting. Is the TUNEL labeling observed in the light damaged region of the retina conclusively due to triggering of the apoptotic process, as

determined by the Ladder technique?

Specific Methods: Generally, the methods of Tso et al. (1994) were followed (see Section 7, General Methods and Procedures, Part G). Rats were light damaged for 2 h, and then kept under dim cycled light for 15, 20, 25, 30, 45, and 60 h (see Section 7, General Methods and Procedures, Part C). Non-stimulated controls were also used. Retinas were isolated from treated rats according to the protocol outlined above, placed into 2 ml plastic, freezer-safe vials, and dropped into liquid nitrogen. They were stored at -40 °C until needed.

Results: Commercial 123 Ladder DNA and rat thymocytes with naturally occurring apoptosis demonstrated DNA laddering, but nuclei isolated from experimental retinas had a varied response. Control retinas showed no laddering, nor did the 15 and 20 h samples. However, 25, 30, 45, and 60 h nuclei demonstrated laddering, with the strongest response appearing at 30 h (Figure 22). The 25 and 60 h responses were very faint.

Discussions-Conclusions: Electrophoresis, showing precise laddering profiles and lack of DNA smearing, demonstrates that the apoptotic-like cell death triggered by excessive light is, in fact, due to the process of apoptosis. Thymocytes are positive, illustrating the sensitivity of this method, and early treatments are negative, showing that endonuclease activity occurs only after about 25 h post-damage. Peak DNA ladders occurred around 30 h, preceding the peak in nuclear dropout at 48 h (see above experiments) by 18 h. Interestingly, the DNA ladders obtained here also illustrate a gradual, prolonged wave of cell death, evident by faint banding at 60 h. It can be

concluded that the process of retinal photoreceptor cell death triggered by light is apoptotic, resulting from the induction of specific endonucleases.

5 Platelet activating factor (PAF) and its relevance to retinal damage

Brief Background: PAF is produced from an alkyl-acyl-glycerophosphocholine, a minor component of the phosphatidylcholine fraction of cell membranes, by the action of a phospholipase A_2 and an acetyltransferase, and then interacts at specific membrane binding sites to increase intracellular calcium (Bazan, 1990). Large calcium influxes trigger the release of excitatory amino acids, especially glutamate, which over-stimulate NMDA receptors, causing excitotoxicity and eventual cell death. PAF has been located in the retina (Bussolino, et al., 1986), and Remé, et al. (1992) showed that PAF is released in retina following 30 min of damaging fluorescent light (400-450 lux) and 2 h of darkness. Furthermore, the PAF antagonist, BN52021, reduced light damage lesions of rod outer segments, strongly implicating PAF as a primary factor in the mechanism of light damage-induced retinal degeneration.

Question or Statement of Intent: Will the presence of PAF in the retina enhance glutamate release, and if so, can the response be inhibited by the synaptic membrane PAF receptor antagonist BN52021?

Specific Methods: Rat retinas were dissociated by a brief exposure to pronase and DNase I, followed by loading with [3 H]glutamate (5 μ Ci / 50 μ g protein; specific activity, 55 Ci/mmol). A perfusion system (Figure 23) was used to follow the time course of [3 H]glutamate efflux obtained by a pulse of 0.5 ml of 0.3, 0.6, and 1.0 μ M of

PAF solution on the perfusion cell, maintained at a flow rate of 6 ml / min with a saline buffer at room temperature. (For details, see Section 7, General Methods and Procedures, Parts H, I, and J.)

Results: Potassium (40 mM), as well as PAF, enhanced [3 H]glutamate release from loaded cells (Figure 24), while a pulse of 0.5 ml of 40 mM KCl induced the release of more than 40% of total [3 H]glutamate taken up by retinal cells. When cells were subjected to incubation and perfusion in the presence of 1 μ M BN52021, most glutamate released after PAF induction (100 μ M) was inhibited. Isolated synaptosomes showed the same general results (Figure 25). Moreover, the synaptic membrane PAF receptor antagonist BN52021 inhibited PAF-induced [3 H]glutamate release to basal levels. PAF, at 10 nM concentration, stimulated more than 20% release of total label (Figure 25). In retinal tissue, the P_1 fraction, composed mainly of cell debris and nuclei, also contains the large glutaminergic synaptic terminals of photoreceptor cells. When this fraction was loaded with [3 H]glutamate, a concentration-dependent release in the presence of PAF was demonstrated (Figure 26). Also, KCl triggered an increase in glutamate release in the presence of the PAF inhibitor.

Discussions-Conclusions: PAF-induced [3 H]glutamate release in rat retinal fractions was obtained with concentrations as low as 10 nM, producing a 25% increase above basal levels at this value and 40 mM KCl induced an increase of up to 45%. Pretreatments with buffer containing 1 μ M BN52021 inhibited PAF-induced [3 H]glutamate release, but did not inhibit the KCl-induced release. Photoreceptors possess a glutamate uptake system, utilizing this compound as their transmitter.

Moreover, glutamate, present in numerous vesicles within the large photoreceptor terminals, is more abundant in the outer plexiform layer than in any other region of the retina. [^3H]glutamate release was more efficiently inhibited in the photoreceptor synaptosomal membrane preparations than from membranes obtained from the rest of retina, probably because of the greater amounts of glutamate and an abundance of PAF receptors on photoreceptor terminals. Remé et al. (1992) have shown that PAF is released in the retina following light damage, and that PAF inhibitors will block the damaging effects of light. Our study demonstrates the presence of PAF receptors in photoreceptor synaptosomes (Marcheselli and Bazan, 1993), showing that their activation is coupled to glutamate release, probably through the action of calcium influx, and suggests that the initial site of BN52021 protection lies in the photoreceptor synaptic terminal membrane.

6 Summary

Our studies on the effects of light damage and the pathophysiological events triggered in the retina have resulted in the development of two models of light damage; a long-term (several days) form induced by normal levels of fluorescent light and a short-term (several hours) form triggered by excessive amounts of light. Use of both models reveals the sequence of events leading to delayed photoreceptor cell death.

The fluorescent lights used to damage retinas does not affect the retinal pigment epithelium or the Müller cells, since both cell types contribute to the phagocytosis of dead cells and remain after the loss of photoreceptors. The first effects of light damage

appear as enlarged regions at the photoreceptor outer segment tips, where the disc membranes have swollen and separated. This response slowly moves down the outer segment to the inner segment, disrupting the structure of the light-sensitive membranes in a manner suggesting edema. Once the outer segments have fragmented, the inner segments begin to undergo changes. Photoreceptors drop out as inner segments die. This is evident by the dramatic decrease in nuclei. In the short-term model, 2 hours of excessive light will reduce the number of photoreceptors to 50% within 2 days, and leave only about 10-20% after 1 week. The remaining cells are cone photoreceptors, indicating that rod cells are the most light sensitive. However, given longer time intervals, most cones will also die.

This delayed photoreceptor cell death results from light triggering apoptotic mechanisms that induce specific endonucleases to cleave DNA, and has been demonstrated by techniques that label cut DNA (TUNEL) as well as by methods that show unique DNA fragment lengths (Ladder) characteristic of apoptosis. Finally, it has been shown that PAF receptors are located within the synaptic membranes of photoreceptors. Synaptosomes, preloaded with [3 H]glutamate, can be induced to release labeled glutamate by the addition of PAF, while the presence of the PAF inhibitor BN52021 prevents the PAF effect. Since it is known that excessive light will cause the release of PAF in the retina, and that BN52021 can reduce the effects of light damage, it appears that the PAF receptors of the photoreceptor terminals, perhaps through calcium interaction, may be directly involved in initiating photoreceptor damage that will trigger apoptosis and delayed cell death.

7 General Methods and Procedures

A. *Animals*: Male, white Wistar rats, 175-200 g, purchased as needed from Hill Top Laboratory Animals (Scottsdale, PA), were used in this study. Rats arrived within 24 h after ordering and were placed immediately in stainless steel, slotted topped cages on a 12 h light 12 h dark photocycle, with ambient light levels set to about 2 lux. Animals were maintained under these conditions for 1 wk prior to use, and given laboratory rat chow and water, *ad libitum*. Throughout these experiments, animals were kept at room temperature.

B. *Light Source and Intensity Calibration*: Fluorescent lamps (G.E.[®] cool white) supplied all illumination during these experiments. Spectral emissions of these bulbs have been published (Kaufman and Haynes, 1981) and used in previous visual studies (Dahl and Gordon, 1992). A LI-COR[®] (Lincoln, NE) quantum/radiometer/photometer (LI-189) with appropriate sensors was used to measure the photon flux density ($\mu\text{E m}^2 \text{ sec}^{-1}$) from 400-700 nm and the density of luminous flux, or illuminance (lux), measured under the "absolute sensitivity figure established for the standard [human] eye," peaking at 555 nm. We have not yet made use of specific spectral regions of the fluorescent light output in these light damage experiments; all retinal stimulation was conducted under fluorescent "white" light conditions. Intensity was adjusted by the addition of fluorescent lamps above white plastic bins or by moving metal cages away, onto dimly lit shelving. Light measurements, taken from the floor of the cages, were used to establish experimental conditions.

C. Short-term Light Damage: Rats were placed in empty, white, wire topped plastic bins in a constant temperature (25° C) incubator with four 24-inch fluorescent bulbs (G.E.® cool white) supplying approximately 7000 lux (125 $\mu\text{E}/\text{m}^2$ sec, or 7.5×10^{19} photons/ m^2 sec) for 2 hours. Animals were then returned to their normal cages, intensity, and photocycle for 0, 1, 2, 4, or 8 days. All light damage was initiated at 10:00 am, and retinas were normally taken around noon. In some experiments where shorter times were required, retinas were fixed at 5 h intervals following the 2 h light exposure.

D. Preparation of Retinal Tissue: Following light damage, animals were killed by over-anesthetization with ether or CO_2 exposure generated from dry ice. After eyes were removed and corneas slit, tissue was placed in fixative. The front of each eye was then removed, the lens lifted out, and the eyecup trimmed with a razor blade. When fixation had been completed, tissue was dehydrated and embedded in either plastic, for light and electron microscopic analysis, or in paraffin, for TUNEL analysis. All retinal dissections and trimming were done with the aid of a Nikon SMZ-U stereo-zoom dissecting microscope.

Fixation for plastic-based light and electron microscopy followed conventional, published (Gordon and Bazan, 1990, 1993) procedures. Briefly, tissue was placed in primary fixative that consisted of 2% glutaraldehyde and 2% formaldehyde in 0.135 M sodium cacodylate buffer (pH 7.3) overnight at 4° C. After trimming eyecups the next day, retinal pieces were rinsed in cacodylate buffer (0.135 M) three times, 15 min each, and then postfixed for 1 h in 1% OsO_4 in cacodylate buffer (0.135 M), rinsed again three

times in buffer, and run through an ethanol 20% step dehydration series to acetone. Infiltration and plastic embedding occurred in a mixture of Epon-araldite plastic (Mollenhauer, 1963), followed by sectioning.

Glass knives were used to produce 1 μm -thick plastic sections for light microscopy, which were subsequently stained with 1% toluidine blue in 1% boric acid. A diamond knife was used to cut silver-gold sections for electron microscopy, which were then placed on parlodion-coated, 100 mesh, hexagonal nickel grids and contrasted with uranium and lead salts.

Fixation for paraffin-embedded tissue was done according to published methods (Humason, 1972). Tissue was placed in 4% formaldehyde and phosphate buffered saline overnight. Following standard eyecup preparation and trimming of tissue, retinal samples were washed in phosphate buffered saline and dehydrated through an ethanol series to xylene. Tissue was then infiltrated and embedded in paraffin (56-57° C).

Metal knives were used to cut 5 μm -thick paraffin sections, which were then placed in distilled water on glass microscope slides (Superfrost/plus; Fisher Scientific, Pittsburgh, PA), and dried on a slide warmer. After deparaffinizing in xylene, sections were rehydrated and then processed for TUNEL analysis of 3'-nicked end DNA. Subsequently, sections were coverslipped with Aqua-Poly/Mount (Polysciences; Warrington, PA) and allowed to set. Counter staining was not employed.

E. Terminal dUTP Nick End Labeling (TUNEL) Technique: Generally, the technique described by Gavrieli et al. (1992) and Portera-Cailliau et al. (1994) was followed.

Deparaffinized, rehydrated sections were treated with Proteinase K (20 µg/ml) in 10 mM TRIS-HCl (pH 8.0) for 15 min, and then rinsed four times (2 min each). Slides were then placed in 3% H₂O₂ for 5 min to inactivate endogenous peroxidases and then rinsed three times in water. At this point, any positive controls were incubated with DNase I (1 µg/ml) for 10 min at 37° C, and then washed. All slides were then preincubated for 10 min at room temperature in TdT buffer (30 mM TRIS-HCl, 140 mM sodium cacodylate, and 1 mM cobalt chloride; pH 7.2), followed by incubation for 1 h at 37° C in a moist chamber with 25-50 µl of TdT buffer containing 0.5 units/µl buffer and 40 µM biotinylated 16-dUTP. The reaction was stopped by immersing the slides in double strength SSC buffer (300 mM NaCl; 30 mM sodium citrate) for 15 min, and then rinsing in water and PBS buffer. Finally, sections are incubated for 1 h at 37° C in Vectastain® ABC peroxidase standard solution (Vector Laboratories; Burlingame, CA), rinsed twice in PBS, and stained for 30-60 min, using aminoethylcarbazole as a substrate. The reaction was stopped by rinsing in water and sections coverslipped in Aqua-Poly/Mount (Polysciences; Warrington, PA). Apoptotic nuclei appear pink to purple in color, all others are colorless.

F. Microscopy: Light microscope sections were viewed, analyzed, and photographed with a Nikon Optiphot-2 upright microscope, equipped with bright field, dark field, phase contrast, and Nomarski differential interference contrast optics. A Sony, three-color CCD camera system, attached to the microscope, permitted viewing and cell counting on a Sony analog/digital color video monitor, and a Nikon UFX-DX automatic camera

system allowed 35mm photography of the sections.

Ultra thin sections were viewed with a Zeiss C10 transmission electron microscope (Carl Zeiss, Jena, Germany), and photographed on 3¼" x 4" Kodak electron microscope film 4489 (EMS, Ft. Washington, PA). D-19 developer (Kodak, Rochester, NY) was used for 4 min.

G. Ladder Technique: The method of Tso et al. (1994) was used to recover DNA from experimental retinas. Frozen samples were thawed in buffer, consisting of Tris-HCl (10 mM, pH 7.6), Na₂EDTA (100 mM), SDS (0.5%), proteinase K (200 µg/ml), and RNAase A (50 µg/ml) for 3 h at 45 °C. The thick lysate was pushed through 19½-, 22½-, and 26½-gauge needles, and the DNA extracted twice with phenol, chloroform, and isoamylalcohol (25:24:1) and once with chloroform. Following overnight precipitation at -20 °C in ethanol, it was dissolved in 200 µl of TE, containing Tris-HCl (10 mM, pH 7.6) and Na₂EDTA (1 mM). DNA concentration was determined by measuring its absorbance at 260 nm.

Portions of DNA samples (20 µg) were subjected to electrophoresis on a 1.8% agarose gel, containing ethidium bromide (0.5 µg/ml), in a running buffer of 1x TAE (pH 8.0) for 16 h at 35 volts. For calibrations, commercial, 123 DNA ladder samples were run along side. Gels were photographed under UV light.

H. Preparation of retinal membrane fractions: Albino Sprague Dawley rats weighing 150-220 g were killed by decapitation after slight anesthesia. Eyes were rapidly

enucleated and retinas removed and subjected to cell dissociation. A saline buffer, composition 145 mM NaCl, 5 mM KCl, 1.2 mM $MgCl_2$, 2 mM EGTA, 10 mM HEPES, 10 mM D-Glucose, (7.5 pH, 4 °C), was used to resuspend the cells. Retinas were incubated at 37 °C for 10 min in saline buffer containing 1 mg/ml pronase. Medium was removed and replaced with fresh saline buffer containing 10 µg/ml DNase and 0.5% BSA, and incubated for 2 min. After rinsing with 2-3 volumes of saline buffer, the procedure was repeated 3 times. Retinas were dissociated by carefully passing them through pipet tips that had been cut to a 4-mm diameter tip (Lolley et al 1986). Once a homogeneous suspension had been obtained, cells were rinsed with cold saline buffer and pelleted by a short centrifugation of 5000 rpm for 2 min in an Ependorf centrifuge. Dissociated cells were then resuspended in saline buffer at a protein concentration of 1 µg/µl.

When subcellular fractions were used, retinas were rapidly immersed in a buffer containing 50 mM Tris-HCl, 2 mM EGTA, 5 mM $MgCl_2$, 0.1 mM PMSF, and 250 mM sucrose (7.4 pH, 4°C), and then homogenized with 5 strokes of a glass-Teflon Potter-Elvehjem homogenizer. A slow speed centrifugation in a Beckman J2-21M centrifuge with a JA.20.0 rotor at 121 x g for 5 min yielded a pellet containing most cell debris. A second centrifugation at 1090 x g for 11 min yielded the P_1 fraction which contains most nuclear membranes, plasma membranes, and the large photoreceptor synaptic terminals. A third centrifugation step, carried out at 17400 x g for 20 min, produced the P_2 pellet containing most synaptosomes and mitochondria. The P_1 and P_2 fractions were resuspended in the same buffer used for homogenization at a final protein concentration

of 1 µg/µl.

I. ³H-Glutamic acid loading and perfusion: ³H-glutamic acid was loaded to 50 µg of dissociated cells or synaptosomes from P₁ and P₂ fractions by addition of 100 µl of saline buffer containing 2.5 µCi ³H-glutamic ac. (specific activity 17.25 Ci/mmol) and 10 min incubation at room temperature. Samples after incubation were diluted with 350 µl saline buffer and loaded to the perfusion cell. A perfusion cell designed and built in our facilities was employed during this studies. The cells or synaptosomes were loaded on GF/B Watman glass fiber filters. The perfusion cell held the glass fiber filter between the two lucite blocks and the Buna O ring which creates the cell body. The surface of the glass fiber filter was 4.5 mm and the death volume of cell including tubing was proximate 0.5 ml. An HPLC pump was used to deliver saline buffer (as described earlier with the addition of 0.025% BSA) at 6 ml/min of constant flow without pulsations and an injection port was used to inject 200 µl of a solution containing KCl or PAF in the concentrations later specified. When an antagonist was used, a buffer containing the compound was delivered trough a secondary pump. The perfusate were send to a radio-chromatography detector (Radiomatic FLO-ONE Beta series A-500, Packard, Meriden, Connecticut) for onflow detection, or to a fraction collector (Foxy, ISCO, Lincoln, Nebraska) for liquid scintillation analysis or endogenous amino acids analysis.

J. Quantitative analysis of endogenous amino acids: Endogenous amino acids were converted into thio-substituted isoindoles by the o-phthaldialdehyde (OPA) reaction

(Lindroth et al. 1979). The derivatives were immediately separated by HPLC chromatography on a Microsorb™ AAAnalysis™ type 0 column 4.6 mm ID x 10 cm L, provided with a guard column 4.6 mm ID x 1.5 cm L, both column and guard column were loaded with C18 reserved batch, particle size 3 μ (Rainin, Woburn, MA). Detection was obtained with a fluorescence detector Beckman AI 406/fluorescence 157 (Beckman, San Ramon, CA), excitation wavelength 305-395 nm, and emission filter wavelength 420-650 nm, 9 μ l flow cell, sensitivity range was 0.1 pM to 10 pM. The HPLC pumps Beckman 126 (Beckman, Fullerton, CA) delivered a gradient mixture 85 % A - 15% B to 0% A - 100% B in 45 min, with a flow rate of 1 ml/min. The solvent A was 0.1 M NaOAcetate/methanol/tetrahydrofuran (95/4.5/0.5) filtered and saturated with He, the solvent B was methanol. Amino ac. standard (Sigma, St. Louis, MO) were individually resuspended 50% methanol/water and mixed to produce a quantitative standard (1 pM/ μ l). Sample derivatization was as follows, 5 μ l of perfusate, mixed with 5 μ l of 2% SDS in 0.4 M Na_3BO_3 , pH 9.5, and 5 μ l of OPA react (50 mg OPA, 1.25 ml methanol, 11.2 ml 0.4 M Na_3BO_3 , 50 μ l 2-mercaptoethanol). Mix well and incubate 1 min, add 10 μ l of 0.1 M K_2HPO_4 pH 4.0 and 75 μ l running buffer A, 50 μ l reaction mixture were injected into HPLC within 2 min of starting reaction to avoid decomposition of some unstable amino acid derivatives (Jones et al. 1981). Data acquisition and analysis was performed with a System Gold™ Version 7.0 software (Beckman, Fullerton, CA).

7 References

Bazan NG. 1990. Involvement of arachidonic acid and platelet-activating factor in the response of the nervous system to ischemia and convulsions. In: *Lipid Mediators in Ischemic Brain Damage and Experimental Epilepsy. New Trends in Lipid Mediators Res.* 4:241-252.

Bussolino F, Gremo F, Teta C, Pescarmona GP, Camussi G. 1986. Production of platelet-activating factor by chick retina. *J Biol Chem.* 261:16502-16508.

Dahl NA, Gordon WC. 1992. Photomembrane turnover in frog retina: Light intensity and spectral correlates. *Exp Eye Res.* 55:839-852.

Gavrieli Y, Sherman Y, Ben-Sasson SA. 1992. Identification of programmed cell death in situ via specific labeling of nuclear DNA fragmentation. *J Cell Biol.* 119:493-501.

Gordon WC, Bazan NG. 1990. Docosahexaenoic acid utilization during rod photoreceptor cell renewal. *J Neurosci.* 10:2190-2202.

Gordon WC, Bazan NG. 1993. Visualization of [3 H]docosahexaenoic acid trafficking through photoreceptors and retinal pigment epithelium by electron microscopic autoradiography. *Invest Ophthalmol Vis Sci.* 34:2402-2411.

Humason GL. 1972. *Animal Tissue Techniques*, Third Edition. W.H. Freeman: San

Francisco.

Jones B, Pääbo S, Stein S. 1981. J Liquid Chromatography. 4:565-596.

Kaufman JE, Haynes H. 1981. IES Lighting Handbook: Reference Volume.
Illuminating Engineering Society of North America: New York.

Lolly R, Lee R, Chase D, Racz E. 1986. Invest Ophthalmol Vis Sci. 27:285-295.

Marcheselli VL, Bazan NG. 1993. Platelet activating factor (PAF) enhances glutamic acid release in the retina through a presynaptic receptor. Invest Ophthalmol Vis Sci. 34(ARVO suppl):1704.

Mollenhauer HH. 1963. Plastic embedding mixtures for use in electron microscopy. J Stain Tech. 39:111-114.

Portera-Cailliau C, Sung C-H, Nathans J, Adler R. 1994. Apoptotic photoreceptor cell death in mouse models of retinitis pigmentosa. Proc Natl Acad Sci, USA. 91:974-978.

Remé C, Wei Q, Munz K, Jung H, Doly M, Droy-Lefaix MT. 1992. Light and lithium effects in the rat retina: Modification by the PAF antagonist BN-52021. Graefes Arch Clin Exp Ophthalmol. 230:580-588.

Tso MOM, Zhang C, Abler AS, Chang C-J, Wong F, Chang G-Q, Lam TT. 1994.

Apoptosis leads to photoreceptor degeneration in inherited retinal dystrophy of RCS rats.

Invest Ophthalmol Vis Sci. 35:2693-2699.

Figure 1

This light micrograph section of rat retina shows the blood supply within the choriocapillaris at the top, and the retinal pigment epithelium (RPE) immediately below. Photoreceptors extend downward from the RPE to the outer plexiform layer (OPL) where the synaptic terminals are situated. Photoreceptor outer segments (OS) contain the light sensitive disc membranes, while typical metabolic organelles are localized within the inner segments (IS). Because of the relatively small diameter and large number of photoreceptors, their nuclei are packed within a thick outer nuclear layer (N), usually composed of stacks, 10-13 nuclei tall. Everything below the OPL consists of higher order neurons and the glial-like Müller cells that extend from the vitreal interface at the bottom of the retina to near the top of the inner segments. The boxes A, B, C, and D represent the regions along the photoreceptor length from which electron microscopy samples were taken. In subsequent micrographs, the sample level is indicated by the corresponding letter.

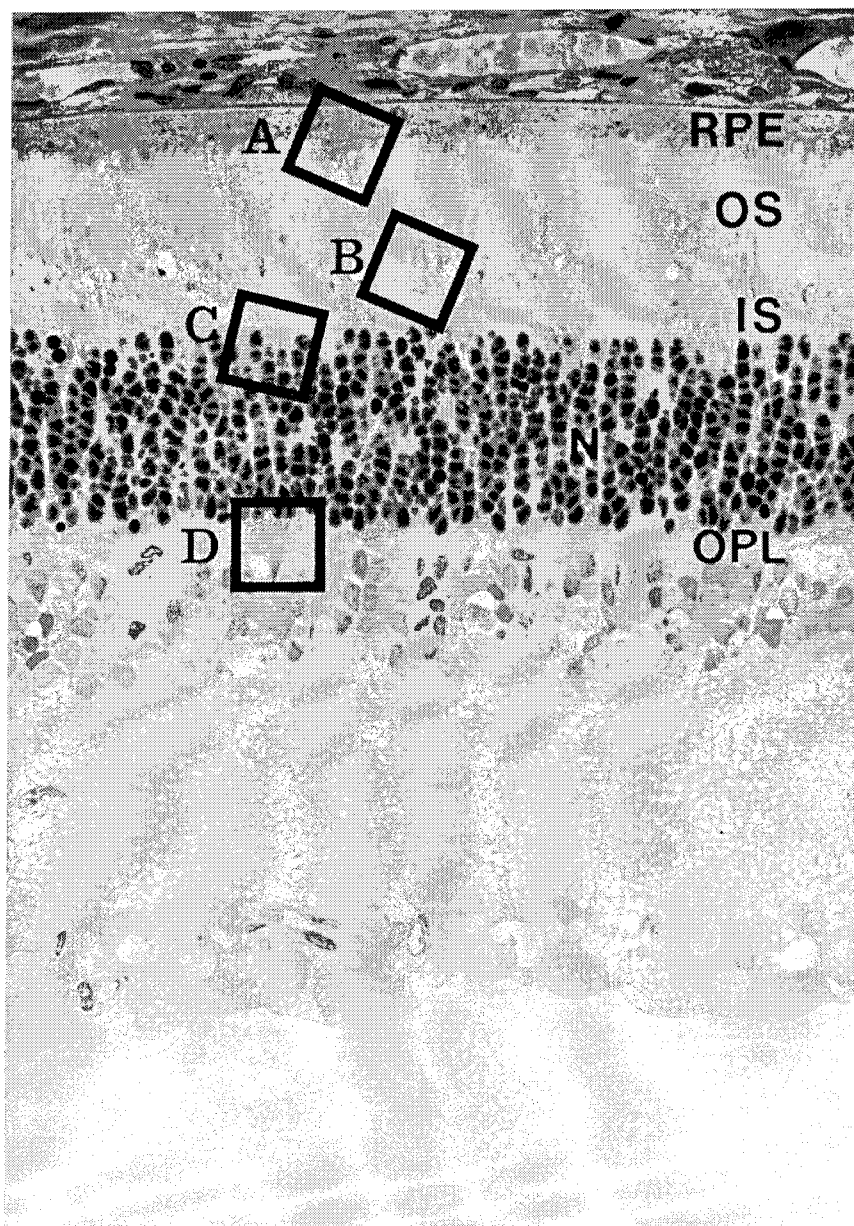
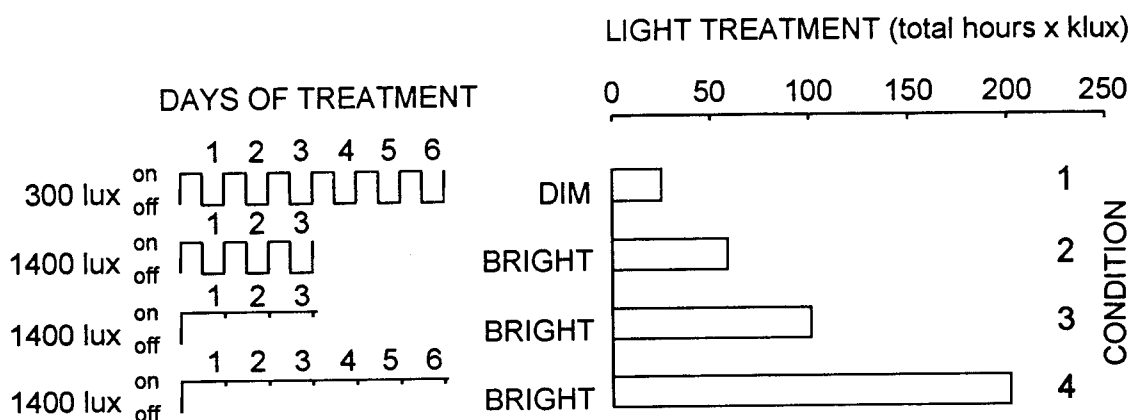


Figure 2

This diagram illustrates the protocol for the long-term light damage. Four conditions, 1-4, are shown. Conditions 1 and 2, lasting for 6 days and 3 days, respectively, used cycled light (14 hours light: 10 hours dark). The amount of light measured at the bottom of a metal cage with narrow slotted top was 300 lux, while the amount at the bottom of a white plastic cage with wire top was 1400 lux. Conditions 3 and 4, also in white plastic cages, used continuous light for 3 days and 6 days, respectively. The amount of light (lux) multiplied by the total number of light-hours for each condition produces a number representative of the light history for each condition. When plotted (upper right), it shows that each successive condition has approximately twice the light of the previous treatment.

LIGHT DAMAGE PROTOCOL



	CAGES	DURATION	LIGHT TREATMENT INDEX
1	METAL	6 DAYS CYCLED LIGHT	84 h, 300 lux → 25
2	PLASTIC	3 DAYS CYCLED LIGHT	42 h, 1400 lux → 59
3	PLASTIC	3 DAYS CONSTANT LIGHT	72 h, 1400 lux → 101
4	PLASTIC	6 DAYS CONSTANT LIGHT	144 h, 1400 lux → 202

Figure 3

Light micrograph of a rat retina treated according to Condition 1. Dark arrow indicates swollen photoreceptor outer segment tips, induced by relatively low levels of light (for human). Stacks of photoreceptor nuclei appear to be normal, with no evidence of cell loss. The majority of these nuclei are of rod photoreceptors. Dark arrow head points to a typical cone photoreceptor nucleus.

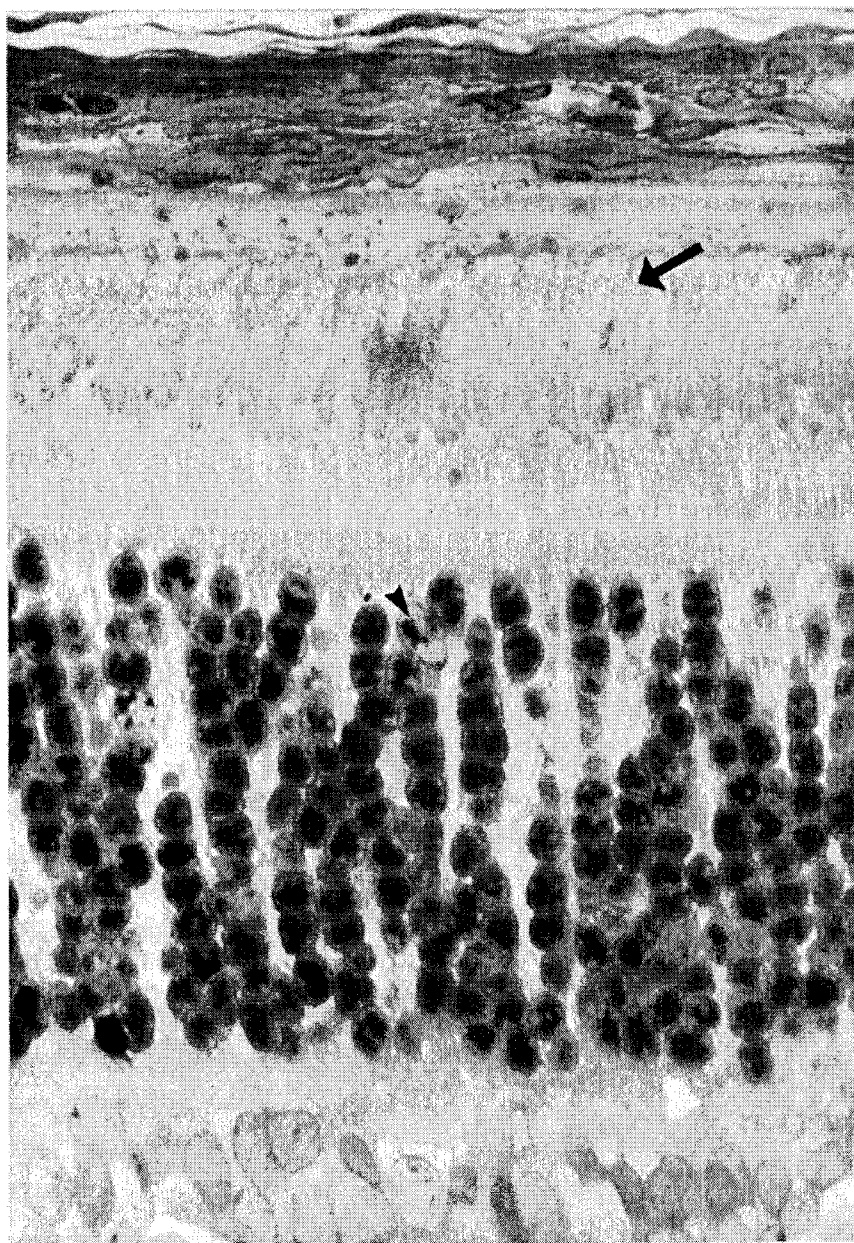
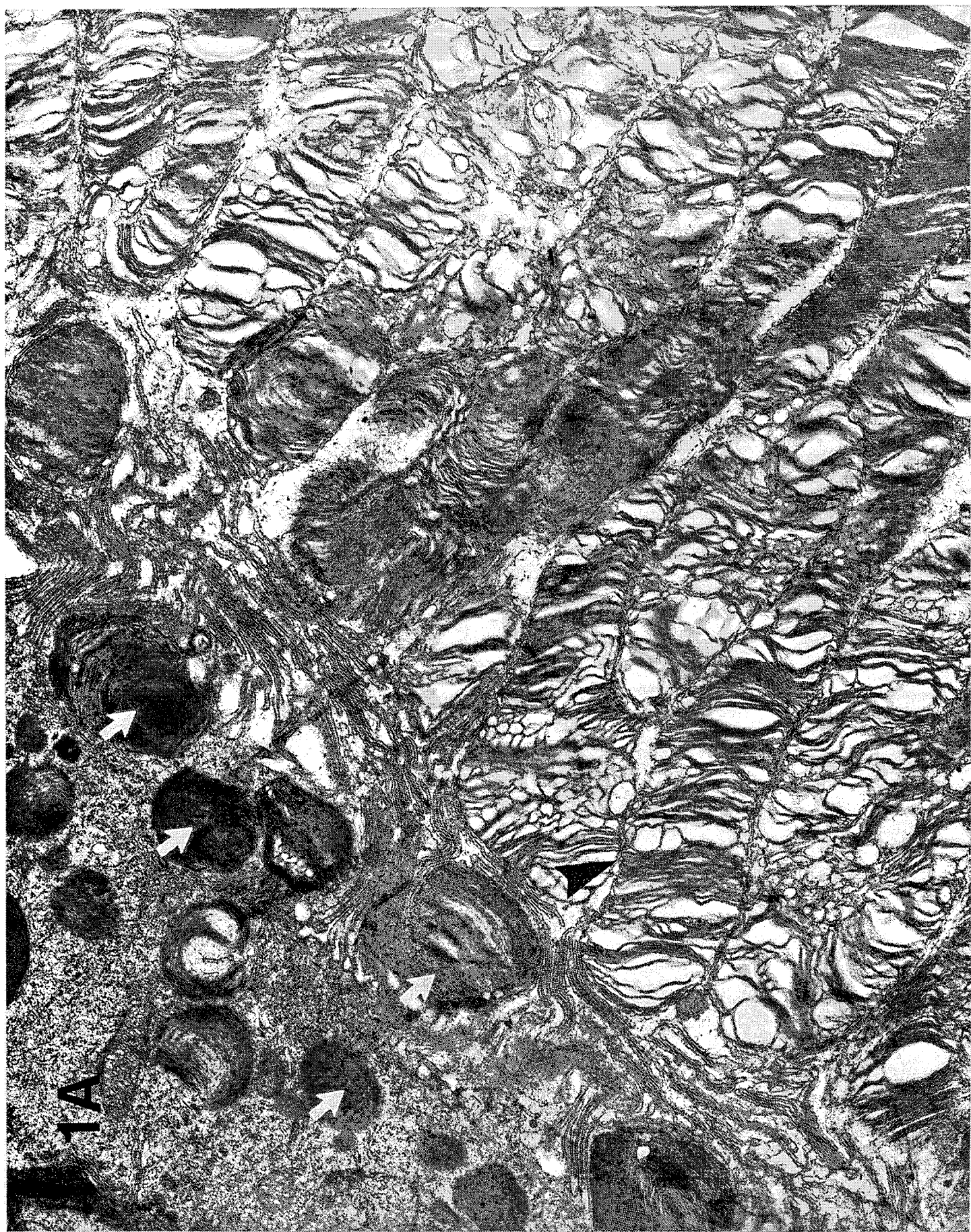


Figure 4

Electron micrograph of a rat retina treated according to Condition 1, level A. (See Figures 1 and 2 for details of light treatment and area of retina.) The tips of the photoreceptor outer segments have become swollen, and the discs within each cell have begun to separate. However, the tight loops at the peripheral borders of each disc remain intact (black arrow head). Numerous phagosomes (shed photoreceptor tips) are present within the retinal pigment epithelium (white arrows). While the photoreceptors have been altered, the pigment epithelium appears to be functioning normally.



1A

Figure 5

Electron micrograph of a rat retina treated according to Condition 1, level B. (See Figures 1 and 2 for details of light treatment and area of retina.) The base of these photoreceptors have normal, intact discs, and do not show any effects from the light treatment. Connecting cilia are evident, and the mitochondrial masses within the distal portions of the inner segments show no osmotic effects.



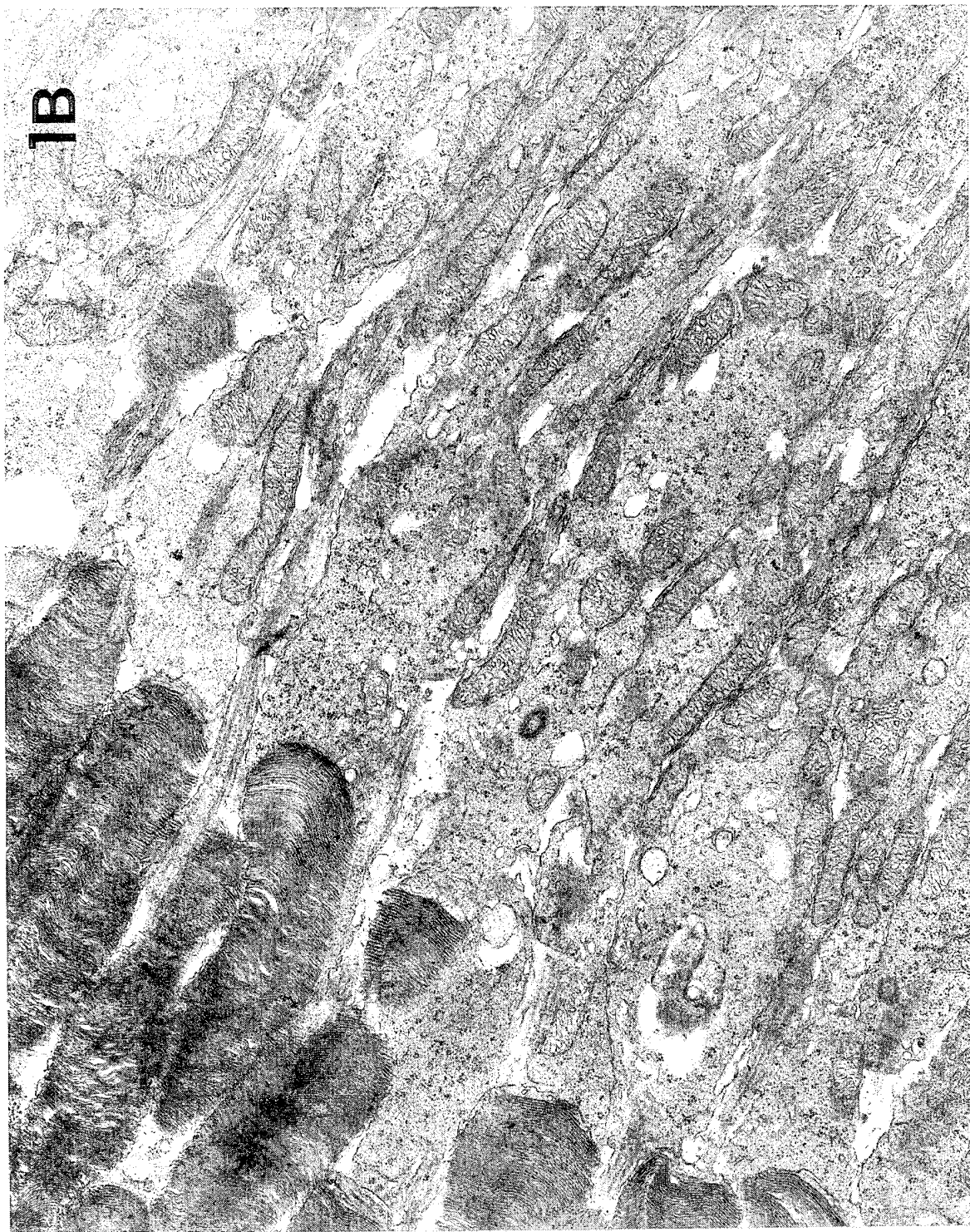


Figure 6

Electron micrograph of a rat retina treated according to Condition 1, level C. (See Figures 1 and 2 for details of light treatment and area of retina.) The photoreceptors near the distal edge of the outer nuclear layer appear to be healthy, with normal mitochondria and endoplasmic reticula. The outer limiting membrane is intact, and the photoreceptor nuclei (N) do not show unusual condensation or rearrangement of chromatin.

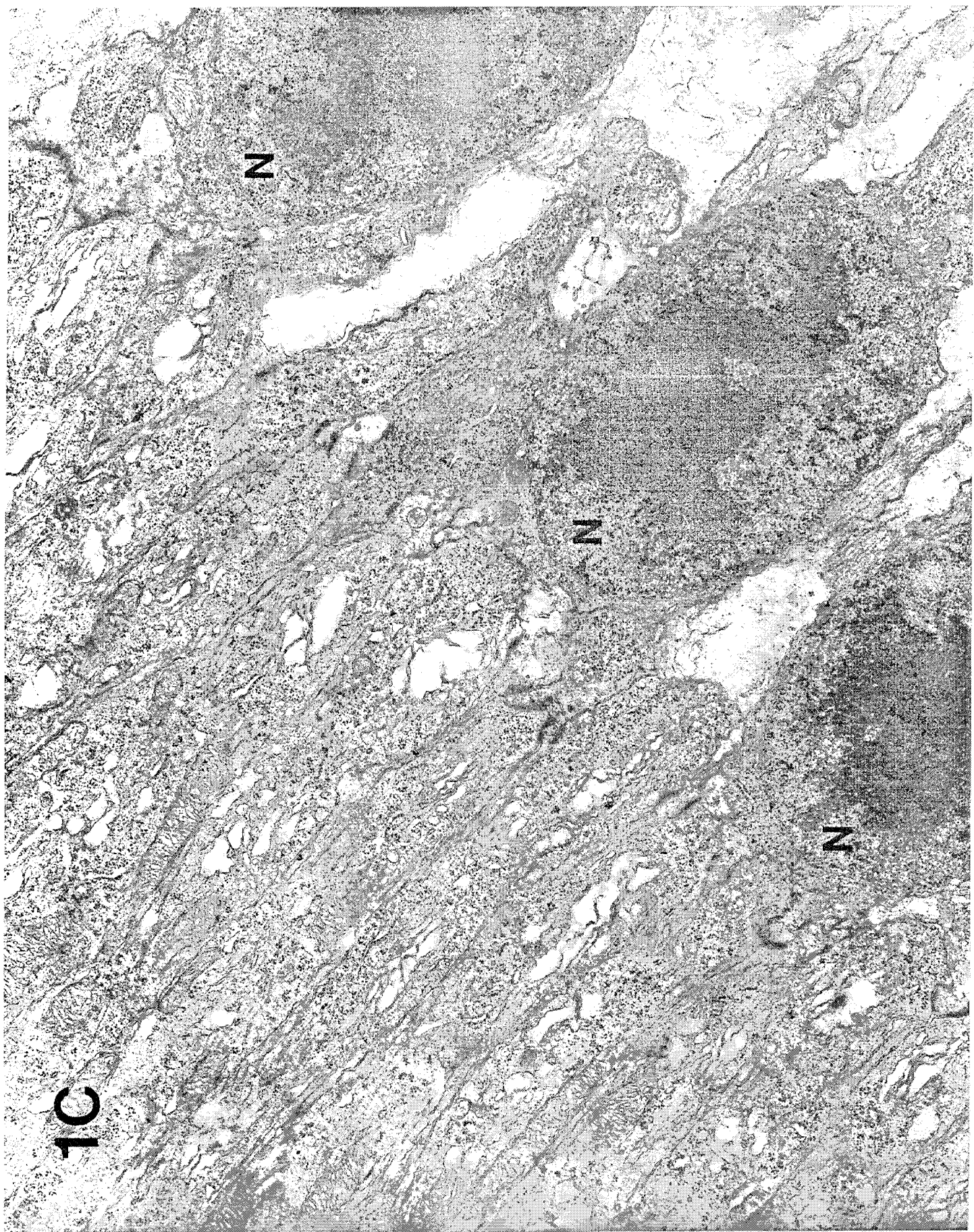
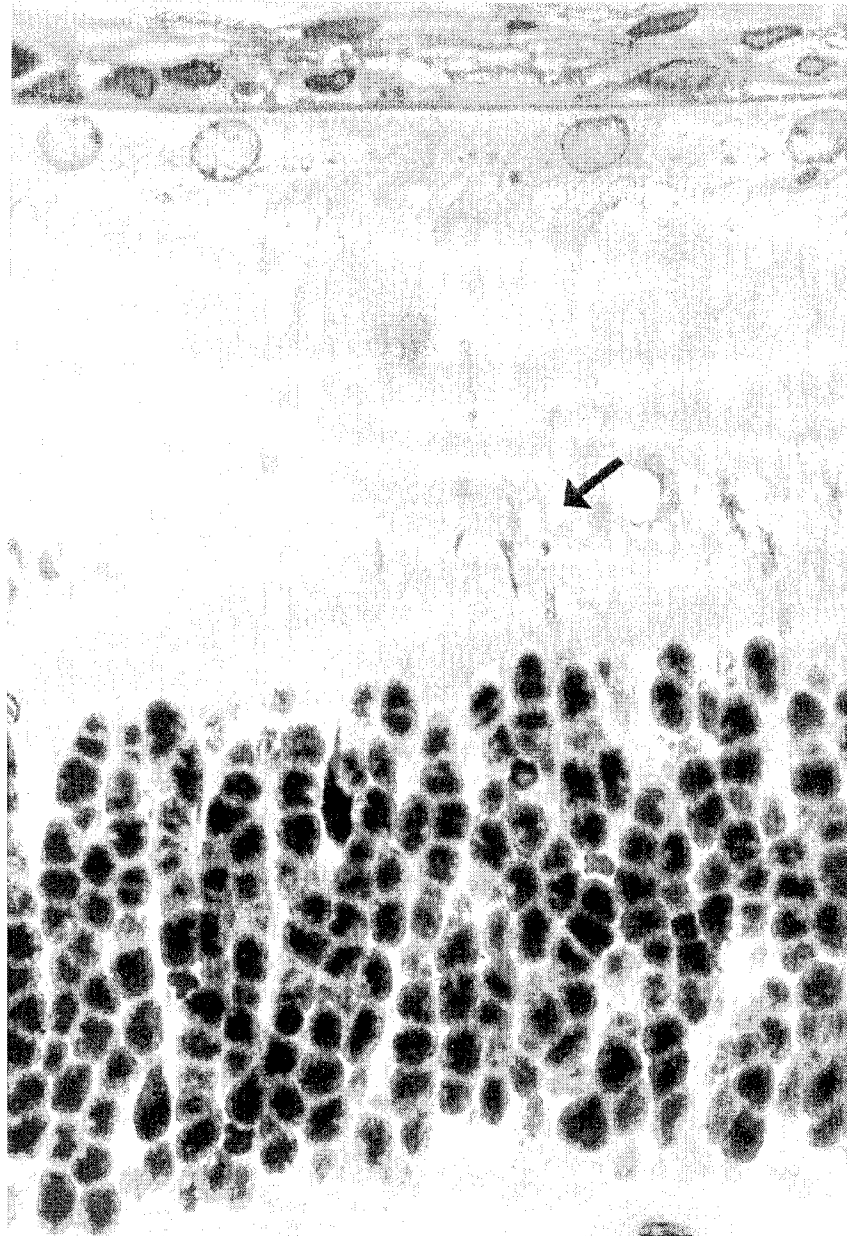




Figure 7

Electron micrograph of a rat retina treated according to Condition 1, level D. (See Figures 1 and 2 for details of light treatment and area of retina.) This section through the photoreceptor synaptic terminals illustrates numerous synaptic vesicles and normal ribbon synapse structures. A nucleus is visible in the upper right.





Handwritten text, likely a signature or name, located at the bottom of the page. The text is faint and appears to be written in cursive or a similar script. It is positioned below the arrow and the large black mass.

Figure 8

Light micrograph of a rat retina treated according to Condition 2. After doubling the amount of light, the entire outer segment becomes affected. The micrographs of Figures 3, 8, 13, 18 are of the same magnification, illustrating that these outer segments have now expanded to almost twice their normal length and diameter. Large gaps near the outer segment-inner segment junctions appear (arrow). While the vertical number of nuclei remain normal, some have now begun to reorganize, appearing dark and misshapen.

Figure 9

Electron micrograph of a rat retina treated according to Condition 2, level A. (See Figures 1 and 2 for details of light treatment and area of retina.) Five to six photoreceptor outer segment tips are arrayed across this section. The disc membranes in several are swollen and separating, as in figure 7, but other outer segments are dramatically disrupted with much disc membrane vesiculation evident. The retinal pigment epithelium (RPE) along the top remains full of phagosomes, but here they appear to be older and more completely degraded. Mitochondria and internal membrane systems within these cells appear normal. An RPE nucleus is visible along the left boarder.

Figure 10

Electron micrograph of a rat retina treated according to Condition 2, level B. (See Figures 1 and 2 for details of light treatment and area of retina.) Along the proximal edge of the photoreceptor outer segments, damage is now evident. Discs have become disrupted (black arrow), and disc membrane vesiculation has begun. While most of the inner segments appear normal, a few have undergone degradation, appearing very dark and condensed (white arrows).



Figure 11

Electron micrograph of a rat retina treated according to Condition 2, level C. (See Figures 1 and 2 for details of light treatment and area of retina.) Inner segments generally appear normal, but occasional vesiculation or swelling of endoplasmic reticulum is present. Some dense, phagocytized bodies appear within the cytoplasm of the Müller cells (white arrow), but photoreceptor nuclei (N) retain their normal structure.



Figure 12

Electron micrograph of a rat retina treated according to Condition 2, level D. (See Figures 1 and 2 for details of light treatment and area of retina.) Again, photoreceptor terminals generally appear normal, containing numerous synaptic vesicles and intact ribbon structures, and nearby nuclei (N) are healthy. However, an occasional photoreceptor terminal has begun degradation (black arrow).



Figure 13

Light micrograph of a rat retina treated according to Condition 3. Photoreceptor outer and inner segments are completely disorganized, and outer segments, when present, are much shorter (dark arrow). The number of photoreceptor nuclei has been reduced by about half, and many remaining nuclei appear dark. Many cone nuclei are present. The photoreceptor terminals occasionally appear enlarged (black arrow heads).

Figure 14

Electron micrograph of a rat retina treated according to Condition 3, level A. (See Figures 1 and 2 for details of light treatment and area of retina.) Under this treatment, the tips of the photoreceptors are greatly disorganized, showing darkening and condensation. While the retinal pigment epithelium contains large phagosomes (white arrow), sometimes consisting of entire outer segments, these cells still retain a normally appearing cytoplasm.



Figure 15

Electron micrograph of a rat retina treated according to Condition 3, level B. (See Figures 1 and 2 for details of light treatment and area of retina.) Photoreceptor outer segments demonstrate much condensation, vesiculation, and fragmentation. Occasionally (upper left), a normally appearing outer segment remains. In this example, it is a cone outer segment.



Figure 16

Electron micrograph of a rat retina treated according to Condition 3, level C. (See Figures 1 and 2 for details of light treatment and area of retina.) The inner segments appear to be greatly disorganized. Large masses of outer segments have been phagocytized by the Müller cells (white arrow), and occasional dark, condensed remains are present. Some nuclei appear normal while others have begun to show reorganization of the chromatin into peripheral dense regions (N).

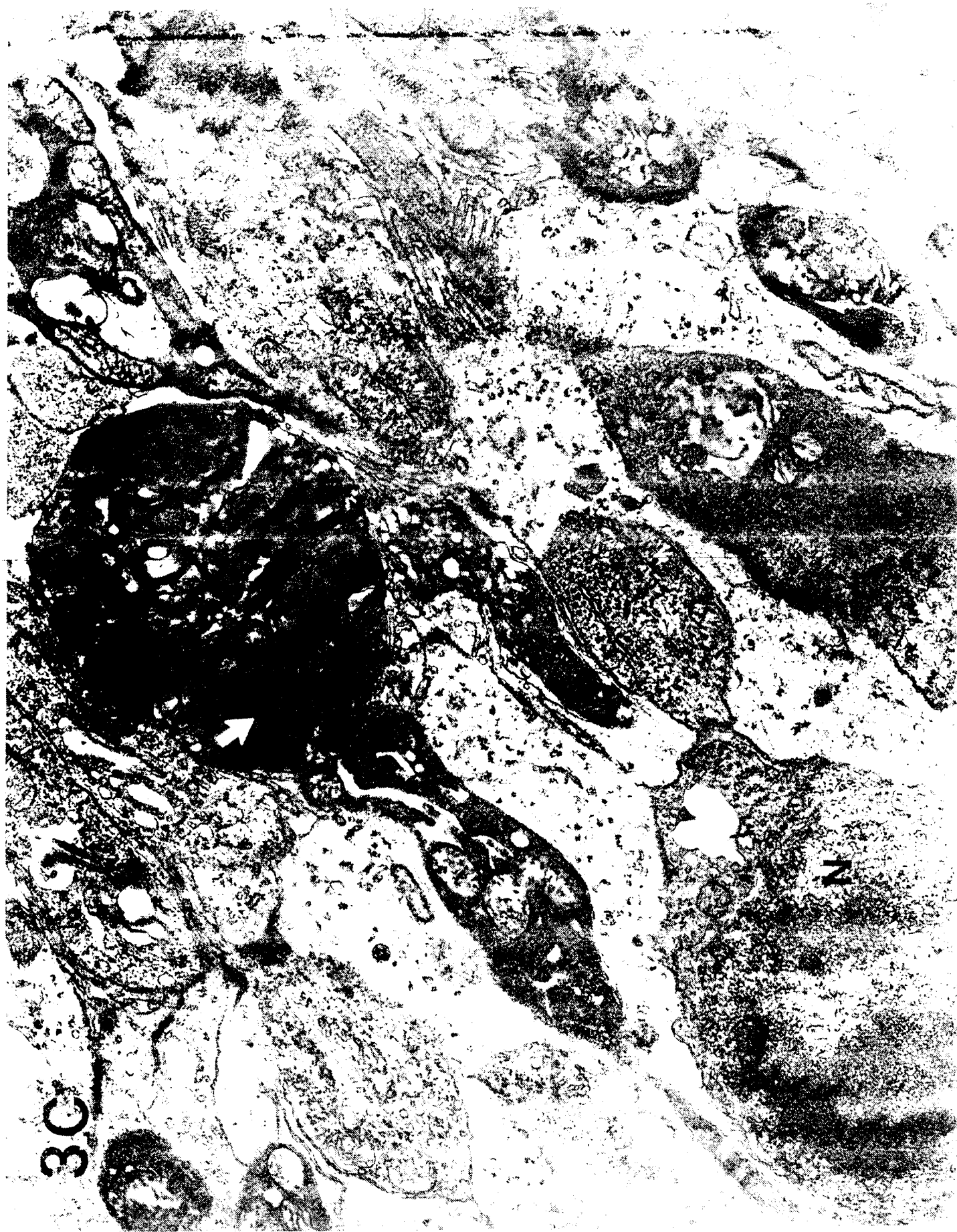


Figure 17

Electron micrograph of a rat retina treated according to Condition 3, level D. (See Figures 1 and 2 for details of light treatment and area of retina.) In this last section, the photoreceptor synaptic terminals appear to be undergoing decomposition. Numerous, dense regions occur as the cytoplasm darkens and condenses, although, situated throughout are normally appearing regions (black arrows). Photoreceptor nuclei (N) generally appear to be altered, with regionally condensed chromatin characteristic of apoptotic nuclei.



Figure 18

Light micrograph of a rat retina treated according to Condition 4. Virtually all photoreceptors have degenerated. The few that remain have no visible outer or inner segments, and their nuclei lie only a short distance below the RPE cells (dark arrow). Most remaining nuclei are dark and condensed, however, some cone nuclei are present (black arrow head).

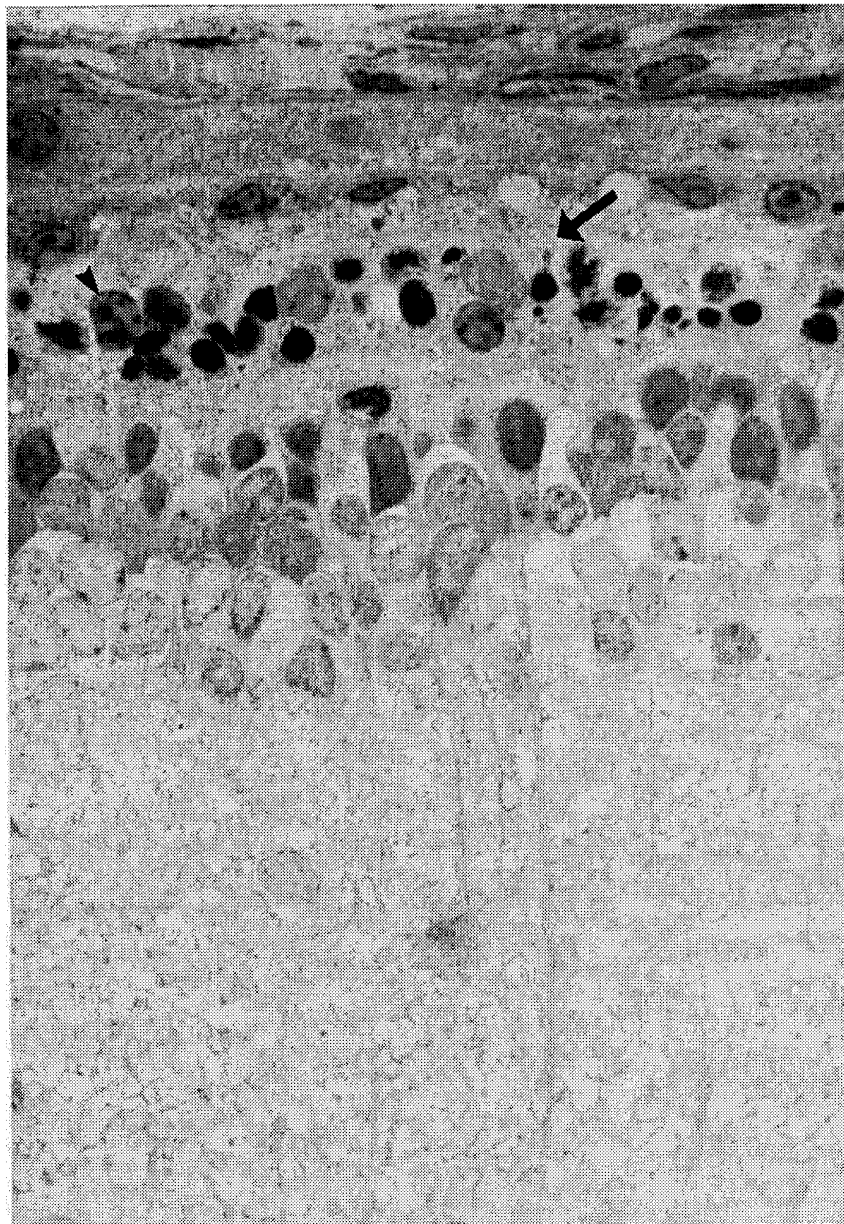


Figure 19

This diagram illustrates the region of the rat retina that becomes light damaged after 2 hours of intense fluorescent light, followed by an interval of normal, dim illumination. In studying these retinas, the inferior half was sectioned along the nasal-temporal line through the optic nerve, and the light damaged region on one side compared with the intact region on the other.

Retina

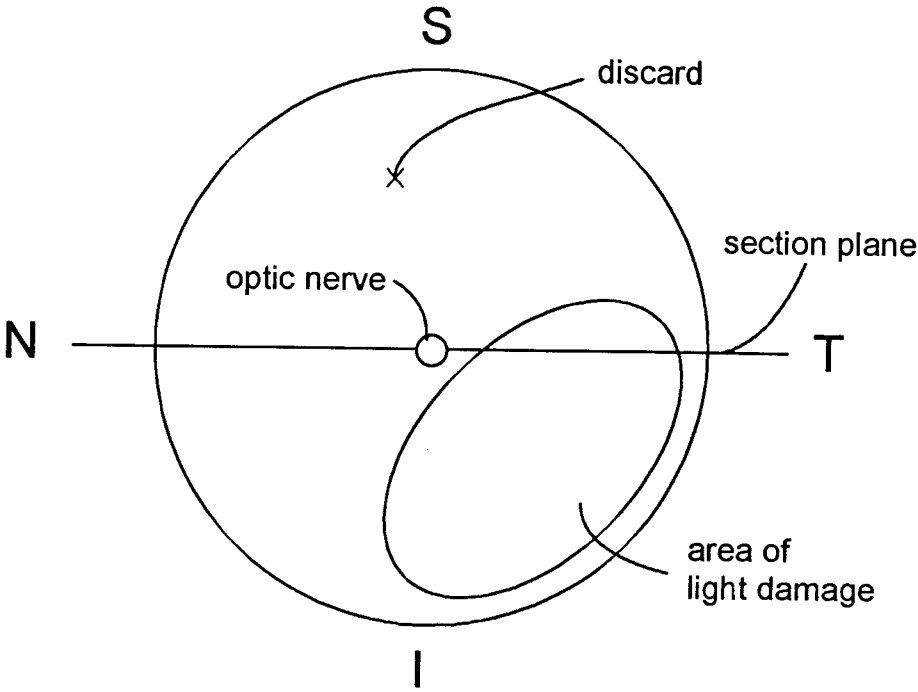


Figure 20

These graphs illustrate the rate at which the rat retina is altered following 2 hours of bright fluorescent light stimulation. Measurements are taken from 1 μm -thick plastic sections, chosen for their higher resolution (however, 5 μm -thick paraffin sections of this same material show the same results). The upper graph illustrates the reduction in photoreceptor cells by measuring the outer nuclear layer (ONL) thickness as light damage progresses, while the lower graph demonstrates the same effect by comparing the thickness of the photoreceptor outer segment layer through time. The intact retinal region of each sample has been normalized to 100% and the light damaged region plotted as percent remaining. The greatest response occurs 48 h following light treatment. Controls (C) represent rat retinas taken just prior to light treatment, while the 0 time point represents samples obtained just after the 2 h treatment.

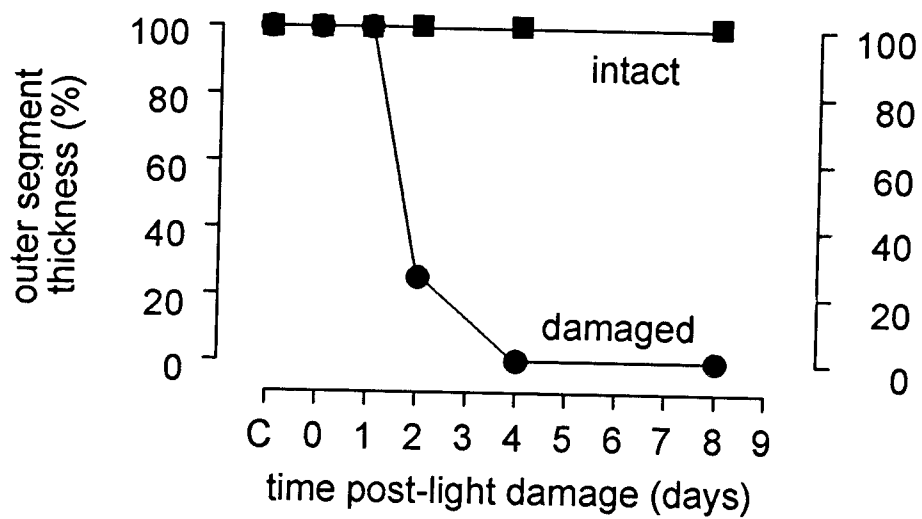
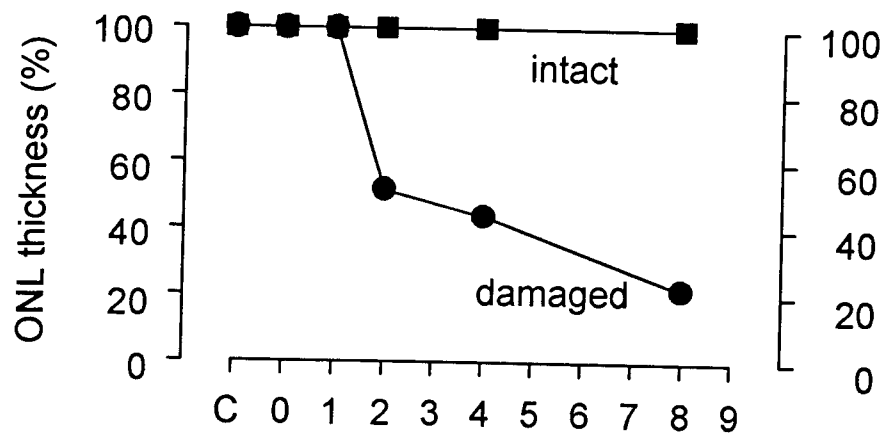


Figure 21

These graphs illustrate the rate at which the rat retina is altered following 2 hours of bright fluorescent light stimulation. The upper graph plots the remaining number of photoreceptor cell nuclei as a percent of the control and 0 time point animals, showing that loss (disappearance) begins 48 hours after treatment. However, even after 8 days, some nuclei remain. The lower graph illustrates the survival ratio of photoreceptors following light treatment. The number of nuclei have been compared between the left and right regions of each retina, and the ratio plotted. Again, dropout appears at 48 hours post-treatment. By plotting the change between each of these values, the rate of loss can be obtained. The greatest loss of photoreceptor nuclei occurs between the 1 and 2 day time points. Thereafter, the rate of loss declines.

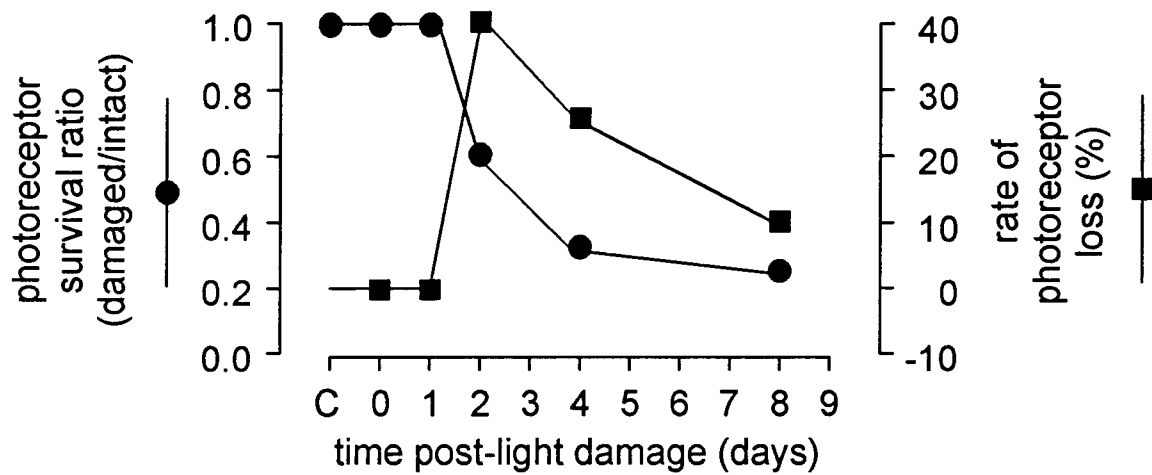
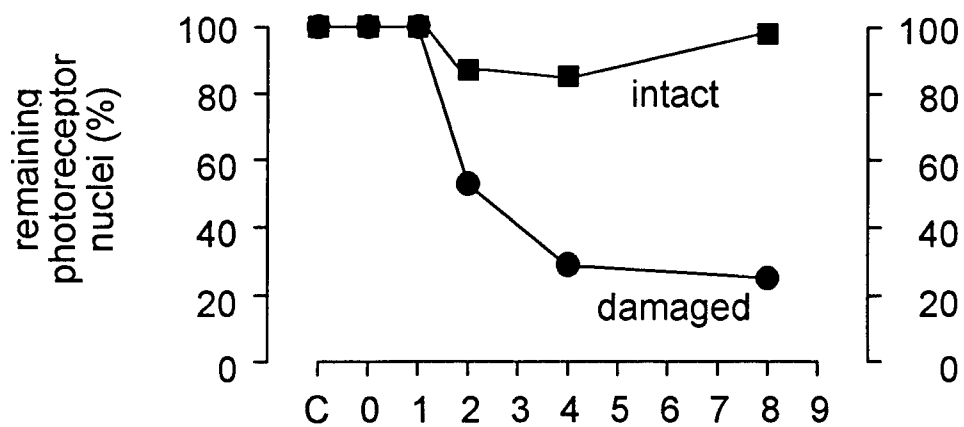
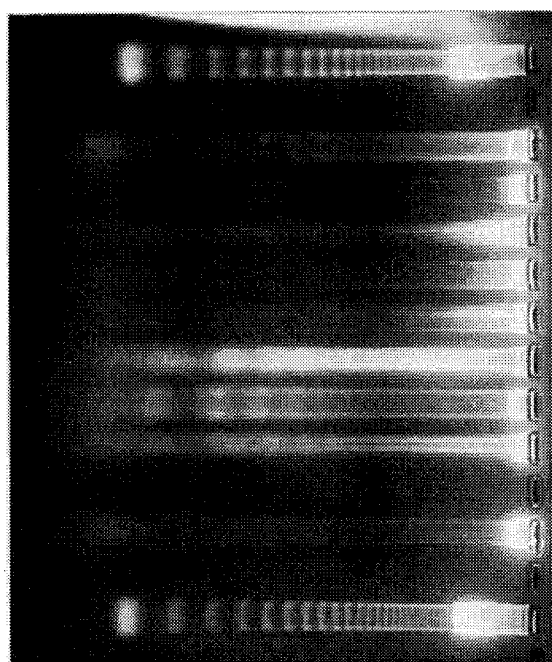


Figure 22

These gel electrophoretic lanes compare commercially prepared 123-DNA ladder with the DNA of naturally occurring apoptotic rat thymocytes and retinal DNA from rats following 2 hours of bright fluorescent light treatment. The commercial ladder (shown at both sides) is composed of DNA fragments that are 123 base pair multimers, the shortest fragments migrating the greatest distance. Rat thymocytes undergo regular apoptotic cell death through a process of DNA fragmentation into multimers of 140-180 base pairs. While faint, the thymocytes (Thy) illustrate this laddering. Two control retinas and retinas taken at 15, 20, and 25 hours after light treatment show no laddering. However, retinas obtained at 30, 45, and 60 hours post-treatment demonstrate DNA laddering, with the strongest image present at 30 hours. This shows that the process of delayed cell death in these treated retinas is a result of apoptosis, and, furthermore, illustrates that the peak of apoptosis (30 h) precedes cell dropout (figures 20 and 21) by about 18 hours.



123

Thy

C

15

20

25

30

45

60

C

123

Figure 23

This diagram illustrates the system used for the assay of excitatory amino acid neurotransmitter release from retinal preparations preloaded with [3 H]glutamate and then treated with PAF and the PAF antagonist BN52021. Dissociated cells or synaptosomes, preloaded with label, were placed into a perfusion chamber, and 6 ml/min saline buffer (room temperature) perfused through the chamber. Two minutes after the cell was loaded, a solution containing 200 μ l PAF or KCl was added. When BN52021 treatment was performed, dissociated cells or synaptosomes were pretreated with saline buffer containing 1 μ M BN52021, and the same buffer perfused through the chamber. A fraction collector, set to collect three drops per vial, was used to harvest perfusates from the preparations (50 μ g protein) loaded with [3 H]glutamate. PAF, KCl, and BN52021 were used to induce [3 H]glutamate release.

ASSAY FOR EXCITATORY AMINO ACID NEUROTRANSMITTERS RELEASE FROM SYNAPTOSOMES

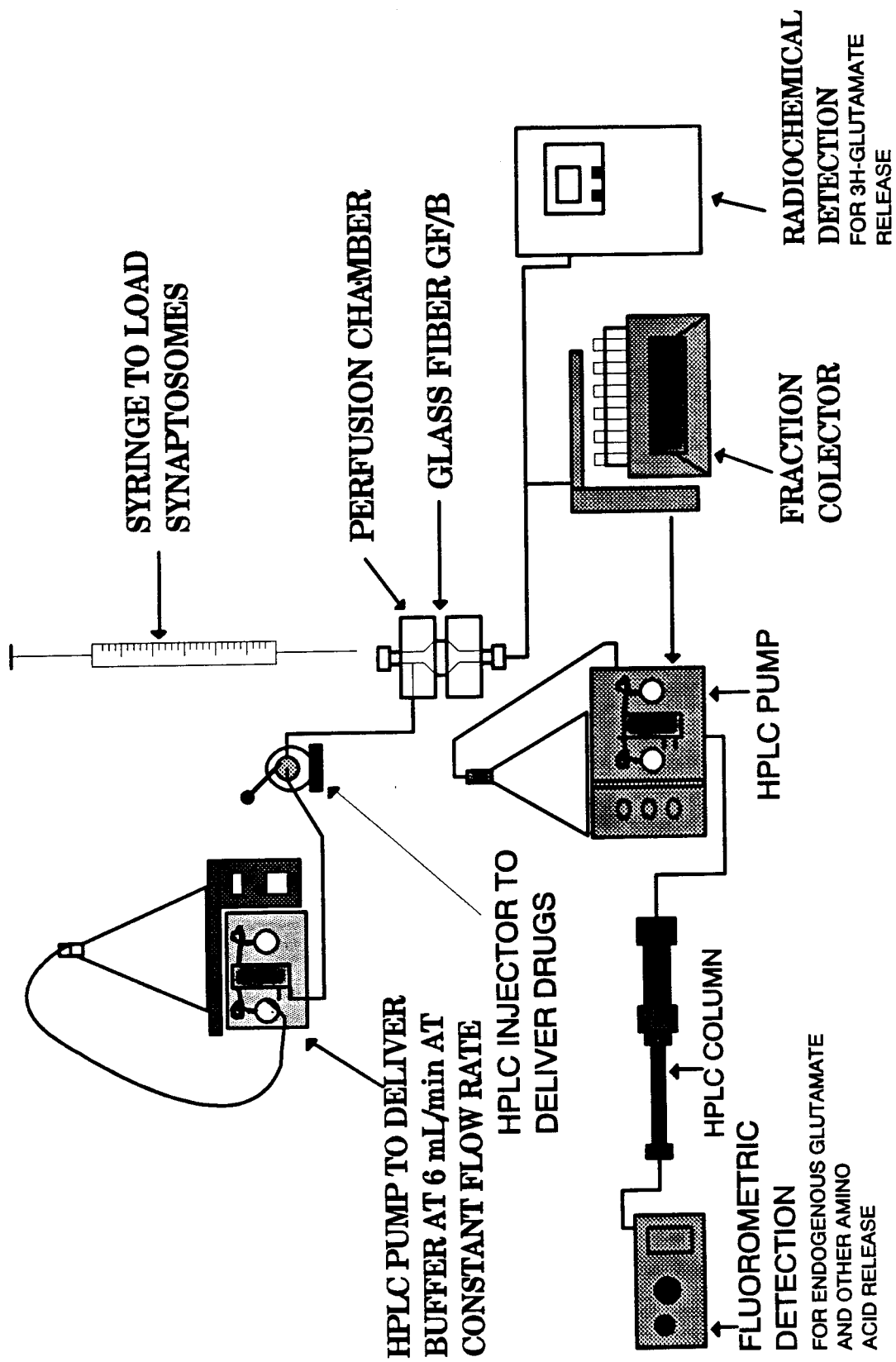


Figure 24

Dissociated cells, which were previously loaded with [3 H]glutamate, were placed in a perfusion cell, and perfused with 6 ml/min saline buffer at room temperature. Two minutes after cell loading, 200 μ l PAF or KCl solution was injected into the chamber. Saline buffer, containing 1 μ M BN52021, was perfused through the cell when treatment with the PAF inhibitor was performed.

PAF INDUCED 3H-GLUTAMIC ACID RELEASE FROM RAT RETINA DISSOCIATED CELLS

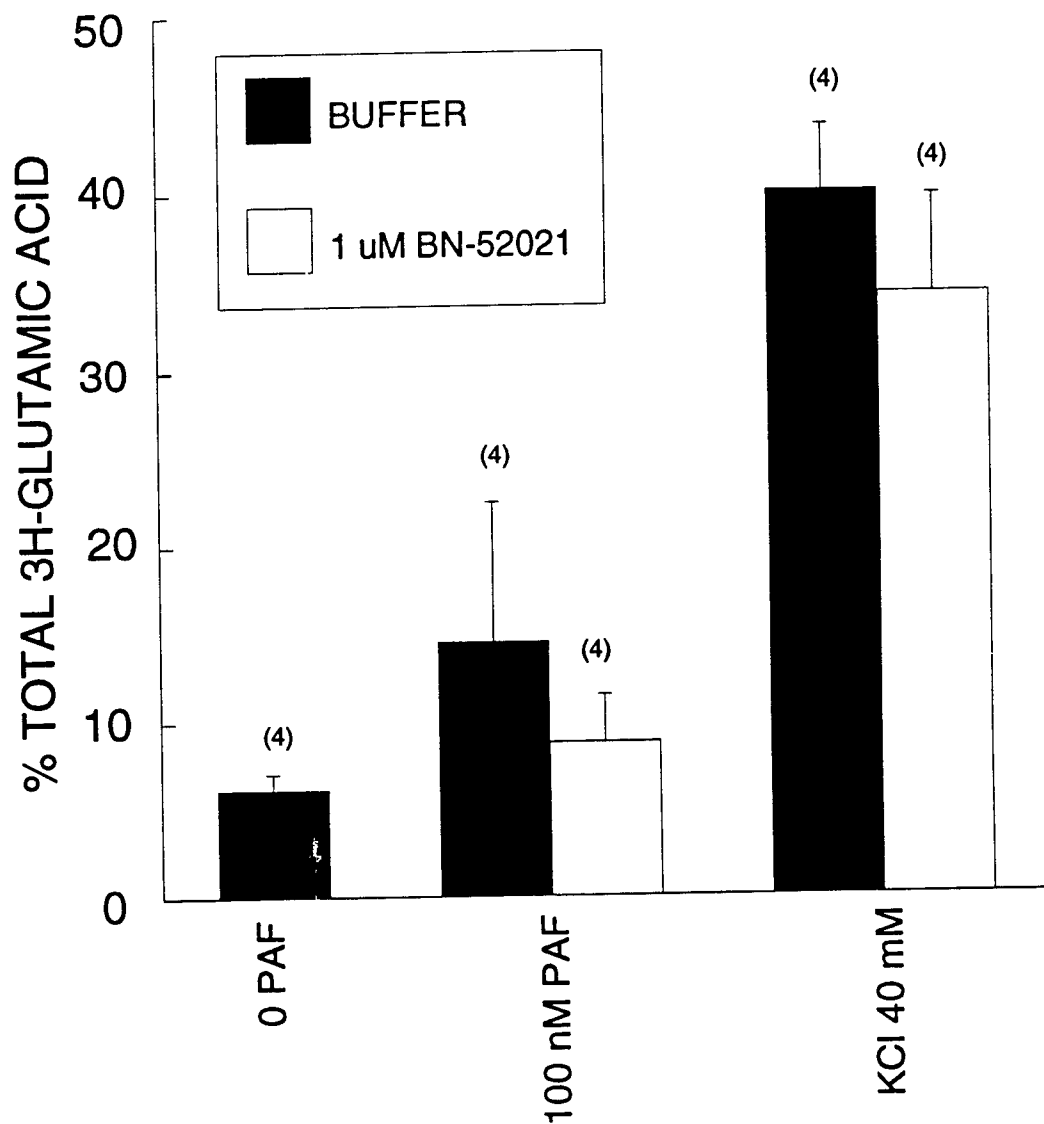


Figure 25

The retina P_2 fractions (50 μ g of protein per treatment), containing most retinal neuronal synaptic endings (but excluding those of the photoreceptors), were incubated at room temperature in a final volume of 150 μ l saline buffer (pH 7.5) with 2.5 μ Ci [3 H]glutamate (specific activity 17.25 Ci/mmol) for 10 min. PAF, KCl, and the PAF antagonist BN52021 (1 μ M) were used to induce [3 H]glutamate release.

PAF INDUCED 3H-GLUTAMIC ACID RELEASE FROM RAT RETINA SYNAPTOSOMES

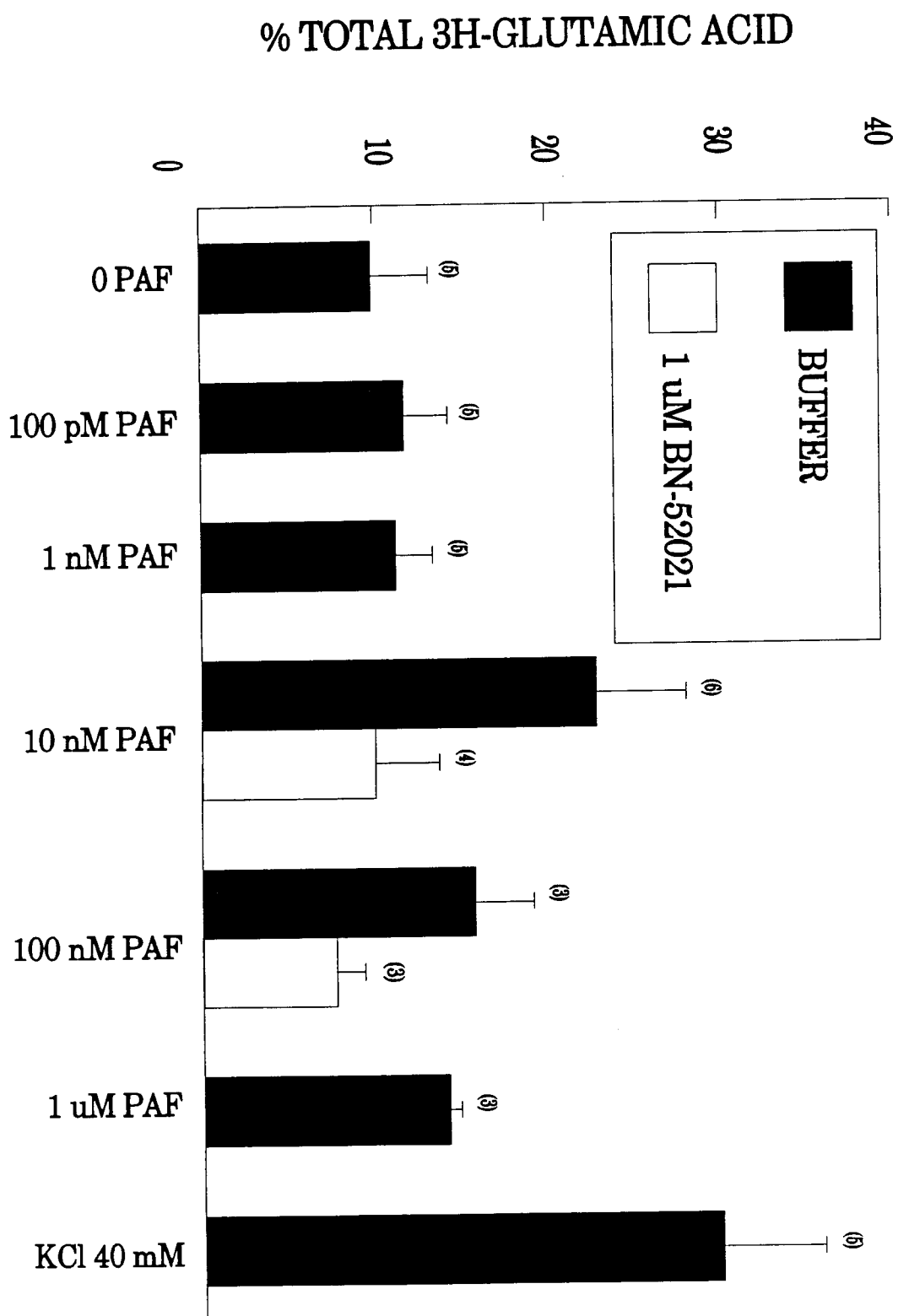


Figure 26

The P1 fraction, containing the photoreceptor synaptosomes, were incubated at room temperature (50 μ g of protein) in a final volume of 150 μ l saline buffer (pH 7.5) with 2.5 μ Ci [3 H]glutamate (specific activity 17.25 Ci/mmol) for 10 min. Synaptosomes, loaded with [3 H]glutamate, were placed in a perfusion chamber, and PAF or KCl injected to trigger [3 H]glutamate release.

3H-GLUTAMIC ACID RELEASE FROM RAT RETINAL SYNAPTOSOMES FROM FRACTION P1

